SYNTHESIS, STRUCTURE AND PROPERTIES OF HIGHERVALENT MANGNAESE COMLEXES

A Thesis

Submitted for the Degree of

Doctor of Philosophy

By

Biju A. R.

School of Chemistry

University of Hyderabad

Hyderabad – 500046

India

DECEMBER 2008

To

THOSE WHO ARE CLOSE TO MY HEART...

CONTENTS

CHAPTER II

Mononuclear manganese(III) complexes of acetyl acetone, unexpected polymorphs

CHAPTER III

DFT and TDDFT studies of mononuclear fluoromanganese complexes

STATEMENT

I hereby declare that the matter embodied in this thesis is the result of investigations carried out by me in the School of Chemistry, University of Hyderabad, Hyderabad, India under the supervision of Prof. M. V. Rajasekharan. In keeping with the general practice of reporting scientific observations, due acknowledgement has been made wherever the work described is based on the findings of other investigators.

Biju A. R.

CERTIFICATE

Certified that the work embodied in this thesis entitled "***SYNTHESIS, STRUCTURE AND PROPERTIES OF HIGHERVALENT MANGANESE COMPLEXES***" has been carried out by **Biju A. R.** under my supervision and the same has not been submitted elsewhere for any degree.

Hyderabad
December 2008

M. V. RAJASEKHARAN
(Thesis Supervisor)

DEAN
School of Chemistry

ACKNOWLEDGMENTS

I thank with immense pleasure Prof. M. V. Rajasekharan, supervisor of my thesis for his generous support and guidance. As a student, I am privileged to work under with an admirable researcher and teacher. I am also grateful to him for the freedom he has given to me. I thank Prof. D. Basavaiah, Dean, School of Chemistry and former Dean(s) for providing all the facilities of the school. I also thank faculty members of the School of Chemistry for their cooperation on various occasions. I thank the Professor-in-charge and the officer-in-charge of Central Instruments Facility (CIL) and Centre for Modelling, Simulation and Design (CMSD) for providing me access to all required facilities.

I thank all the non-teaching staff of the School, CIL and CMSD for their help during the research work. A special word of thanks goes to Mr. Raghavaiah for his help in x-ray data collection, Ms. Asia Parwez for her help in IR measurements, Mr. Prasad at glass blowing centre, Mr. Suresh for his help during ESR measurements and Mr. Nageshwarrao for his help in PXRD measurements.

I thank Dr. J. -P. Tuchagues at Laboratoire de Chimie de Coordination du CNRS, Toulouse, France for the variable temperature magnetic susceptibility measurements, Dr. M. K. Chattopadhyay for his collaborative work on cold adaptation of Antarctic bacterium and the librarian and other staff of Indira Gandhi Memorial Library (IGML) of the university for the books and journals.

Let me also thank the present and former warden(s) of New Research Scholars Hostel for providing the accommodation.

My sincere thanks to UGC, India for the fellowships (JRF/SRF), without which I could not have even dreamt a Ph.D degree.

I am grateful to Paaru for her love, compassion and care and thankful to my mother for her constant support. I am also thankful to current (Mr. Kishore Babu, Ms. Bhargavi, Mr. Krishnachari and Mr.Mehaboob) and former labmates for their assistance and teamwork. I thank Mr. Sreenath Muraleedharan. K and Mr. Jibin A. K. for their wonderful friendship.

My heartfelt thanks also go to all dear friends of the university. Finally, I thank all those who gave suggestions, advices and guidance before and during the research. Omissions of references to any special help or suggestions are unintentional and I express my regret.

Biju A. R.

PREFACE

The studies on highervalent manganese complexes are of great interest due to its relevance not only in various biological systems like oxygen evolving complex of Photosystem II, Mn catalases and Mn superoxide dismutase, but also in the field of single molecular magnetism. The thesis explores synthesis, structure and properties of various highervalent manganese complexes.

Thesis is divided into five chapters and an appendix. Chapter I gives a brief introduction to various manganese(III) complexes and its relevance in various fields. Besides these, a brief account of the background works of mononuclear, dinuclear, trinuclear and tetranuclear manganese complexes are also described.

Chapter II deals with synthesis, structural analysis and lattice energy calculations of four packing polymorphs of mononuclear manganese complexes with acetyl acetone.

Synthesis, structure, reflectance spectra, DFT and TDDFT studies of six mononuclear fluoromanganese complexes are discussed in chapter III. A good correlation was observed with the observed spectra in many cases.

Chapter IV deals with synthesis and structural characterisation of various dinuclear manganese complexes. Variable temperature magnetic susceptibility measurements of two dinuclear manganese complexes are also reported. Rare mononuclear manganese complexes with three monodentate haloacetic acid ligands are also reported.

In chapter V, synthesis and structural characterisation of two trinuclear manganese(IV) complexes and two tetranuclear manganese(III) complexes are discussed.

4,5-Diazafluoren-9-one (dafone) is a bidentate ligand. It is a derivative of 1,10-phenanthroline (phen), having an exocyclic keto function. Coordination mode of the dafone is not known for silver(I) and platinum(II). Appendix 1 deals with synthesis and structural characterisation of two silver complexes and one platinum complex of dafone.

A copy of this thesis (.pdf), file containing crystallographic information (.cif) and a .cif file viewer is available in a CD-ROM at the back cover of the thesis.

Part of the work reported in this thesis has been published are given at the end of the thesis.

Abbreviations and definitions

$R1$	$= \Sigma\|\|F_o\| - \|F_c\|\| \,/\, \Sigma\|F_o\|$
$wR2$	$= \{\Sigma\,[w(F_o^2 - F_c^2)^2]/\,[\Sigma(w(F_o^2)^2)]\}^{1/2}$
w	$= 1/[\sigma^2(F_o)^2 + (AP)^2 + BP];\ P = [2F_c^2 + \mathrm{Max}\,(F_o^2, 0)]/3$
GooF	$= \{\Sigma[w(F_o^2 - F_c^2)^2]/(n\text{-}p)\}^{1/2}$
$\Delta\rho_{max}$, $\Delta\rho_{min}$	= Maximum, minimum residual electron density on the final Fourier map.

CHAPTER 1

Manganese(III) complexes: A brief introduction

1.1 Introduction

The coordination chemistry of manganese(III) has been increasingly studied in an effort to simulate the biological systems like oxygen evolving complex of Photosystem II, Mn catalases and Mn superoxide dismutase that have been found to contain this oxidation state or go though this oxidation state in their catalytic cycles. Moreover manganese(III) has been extensively studied in the field of single molecular magnetism.

1.1.1 Photosystem II

Photosystem(II) is the unique enzyme that found in thylakoid membranes of oxygenic photosynthetic organisms which splits water producing molecular oxygen. It is expected that unraveling the structural and functional principles of this catalyst site of water oxidation will inspire the development of artificial catalysts for solar light powered water splitting into molecular oxygen and hydrogen. Although PSII is a large protein complex, much of its bulk is involved in harvesting and transferring photonic energy. The actual oxidation of water to oxygen is carried out at a cluster of metal ions referred to as oxygen-evolving complex (OEC). The OEC consists of an inorganic core comprising four manganese, one calcium, and at least five oxygen bridges (Mn_4OxCa cluster)[1] that

is surrounded by a functionally important protein matrix. Cofactors are Cl^- and possibly bicarbonate[2]. Two recent crystal structures[1,3] have resolved the electron density of the OEC and proposed that it can be best fit by a trimanganese cluster with a single "dangler" manganese a slightly longer distance away (Figure 1.1). For the water oxidation reaction to take place, the cluster cycles through five oxidation states (S_n states, S_0 to S_4). The stabilization of higher oxidation states (S_2 and S_3) in the Mn_4Ca cluster is both due to the delocalization of positive charge among metal centers and also from the local electrostatic effect generated by the strong electro static effect generated from the strong sigma donor ligands such as aspartate, glutamate and histidine that surround the cluster in the active site.

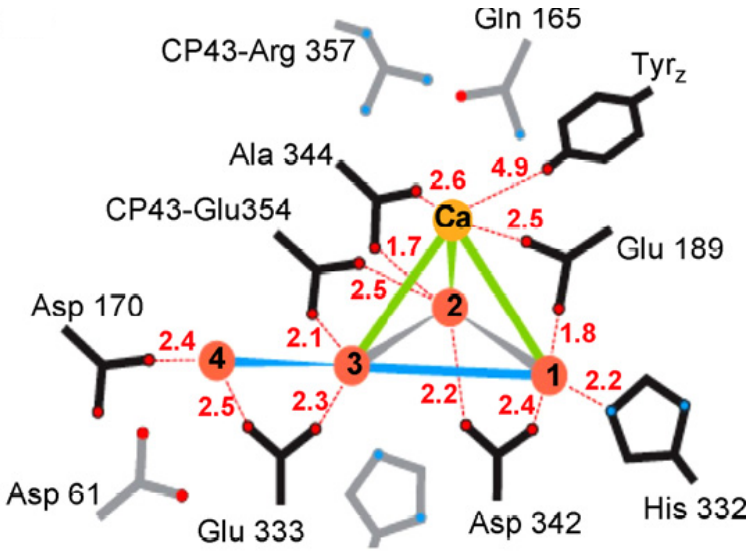

Figure 1.1 3.0 Å crystal structure model of the OEC[3]

We can explain the process by a conceivable mechanism, which is linear four quantum process in which four consecutive flashes induces four increasingly oxidized sates of a trapping centre ($S_{0\rightarrow4}$), each excitation state adding one oxidation state. A schematic diagram of the OEC is shown in Figure 1.2.

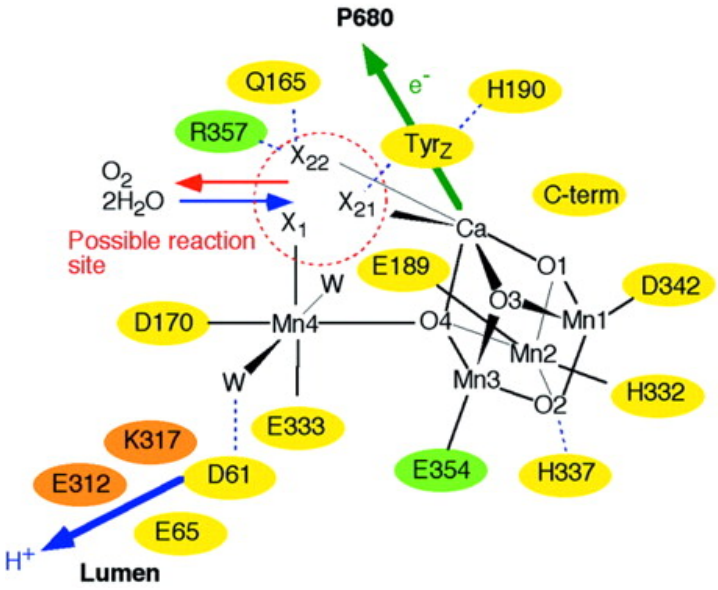

Figure 1.2 Schematic view of the OEC[1].

1.1.2 Mn-catalases

Manganese binuclear complexes with carboxylate ligand have attained much attention due to their presence in metalloezyme called Mn-catalases. Catalases catalyse the disproportionation of hydrogen peroxide into water and oxygen.

$$2H_2O_2 \rightleftharpoons O_2 + 2H_2O$$

Thereby they protect cells from oxidative damage by hydrogen peroxide, which is produced during the oxygen metabolism. Hydrogen peroxide levels may be as high as 10% of the oxygen that is consumed in cellular respiration. Hydrogen peroxide readily reacts with many reductants usually found in cells and the hydroxyl radicals that are formed in turn are very potent oxidizing agents that react immediately with most molecules in the cell.

Figure 1.3. Ribbon diagram of the 1.0 Å resolution X–ray structure of a dimanganese catalase monomer from *Thermus thermophilus*[6]. The two Mn ions are located within the four-helix-bundle.

Possibly they also play a role in the prevention of cell aging and cancer development[4]. It has been found in several microorganisms, for example *Thermus thermophilus* and *Lactobacillus plantarum*[5]. The enzymes from both species were isolated and found to be highly homologous. Recently, very high resolution (1.0 Å) X–ray structures were obtained of the enzyme isolated from both organisms in the $Mn^{III}Mn^{III}$ oxidation state[6,7]. The central motif found in these structures is a four-helix bundle which is depicted in Figure 1.3. The Mn binding sites in the *thermophilus* enzyme are the amino-acid residues of GLU36, HIS73, GLU70, HIS168 and GLU155. Four oxidation states can be realised in the Mn catalases, $Mn^{II}Mn^{II}$, $Mn^{II}Mn^{III}$, $Mn^{III}Mn^{III}$ and $Mn^{III}Mn^{IV}$. Only the homovalent $Mn^{II}Mn^{II}$ and $Mn^{III}Mn^{III}$ states, however, show extremely high reaction rates for the catalytic reaction. First evidence for a dinuclear Mn active site came from EPR spectroscopy[8]. Since then all four oxidation states have been investigated[9-11].

1.1.3 Mn-Superoxide dismutases

Superoxide dismutases are biological metal complexes that function as radical scavengers inside the living cells and thus protect the macromolecular structures from oxidative stress. Superoxide is a normal byproduct of metabolism in many of the key biological process. It is for this reason that enzyme susperoxide dismutase exists as an almost ubiquitous component of aerobically living systems to catalyse the disproportionation of superoxide to oxygen and hydrogen peroxide.

$$2O_2^- + 2H^+ \rightarrow O_2 + H_2O_2$$

Three basic types of SODs have been found based on mononuclear Mn or Fe or a dinuclear Cu/Zn active site.

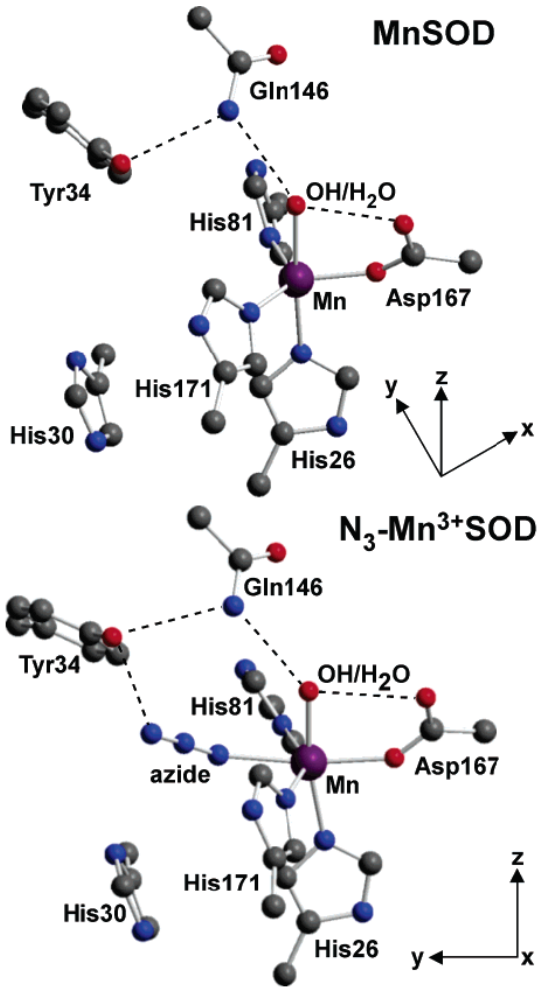

Figure 1.4 Active-site structures of *E. coli* MnSOD (top) and *T.thermophilus* N_3-Mn^{3+}SOD[12]

Mn-SODs are typically isolated as dimers or tetrames containing one Mn ion per subunit. X-ray crystallographic structures[12] of Mn-SOD reveals that active site, Mn ion is ligated by four amino acid unit and one solvent molecule in trigonal bipyramidal geometry (Figure 1.4). Both experimental and theoretical studies

have shown that axially ligated solvent molecule is OH^- in Mn^{3+}-SOD but acquires a proton to become H_2O upon reduction of metal ion to Mn^{2+}-SOD[13, 14]. The structure of the azide complex of the *T.thermophylus* MnSOD has been solved by X-ray crystallography[15,16]. Azide binds directly to the metal ion in the crystal forming a complex that retains all four protein ligands. The persistence of electron density in the axial water site implies six coordination for the Mn in anion complex.

1.1.4 Single molecular magnets

One of the most fascinating recent developments in molecular magnetism is the discovery that simple coordination compounds containing paramagnetic metal ions can function as single-domain magnetic particles at low temperatures in the absence of an external magnetic field. Such molecules are now termed as "single-molecule magnets" (SMMs). Although complexes displaying SMM behavior are known with a number of metal ions[17], homometallic manganese carboxylate clusters have to date proven to be the most fruitful source of SMMs. Manganese(III) clusters with its high spin ground state and high zero filed splitting parameters have made an ideal selection for the development of single molecular magnets. After the discovery of first single molecular magnet $[Mn_{12}O_{12}(O_2CCH_3)_{16}(H_2O)_4]$ $2HOAc.\ 4H_2O$, a plethora of complexes have been reported with single molecular magnetic property[18].

1.2 Manganese complexes

1.2.1 Synthetic strategies

A dominant feature of the inorganic chemistry of manganese is the variety of complexes that can be made with different oxidation level of manganese. Mn shows variable oxidation states from –3 to +7. Among these the divalent state is the most common and stable one. In neutral or acidic aqueous solution it exists as the very pale pink hexaaqua ion, $[Mn(H_2O)_6]^{2+}$ which is quite resistant as shown by the potential.[19]

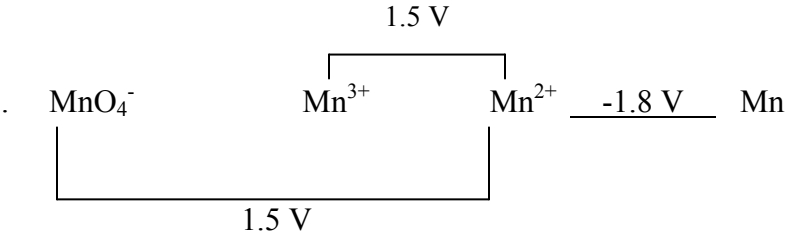

In basic media however the hydroxide $Mn(OH)_2$ is formed and this is very easily oxidized even by air, as shown by the potentials.[19]

$MnO_2.yH_2O$ —0.1 V— $Mn_2O_3.xH_2O$ —0.2 V— $Mn(OH)_2$

1.2.1.1 Oxidation

In situ oxidation of Mn(II) complexes by $XMnO_4$ ($X= K^+$, $(N^nBu_4)^+$)[20] is the common procedure for the preparation of manganese(III) complexes. Other reagents like Ce(IV) and O_2 have also been used as oxidizing agents[21]. In many cases manganese(III) acetate, which was prepared from manganese(II) acetate by $KMnO_4$ oxidation have been used as starting material[22]. In addition, a clever selection of ligand and reaction media is important in the synthetic procedure[23].

Some of the important strategies for the synthesis of various manganese complexes are given below.

1.2.1.2 Self assembly

For polynuclear complexes two successful methodologies have emerged: the first is based on "serendipitous self-assembly", whereby suitable flexible bridging ligands (e.g., carboxylates) are mixed with simple metal salts or premade polymetallic compounds in a particular solvent[24] or mixture of solvents, and the second is the "rational design" of molecules, whereby inflexible ligands (e.g., cyanide) direct the formation of complexes whose overall formulas and topology can, in many cases, be wholly or partly predicted, suggesting a more "customized preparation of SMMs[25].

1.2.1.3 Microwave

Microwave heating is an increasingly common tool in chemical synthesis, and the advantages and convenience of microwave dielectric heating are now well documented.[26,27]. Despite the range of applications and advantages of this heating method, reactions involving liquid-phase inorganic syntheses have not yet received great attention. George Christou et al have been used[28] microwave as synthetic tool for the preparation of Mn(III) single molecular magnet.

1.2.1.4 Reductive method.

Reductive method is the process in which high oxidation state mononuclear permanganate (MnO_4^-) ion is reduced by MeOH in the presence of excess of carboxylic acid. There have been few complexes[29-31] reported by this method.

1.2.2 Mononuclear manganese(III) complexes

Coordination chemistry of manganese has gained much attention for the replication of the biological systems. However the growth of manganese(III) chemistry is slow due to the fact that Mn(III) is prone to disproportionation, particularly in aqueous solution into manganese(IV) and manganese(II). Manganese (III) has d^4 electronic configuration and thus its octahedral complexes are Jahn-Teller active. In ions possessing more than one unpaired electron, the interaction of the individual magnetic moments with the local fields of the other electrons leads to a removal of degeneracy of the spin levels even without an external magnetic field. Therefore this interaction is called zero-field interaction or zero-field splitting (ZFS). ZFS can be axial or rhombic. The axial zero field splitting remove the degeneracy of the ground state spin multiplet yielding a spin ground state that is doublet for the negative ZFS. Applied magnetic field will remove the degeneracy of the ground state, the transitions which involves M_S = 0↔±1, ±1↔±2, etc. are EPR allowed, but if zfs is larger than the microwave quantum (at X band and Q band) then there is either not enough energy to achieve resonance or the resonance would appear at magnetic field far exceeding those available on standard EPR spectrometer. This makes it difficult to retrieve reliable information from conventional 9 GHz EPR spectrum. In contrast when microwave excitation frequency and field are very high we can get the characteristic electronic structures of such integral spin ions. In fact Jahn-Teller distortion and the absence of an EPR signal in the X-band frequency often serve to identify manganese(III) centers in complexes with mixed valence state.

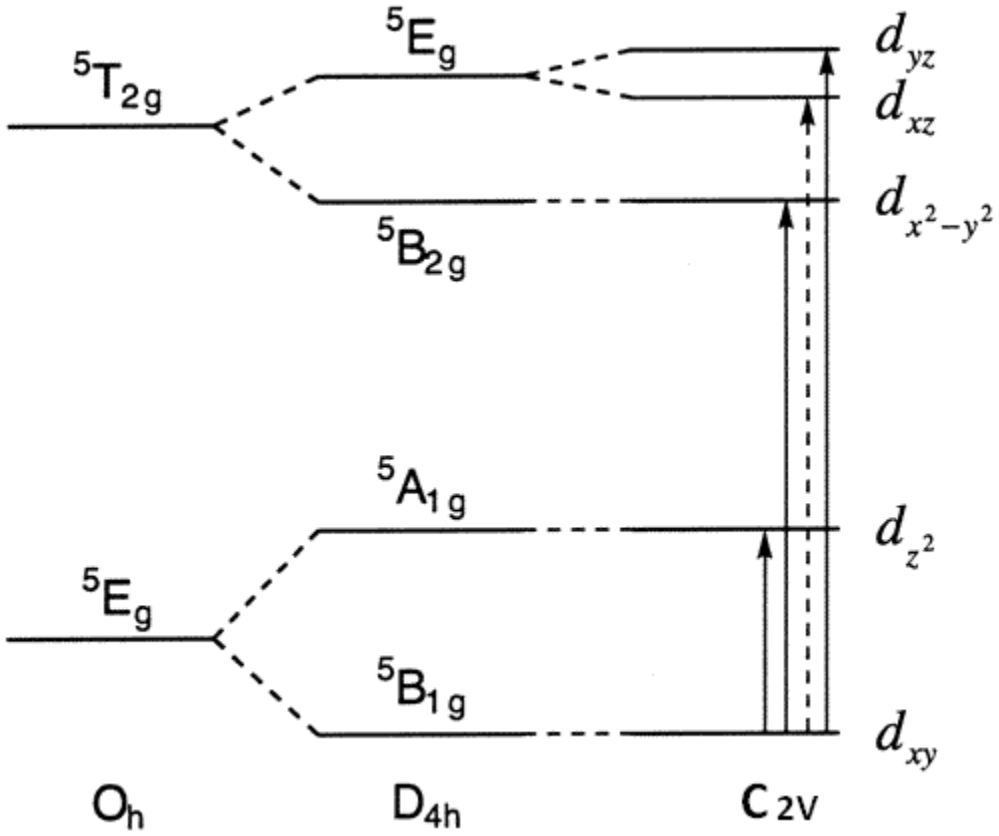

Figure 1.5 Splitting of the spectroscopic terms when lowering the symmetry from O_h to C_{2V} with the elongation axis perpendicular to the C_2 rotation axis. The solid and dashed arrows show the allowed and forbidden *d-d* transitions, respectively[35].

Mononuclear manganese complexes are rare especially with diimine ligands like bpy and phen[32-34] since in aqueous solution it readily undergo disproportionation into Mn(IV) and Mn(II). Detailed assignments of the optical transitions (Figure. 1.5) based on polarized absorption studies have been made in $Mn(bpy)F_3(H_2O)$[34]. Later DFT calculations on $[(Py_2(NMe)_2)MnF_2](PF_6)$[35] supported the above assignments. In order to isolate carboxylate mononuclear complex, carboxylate

has to be at least bidentate. Some of the mononuclear complexes reported are with citric acid and β-diketone and related ligands[33,36]. The chemistry of manganese(III) with monodentate carboxylates, such as acetate and benzoate or their derivatives, results in the formation of complexes with higher nuclearities.

1.2.3 Dinuclear manganese(III, III) complexes

Different coordination modes have been reported for Mn(III, III) dimers (Figure 1.6). Dinuclear manganese(III) complexes fall into two categories (i) those with one or two alkoxo bridge(s) (ii) those with one μ_2-O^{2-} bridge. With the exception of one complex[37a], all other complexes of the type (I) core (Figure 1.6) contain a Schiff base coligand[37b]. Type (II) categories are very rare. Only benzoate analogue was reported earlier[37c] many years ago and it was structurally characterized later[38]. There has been rigorous effort directed towards the chemistry of complexes with $[Mn_2(\mu\text{-}O)(\mu\text{-}OAc)]^{3+}$ (type III) and $Mn_2(\mu\text{-}O)(\mu\text{-}OAc)_2]^{2+}$ (type IV) cores due to their relevance to biological systems. However there are only few systems with type III core reported[39-41].

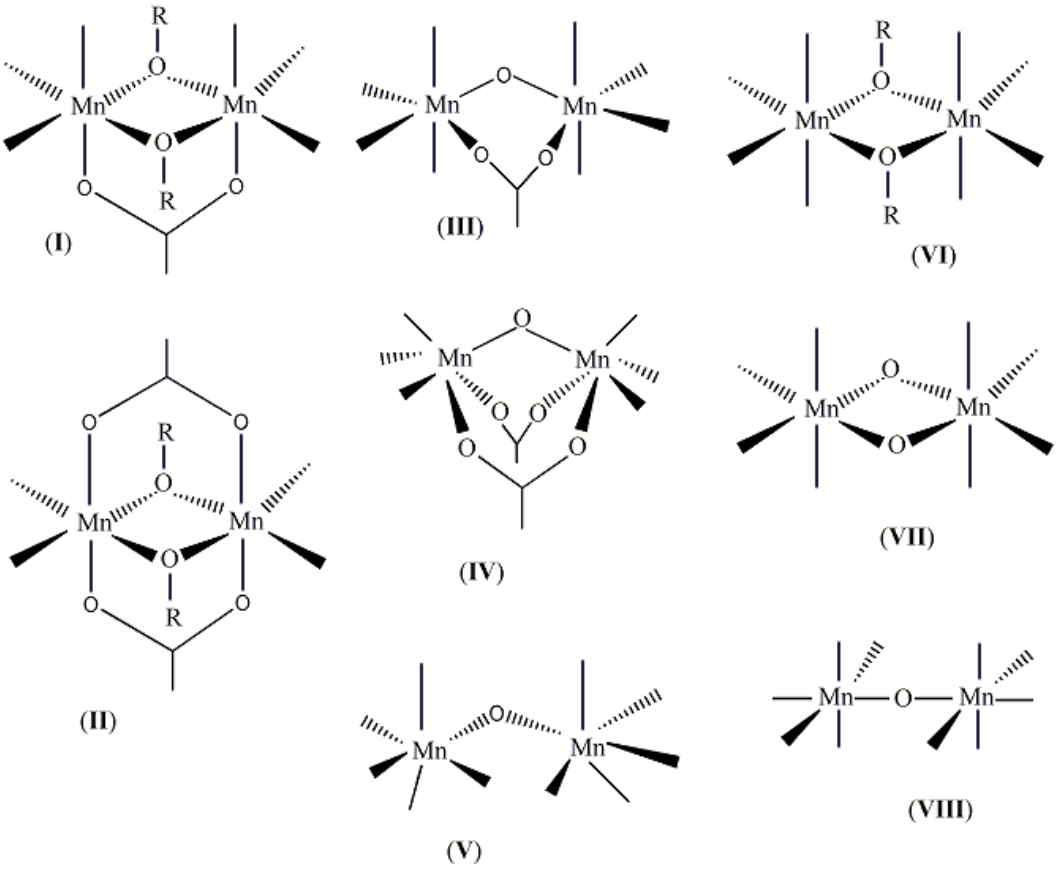

Figure 1.6. Schematic view of Mn(III) dimeric complexes.

Since 1980 a large number of complexes containing type IV core have been prepared with various bidentate, tridentate and polydentate and poly pyridyl coligands[42-63]. But only few of them are characterized by X-ray diffraction and magnetic studies[51-63]. The use of bidentate ligands leaves one coordination site free on each manganese(III) centre to be filled by easily exchangeable ligands such as water, nitrate, chloride or azide. In most of the complexes monocarboxylate such as acetate, benzoate and its derivatives have been used as bridging ligand. It is well known that the magnetic interactions for these

complexes are weak and could be antiferro- or ferro-magnetic[64]. Octahedron of the complexes can have three types of possible distortions viz (i) compression in the direction of oxo- bridge, i.e. the bond trans to oxo ligand is appreciably shortened. This shortening is expected if N_{trans}-Mn-O_{oxo} becomes Jahn-Teller axis because the Mn-O_{oxo} distance is already the shortest distance in the octahedron. (ii) Elongation in the direction of one of the blocking ligand. (iii) Rhombic distortion in which elongation along the trans-X-Mn-O(OAc) axis, where X is a monodentate ligand. This kind of distortion is found in all the previously reported complexes containing monodentate ligand (X). In general tridentate ligand favors mode(i) distortion. Tridentate amines (Me_3(N,N',N''-trimethyl-1,4,7-triazacylononae) favor a compressed octahedron[54,55]. However, tridentate amines TMIP (tris(M-methylimidazole-2-yl)phosphane) and HB-$(pz)_3$(hidrotris(1-pyrazolyl)borate) lead to a rhombic distortion [59, 60].

1.2.4 Dinuclear Manganese(II, III) complexes

Structurally characterized valence trapped Mn(II,III) complexes are few in number[65]. Most of these were prepared by the oxidation of Mn(II) complexes by O_2. Mn(II,III) structures show development of hyperfine structures at low temperature which related to the strength of the Mn…Mn magnetic coupling. High spin Mn(II) d^5 and Mn(III) d^4 have spin S_{II} = 5/2 and S_{III} = 2 respectively and their coupling results in spin sates 1/2, 3/2, 5/2, 7/2 and 9/2. At 4 K population of ground state (S = ½) predominates and complexes give 16 line EPR spectra[66] (Figure 1.7).

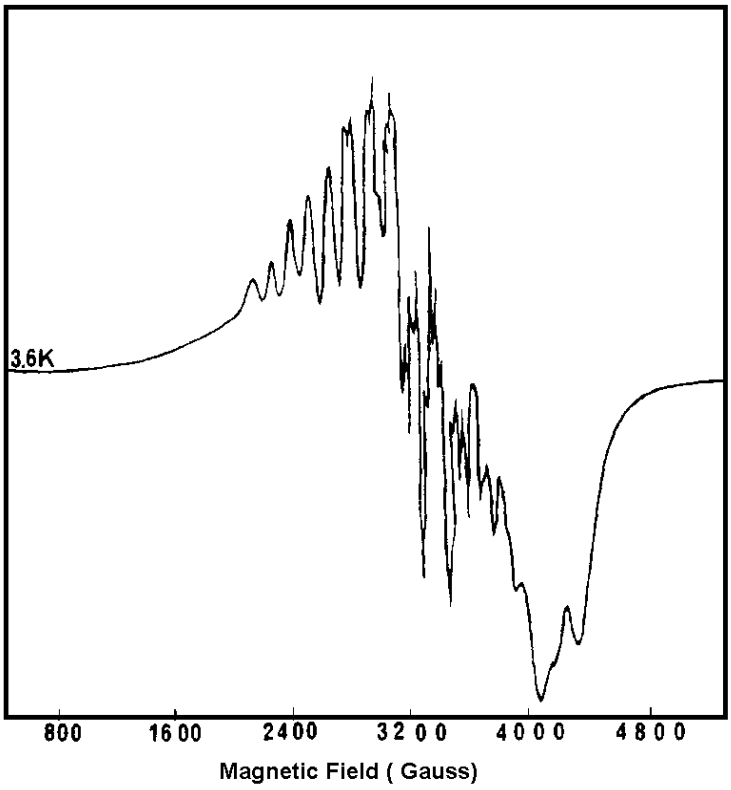

Figure 1.7. X-band EPR spectra of complex [Mn2(L-Im)(μ-OAc)2]$(ClO_4)_2$[66]

The complexes $[Mn_2LCl_2Br].H_2O$ and $[Mn_2LBr_3]0.5CH_2Cl_2$ have been reported[65k], where LH_2 is the macrocyclic ligand formed by condensation product of 1,3-diaminopropane and 2,6-dimethyl-4-t-butylphenol. The X-ray structure of the complexes shows the bound macrocycle to be essential planar; however each manganese(II) ion is displaced 0.69 Å for former and 1.25 Å for the later complexes on either side of the ligand plane. It was noted that relatively weak antiferromagnetic interactions are seen for such binuclear Mn(II,III) complexes,

which contrast with the strong antiferromagnetic interactions that are generally observed for the binuclear Mn(III, IV) complexes.

1.2.5 Mn3 complexes

All of the trinuclear manganese(III) carboxylate complexes have similar core structure as Manganese(III) acetate $[Mn(\mu_3\text{-}O)(\mu\text{-carboxylato})_6]^+$. Even though one electron reduced species Mn(II,III,III) have many reports[67], $[Mn(\mu_3\text{-}O)(\mu\text{-carboxylato})_6]^+$ core has limited number of reports[68]. $[Mn_3O_4]^{4+}$ complexes of α-diimine ligands, which have important features common to oxygen evolving complex (OEC) of PSII[69-71]: Very few structures have been reported earlier[72]. Oxo-bridged Mn ions in higher oxidation state, two sets of Mn…Mn contacts ca 2.7 Å and 3.3 Å and two fully protonated water molecule coordinated to two manganese centers. Total spin of the $[Mn_3O_4(bpy)_4(OH_2)_2]^{4+}$ unit is ½ which was determined by using EPR spectroscopy[72a]. There was an attempt to predict the relative stability of the states of different spin multiplicity in the Mn trimer $[Mn_3O_4(bpy)_4(OH_2)_2]^{4+}$ by using hybrid B3LYP functionals[73]. However, the DFT/B3LYP methodology does not correctly predict the relative stabilization of lowest spin states.

1.2.6 Mn4 complexes

Tetranuclear manganese carboxylate complexes have three different configurations for their metal centers: fused open cubane[74] planar[75] or butterfly[76] (Figure 1.8). The difference between the planar tetranuclear complexes with a $[Mn_4O_2(OAC)_6]^{2+}$ core and the butterfly tetranuclear complexes with a $[Mn_4O_2(OAC)_7]^+$ core is due to the seventh bridging carboxylate in the latter. In $[Mn_4O_2(OAC)_6]^{2+}$ complexes, coordination sites of inner or outer manganese

atom can often be vacant or occupied by monodentate ligands. In case of monodentate ligand (L) bound to two inner manganese atoms, there are two possible stereochemical configurations, *cis* and *trans* for the $Mn_4O_2L_2$ centre (Figure 1.9).

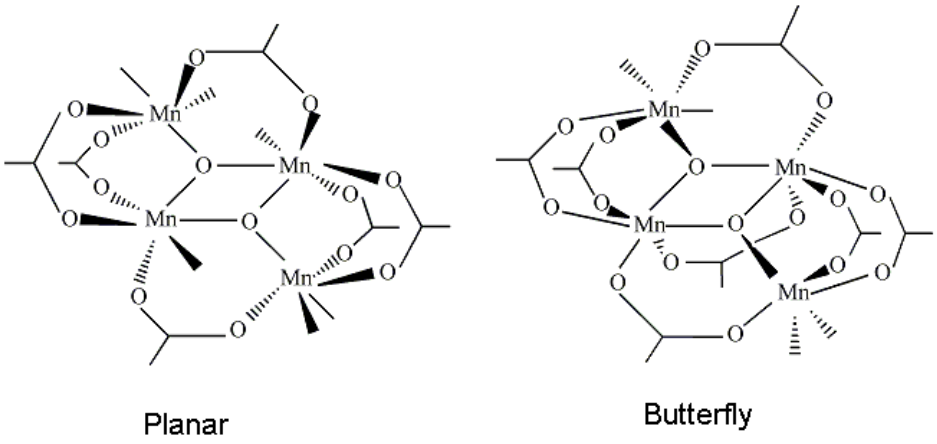

Figure 1.8 Planar and butterfly core types of Mn_4O_2 complexes

Generally *cis* configuration is consistent with non-planar $Mn_4O_2L_2$ centre and *trans* configuration is consistent with the planar $Mn_4O_2L_2$ centre.

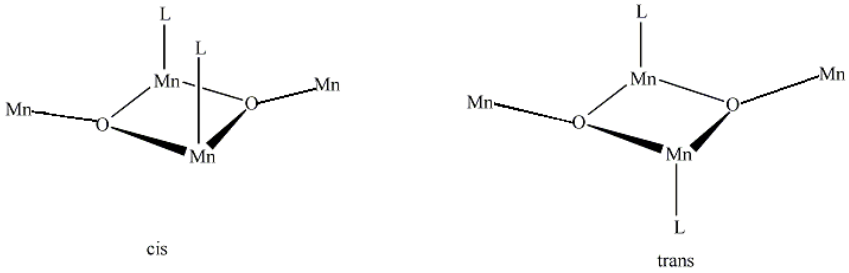

Figure 1.9 *Cis* and *trans* configuration of $Mn_4O_2L_2$ centre

1.3 References

[1] Ferreira, K. N.; Iverson, T. M.; Maghlaoui, K.; Barber, J.; Iwata, S. *Science* **2004**, *303*, 1831.

[2] Olesen, K.; Andréasson L. E. *Biochemistry* **2003,** *42,* 2025.

[3] Loll, B.; Kern, J.; Saenger, W.; Zouni, A.; Biesadka, J. *Nature* **2005**, 438.

[4] (a) Halliwell, B.; Gutteridge, J. M. C. *Academic Press*, San Diego. **1990.** (b) Stadtman, E. R.; Berlett, P.; and Chock, P. B. *Proc. Natl. Acad. Sci. U.S.A.* **1990**, *87*, 384.

[5] (a) Barynin, V. V.; Hempstead, P. D.; Vagin, A. A.; Antonyuk, S. V.; Melik-Adamyan, W. R.; Lamzin, V. S.; Harrison, P. M.; Artymiuk, P. J. *J. Inorg. Biochem.* **1997**, *67*, 196. (b) Antonyuk, S. V.; Melik-Adamyan, W. R.; Popov, A. N.; Lamzin, V. S.; Hempstead, P. D.; Harrison, P. M.; Artymiuk, P. J.; Barynin, V. V. *Crystallogr. Rep.* **2000**, *45*, 105. (c) Barynin, V. V.; Whittaker, M. M.; Antonyuk, S. V.; Lamzin, V. S.; Harrison, P. M.; Artymiuk, P. J.; Whittaker, J. W. *Structure* **2001**, *9*, 725.

[6] Antonyuk, S. V., Melik-Adamyan, V. R.; Lamzin, A. N. P. V. S., Hempstead, P. D.; Harrison, P. M.; Artymyuk, P. J.; and Barynin, V. V. *Crystallography Reports* **2000**, *45*, 111.

[7] Barynin, V. V.; Whittaker, M. M.; and Antonyuk, S. V. *Structure* **2001**, *9(8)*, 725.

[8] Khangulov, S. V.; Barynin, V. V.; Melik-Adamyan, V. R.; Grebenko, A. I., Voevodskay, N. V., Dobrykov, S. N., Iĺysova, V. N. *Bioorgan. Khim.* **1986**, *12*, 741.

[9] Khangulov, S. V., Barynin, V. V., Voevodskaya, N. V., Grebenko, A. I. *Biochim. Biophys. Acta* **1990**, *1020*, 305.

[10] Fronko, R. M.; Penner-Hahn, J. E.; Bender, C. J. *J. Am. Chem. Soc.* **1988**, *110*, 7554.

[11] Meier, A. E.; Whittaker, M. M.; Whittaker, J. W. *Biochemistry* **1996**, *35*, 348.

[12] Jackson, T. A.; Karapetian, A.; Anne-Frances Miller, A.-F,; Brunold, T. C *Biochemistry* **2005**, *44*. 1504.

[13] Miller, A.-F.; Padmakumar, F.; Sorkin, D.; Karapetian, A.; and Vance, C. K. *J. Inorg. Biochem.* **2003**, *93*, 71-83.

[14] Han, W.-G.; Lovell, T.; Noodleman, L. *Inorg. Chem.* **2002**, *41*, 205.

[15] Lah, M. S.; Dixon, M. M.; Pattridge, K. A.; Stallings, W. C.; Fee, J. A.; Ludwig, M.L. *Biochemistry* **1995**, *34*, 1646.

[16] Ludwig, M. L.; Metzger, A. L.; Pattridge, K. A.; Stallings, W.C. *J. Mol. Biol.* **1991**, *219*, 335.

[17] Spina, G.; Del Giallo, F.; Pieralli, F. *J. Am. Chem. Soc.* **1995**, *117*, 2491. (b) Gatteschi, D.; Sessoli, R.; Cornia, A. *Chem. Commun.* **2000**, 725. (c) Oshio, H.; Hoshino, N.; Ito, T. *J. Am. Chem. Soc.* **2000**, *122*, 12602. (d) Cadiou, C.; Murrie, M.; Paulsen, C.; Villar, V.; Wernsdorfer,W.; Winpenny, R. E. P. *Chem. Commun.* **2001**, 2666. (e) Ochsenbein, S. T.; Murrie, M.; Rusanov, E.; Stoeckli-Evans, H.; Sekine, C.; Gu¨del, H. U. *Inorg. Chem.* **2002**, *41*, 4604. (f) Sokol, J. J.; Hee, A. G.; Long, J. R. *J. Am. Chem. Soc.* **2002**, *124*, 7656. (g) Boudalis, A. K.; Donnadieu, B.; Nastopoulos, V.; Clemente-Juan, J. M.; Mari, A.; Sanakis, Y.; Tuchagues,

J. P.; Perlepes, S. P. *Angew. Chem., Int. Ed*. **2004**, *43*, 2266. (h) Osa, S.; Kido, T.; Matsumoto, N.; Re, N.; Pochaba, A.; Mrozinski, J. *J. Am. Chem. Soc.* **2004**, *126*, 420. (i) Berlinguette, C. P.; Vaughn, D.; Canada-Vilalta, C.; Galan- Mascaras, J. R.; Dunbar, K. R. *Angew. Chem., Int. Ed.* **2003**, *42*, 1523. (j) Andres, H.; Basler, R.; Blake, A. J.; Cadiou, C.; Chaboussant, G.; Grant, C. M.; Gudel, H.-U.; Murrie, M.; Parsons, S.; Paulsen, C.; Semadini, F.; Villar, V.; Wernsdorfer, W.; Winpenny, R. E. P. *Chem. Eur. J*. **2002**, *8*, 4867. (k) Dendrinou-Samara, C.; Alexiou, M.; Zaleski, C. M.; Kampf, J. W.; Kirk, M. L.; Kessissoglou, D. P.; Pecoraro, V. L. *Angew. Chem., Int. Ed.* **2003**, *42*, 3763.

[18] (a) Christou, G., Gatteschi, D., Hendrickson, D.N., Sessoli, R. *MRS Bulletin*, **2000**, *25*, 66. (b) Chistou, G. *Polyhedron* **2005**, *24*, 2065. (c) Milios, C. J.; Vinslava, A.; Wernsdorfer, W.; Moggach, S.; Parsons, S.; Perlepes, S. P.; Christou, G.; Brechin, E. K. *J. Am. Chem. Soc.* **2007**, *129*, 2754. (d) Milios, C. J.; Vinslava, A.; Wernsdorfer, W.; Prescimone, A..; Wood, P. A.; Parsons, S.; Perlepes, S. P..; Christou, G.; Brechin, E. K. *J. Am. Chem. Soc.* **2007**, *129*, 6547; (e) Milios, C. J.; Inglis, R.; Vinslava, A.; Bagai, R.; Wernsdorfer, W.; Parsons, S.; Perlepes, S. P.; Christou, G.; Brechin, E. K. *J. Am. Chem. Soc.* **2007**, *129*, 12505. (*f*) Brechin, E.K., Milios, C.J., Piligkos, S. *Dalton Trans*. **2008**, 1809. (*g*) Mishra, A.; Pushkar, Y.; Yano, J.; Yachandra, V. K.; Wernsdorfer, W.; Abboud, K. A.; Christou, G. *Inorg. Chem.* **2008**, *47* ,1940. (*h*) Barra, A.-L., Caneschi, A., Cornia, A., Gatteschi, D., Gorini, L., Heiniger, L.-P., Sessoli, R., Sorace, L. *J. Am. Chem. Soc.*, **2007**, *129*,10754. (*i*) Stamatatos, T.C.,

Foguet-Albiol, D., Lee, S.-C., Stoumpos, C.C., Raptopoulou, C.P., Terzis, A., Wernsdorfer, W., Hill, S.O., Perlepes, S.P., Christou. G. *J. Am. Chem. Soc.* **2007**, *129*, 9484. (*j*) Saalfrank, R.W., Scheurer, A., Prakash, R., Heinemann, F.W., Nakajima, T., Hampel, F., Leppin, R., Pilawa, B., Rupp, H., Muller, P. *Inorg. Chem.* **2007**, *46*, 1586. (*k*) Milios, C.J., Vinslava, A., Wood, P.A., Parsons, S., Wernsdorfer, W., Christou, G., Perlepes, S.P., Brechin, E. K. *J. Am. Chem. Soc.* **2007**, *129*, 8.

[19] Cotton, F. A; Wilkinson, G. *Advanced Inorganic Chemistry,* 5 ed; Wiley – Interscience; **1988**, 846.

[20] Baca, S. G.; Stoeckli-Evans, H.; Ambrus, C.; Malinovskii, S. T.; Malaestean, L.; Gerbeleu, N.; Decurtins, S. *Polyhedron* **2006**, 25, 3617. (b) Cañada-Vilalta, C.; Huffman, J. C.; Streib, W. E.; Davidson, E. R.; Christou, G. *Polyhedron* **2001**, 20, 1375. (c) Ribas, J.; Albela, B.; Stoeckli-Evans, H. Christou, G. *Inorg. Chem*. **1997**, 36, 2352. (d) An, J.; Chen, Z.-D, Bian, J.; Jin, X.-L,Wang, S.-X. Xu. *Inorg. Chim. Acta* **1999**, 287, 82.

[21] McCrea, J.; McKee, V.; Metcalfe, T.; Tandon, S. S.; Wikaira, J. *Inorg. Chim. Acta* **2000**, *297*, 220 (b) Yang, C.-I.; Lee, G.-H.; Wur, C.-S.; Lin, J. G.; Tsai, H.-L. *Polyhedron* **2005**, *24*, 2215. (c) Boskovic, C.; Bircher, R.; Philip L. W.; Tregenna-Piggott, Güdel, H. U.; Paulsen, C.; Wernsdorfer, W. Barra, A.-L.; Khatsko, E.; Neels, A.; Stoeckli-Evans, H. *J. Am. Chem.* soc. **2003**, *125*, 14046. (d) Yang, C.-I.; Wernsdorfer, W .; Cheng, K.-H.; Nakano, M.; Lee,

G.-H.; Tsai, H.-L. *Inorg. Chem*. **2008**, *47*. 10184. (e) Mitra, K.; Mishra, D.; Biswas, S.; Lucas, C. R.; Adhikary, B. Polyheron 2006, 25, 1681.

[22] Bashkin, J. S.; Chang, H.-R.; Streib, W. E.; Huffman, J. C.; Hendrickson, D. N. Christou, G. *J. Am. Chem. Soc.* **1987,** *109,* 6502. (b)Weighardt, K.; Bossek, K. U.; Nuber, B.; Weiss, J.; Bonvoisin, J.; Corbella, M.; Vitols, S. E.; Girerd, J. J. *J. Am. Chem. Soc*. **1988**, *110*, 7398. (c) Pal, S.; Chan, M. K.; Armstrong, W. H.; *J. Am. Chem. Soc*. **1992**, *114*, 6398. (d) Hendrickson, D. N.; Christou, G.; Schmitt, E. A.; Libby, E.; Bashkin, J. S.; Wang, S.; Tsai, H.-L.; Vincent, J. B.; Boyd, P. D. W.; Huffman, J. C.; Folting, K.; Li, Q.; Streib, W. E. *J. Am. Chem. Soc.* **1992**, *114*, 2455. (e) Chandra, S. K.; Chakravorty, A. *Inorg. Chem*. **1992**, *31*, 760. (f) Larson, E.; lah, M. S.; Li. X.; Bonadies, J. A.; Pecorado, V. L. *Inorg. Chem*. **1992**, *31*, 373.

[23] Roubeau, O.; Clérac, R. *Eur. J. Inorg. Chem*. **2008**, 4325.

[24] (a) Winpenny, R. E. P. *Dalton Trans.* **2002**, 1. (b) Christou, G. *Polyhderon* **2005**, *24*, 2065. (c) Aromí, G.; Brechin, E. K. *Struct. Bonding* **2006**, *122*, 1.

[25] (a) Rebilly, J.-N.; Mallah, T. *Struct. Bonding* **2006**, *122*, 103. (b) Beltran, L. M. C.; Long, J. R. *Acc. Chem. Res*. **2005**, *38*, 325. (c) Parker, R. J.; Spiccia, L.; Berry, K. J.; Fallon, G. D.; Moubaraki, B.; Murray, K. S. *Chem. Commun*. **2001**, 333. (d) Marvaud, V.; Decroix,C.; Scuiller, A.;

Guyard-Duhayon, C.; Vaissermann, J.; Gonnet, F.; Verdaguer, M. *Chem. Eur. J.* **2003**, *9*, 1677. (e) Marvaud, V.; Decroix, C.; Scuiller, A.; Tuyeras, F.; Guyard-Duhayon, C.; Vaissermann,J.; Marrot, M.; Gonnet, F.; Verdaguer, M. *Chem. Eur. J.* **2003**, *9*, 1692.

[26] Whittaker, A. G.; Mingos, D. M. P. *J. Microwave Power Electromagn. Energy* **1994**, *29*, 195.

[27] Mingos, D. *Res. Chem. Intermed.* **1994**, *20*, 85.

[28] Milios, C. J.; Vinslava, A.; Whittaker, A. G.; Parsons, S.; Wernsdorfer, W.; Christou, G.; Perlepes, S. P.;| Brechin, E. K. *Inorg. Chem*. **2006**, *45*, 5272.

[29] King, P.; Wernsdorfer, W.; Abboud, K. A.; Christou, G. *Inorg. Chem.* **2004**, *43*, 7315.

[30] Tasiopoulos, A. J.; Wernsdorfer, W.; Abboud, K. A.; Christou, G. *Inorg. Chem.* **2005**, *44*, 6324.

[31] King, P.; Wernsdorfer, W.; Abboud, K. A.; Christou, G. *Inorg. Chem.* **2005**, *44*, 8659.

[32] Reddy, K. R.; Rajasekharan, M.V. *Polyhedron* **1994**, *13*, 765.

[33] Swarnabala, G; Reddy, K. R.; Tirunagar, J.; Rajasekharan, M.V. *Transition Met. Chem*. **1994**, *19*, 506.

[34] Nunez, P.; Elias, C.; Fuentes, J.; Solans, X.; Tressaud, A.; de Lucas, M.C.M.; Rodriguez, F. *J. Chem. Soc., Dalton Trans*. **1997**, 4335.

[35] Albela, B.; Carina, R.; Policar, C.; Poussereau, S.; Cano, J.; Guilhem, J.; Tchertanov, L.; Blondin, G.; Delroisse, M.; Girerd, J.-J. *Inorg. Chem.* **2005**, *44*, 6959.

[36] (a) Matzapetakis, M.; Karligiano, N.; Bino, A.; Dakanali, M.; Raptopoulou, C. P.; Tnagoulis, V.; Terzis, A.; Giapintzakis, J.; Salifoglou, A. *Inorg. Chem*. **2000**, *39*. 4044. (b) Bouwman, E.; Caulton, K. G.; Christou, G.; Folting, K.; Gasser, C.; Hendrickson, D. N.; Huffman, J. C.; Lobkovsky, E. B.; Martin, J. D. *Inorg. Chem*. **1993**, *32*, 3463. (c) Weighardt, K.; Pohl, K.; Bossek, U.; Nuber, B.; Weiss, J. *Z. Naturforsch. B*, **1998**, *43*, 1184. (d) Barra, A-L.; Gatteschi, D.; Sessoli, R.; abbati, G. L.; Cornia, A.; Fabretti, a. C.; Uytterhoeven, M. G.; *Angew. Chem.; Int. Ed.* **1997**, *36*, 2329. (e) Yamaguchi, K. S.; Sawyer, D. T. *Inorg. Chem*. **1985**, *24*, 971.

[37] (a) Saadeh, S. M.; Lah, M. S.; Pecoraro, V. L. *Inorg. Chem.* **1991**, *30*. 8. (b) Weatherburn, D. C; Mandal, s.; Mukhopadhyay, S.; Bhaduri, S.; Lindoy, L. F. Manganese. *In Comprehensive Coordination Chemistry* **2003**, *5*, 1. (c) Chiswell, B.; McKenzie, E. D.; Linoy, L. F. Manganese. *In Comprehensive Coordination Chemistry*: Wilkinson, G.; Gillard, R. D., McCleverty, J. A. Eds. Pergamon, Oxford, **1987**.

[38] Zhang, C. G.; Janiak, C. *Acta Cryst.*. **2001**, *C57*, 719.

[39] Oberhausen, K. J.; O' Brien, R. L.; Richardson, J. f.; Buchana, R. M.; Costa, R.; Latour, J. M.; Tsai, H. L.; Hendrickson, D. N. *Inorg. Chem.* **1993**, *32*, 5461.

[40] Arulsamy, N.; Glerup, J.; Hazell, A.; Hodgson, D. J.; McKenzie, C. J.; Toftlund, H. *Inorg. Chem*. **1994**, *33*, 3023.

[41] Triller, M. U.; Hsich, W. Y.; Pecoraro, V. L.; Rompel, A.; Krebs, B. *Inorg. Chem*. **2002**, *41*, 5544.

[42] Dave, B. C.; Czernuszewickz, R. S. *Inorg. Chim. Acta*. **1998**, *281*, 25.

[43] Ruiz, R.; Sangregorio, C.; Caneschi, A.; Rossi, P.; Gaspar, A. B.; Real, J. A.; Muňoz, M. C. *Inorg. Chem. Commun*. **2000**, *3*, 361.

[44] Reddy, K. R.; Rajasekharan, M. V.; Sukumar, S. *Polyhedron* **1996**, *15*, 4161.

[45] Albela, B.; Corbella, M.; Ribas, J. *Polyhedron* **1996**, *15*, 91.

[46] Corbella, M.; Costa, R.; Ribas, j. Fries, P. H.; Latour, J. M.; Ohstrom, L. Solans, X.; Rodríguez, V. *Inorg. Chem*. **1996**, *35*, 1857.

[47] Romakh, V. B.; Therrien, B.; Karmazin-Brelot, L.; Labat, G.; Stoeckli-Evans, H.; Shuĺpin, G. B.; Süss-Fink, G. *Inorg. Chim. Acta* **2006**, *359*, 1619.

[48] de Boer, J. W.; Brinksma, Browne, W. R.; Meetsma, A.; Alsters, P. L.; R.; Hoge, R.; Feringa, B. L. *J. Am. Chem. Soc*. **2005**, *125*, 7990.

[49] Bolm, C.; Meyer, N.; Raabe, G.; Weyhermüller, T.; Bothe, E. *Chem. Commun*. **2000**, 2435.

[50] Caňada-Vilalta, C.; Streib, W. E.; Huffman, J. C.; O'Brien, T. A.; Davidson, E. R.; Christou, G. *Inorg. Chem.* **2004**, *43*, 101.

[51] Caňada-Vilalta, C.; Huffman, J. C.; Streib, W. E.; Davidson, E. R., Christou, G. *Polyhedron* **2001**, *20*, 1375.

[52] Ménage, S.; Girerd, J.-J.; Gleizes, A. *J. Chem. Soc., Chem. Commun.*

1988, 431.

[53] Corbella, M.; Costa, R.; Ribas, J.; Fries, P. H.; Latour, J. M.; Ohrstrom, L.; Solans, X.; Rodríguez, V. *Inorg. Chem.* **1996**, *35*, 1857.

[54] Wieghardt, K.; Bossek, U.; Ventur, D.; Weiss, J. *J. Chem. Soc., Chem. Commun.* **1985**, 347.

[55] Wieghardt, K.; Bossek, U.; Nuber,B.; Weiss, J.; Bonvoisin, J.; Corbella, M.; Vitols, S. E.; Girerd, J. J. *J. Am. Chem. Soc.* **1988**, *110*, 7398.

[56] Bolm, C.; Meyer, N.; Raabe, G.; Weyhermüller, T.; Bothe, E. *Chem. Commun.* **2000**, 2435.

[57] Vincent, J. B.; Folting, K.; Huffman, C. J.; Christou, G. *Biochem. Soc. Trans.* **1988**, *16*, 2.

[58] Vincent, J. B.; Tsai, H. L.; Blackman, A. G.; Wang, S.; Boyd, P. D.; Folting, K.; Huffman, J. C.; Lobkovsky, E. B.; Hendrickson, D. N.; Christou, G. *J. Am. Chem. Soc.* **1993**, *115*, 12353.

[59] Sheats, J. E.; Czernuszewicz, R. S.; Dismukes, G. C.; Rheingold, A. L.; Petrouleas, V.; Stubbe, J. A.; Armstrong, W. H.; Beer, R. H.; Lippard, S. J. *J. Am. Chem. Soc.* **1987**, *109*, 1435.

[60] Wu, F. J.; Kurtz, D. M., Jr.; Hagen, K. S.; Nyman, P. D.; Debrunner, P. G.; Vankai, V. A. *Inorg. Chem.* **1990**, *29*, 5174.

[61] Mitra, K.; Mishra, D.; Biswas, S.; Lucas, C. R.; Adhikary, B. *Polyhedron* **2006**, *25*, 1681.

[62] Fernández, G.; Corbella, M.; Alfonso, M.; Stoeckli-Evans, H.; Castro, I. *Inorg. Chem.* **2004**, *43*, 6684.

[63] Fernández, G.; Corbella, C.; Aullón, G.; Maestro, M. A.; Mahía, J. *Eur. J. Inorg. Chem*. **2007**, 1285.

[64] Hotzelmann, K.; Wieghardt, K.; Flörke, U.; Haupt, H, -J.; Weatherburn, D. C.; Bonvoisin, J.; Blondin, G. Girerd, J. –J. *J. Am. Chem. Soc*. **1992**, *114*, 1681.

[65] (a) Dubois, L.; Xiang, D.-F.; Tan, S.-S.; Pecaut, J.; Jones, P.; Baudron, S.; Le Pape, L.; Latour, J.-M.; Baffer, C.; Chardon-Noblat, S.; Collomb, M.-N.; Deronzier, A. *Inorg. Chem*. **2003**, *42*, 750. (b) Suzuki, M.; Mikuriya, M.; Murata, S.; Uehara, A.; Oshio, H.; Kida, S.; Saito, K. *Bull. Chem. Soc. Jpn.* **1987**, *60*, 4305. (c) Karsten, P.; Neves, A.; Bortoluzzi, A.; Strhle, J.; Maichle-Mossmer, C. *Inorg. Chem. Commun.* **2002**, *5*, 434. (d) Mikuriya, M.; Fujii, T.; Tokii, T.; Kawamori, A. *Bull. Chem. Soc. Jpn.* **1993**, *66*, 1675. (e) Huang, P.; Shaikh, N.; Anderlund, M. F.; Styring, S.; Hammarström, L. *J. Inorg. Biochem*. **2006**, *100*, 1139. (f) Jensen, K. B.; Johansen, E.; Larsen, F. B.; McKenzie, C. J. *Inorg. Chem*. **2004**, *43*, 3801. (g) Darovsky, A.; Kezerashvili, V.; Coppens, P.; Weyhermüller, T.;H. Hummel, H.; Wieghardt, H. *Inorg. Chem.* **1996**, *35,* 6916 (h) Chang, H.R.; Drill, H.; Nilges, M. J.; Zhang, X.; Potenza, J. A.; Schugar, H. J.; Hendrickson, D. N.; Isied, S. S. *J. Am. Chem. Soc.* **1988**, *110*, 625. (i) Boisen, A; Hazell, A.; McKenzie, C. J. *Chem. Commun.* **2001**, 2136. (j) Gou, S.; Zeng, Q.; Yu, Z.; Qian, M.; Zhu, J.; Duan, C.; You, X. *Inorg. Chim. Acta* **2000**, 303, 175. (k) Chang, H. R.; Larsen, S. K.; Boyd, P. D. W.; Pierpont, C .G.; Hendrickson, D. N. *J. Am. Chem. Soc*. **1988**, *110*, 4565. (l) Drill, H.; Chang, H. R.; Zhang, X.; Larsen, S. K.; Potenza, J. A.;

Pierpont, C. G.; Schugar, H. J.; Isied, S. S.; Hendrickson, D. N. *J. Am. Chem. Soc.* **1987**, 109, 6207.

[66] Buchanan, R. M.; Oberhausen, K. J.; Richardson, J. F. *Inorg. Chem.* **1988**, *27*, 971.

[67] (a) Baikie, A. R. E.; Hursthouse, M. B.; New, L.; Thornton, P.; White, R. G. *Chem. Commun.* **1980**, 684. (b) Yan, B. *Chem. Papers ,* **2003**, *57,* 102.(c) Canada-Vilalta, C.; Streib, W. E.; Huffman, J. C.; O'Brien, T. A.; Davidson, E. R.; Christou. G. *Inorg. Chem.* **2004**, *43*, 101. (d) An, J.; Chen, Z.-D.; Bian, J.; Jin, X.-L.; Wang, S.-X.; Xu, G.-X. *Inorg. Chim. Acta* **1999**, *287*, 82. (e) Vincent, J. B.; Chang, H.-R.; Folting, K.; Huffman, J. C.; Christou, G.; Hendrickson, D. N. *J. Am. Chem. Soc.* **1987**, *109,* 5703. (f) Zhao, H.; Berlinguette, C. P.; Basca, J.; Tichy, S. E.; Dunbar, K. R.; *J. Cluster Sci.* **2003***, 14,* 235. (g) Kim, J.; Cho, H. *Inorg. Chem. Commun.* **2004**, *7*, 122. (h) Lis, T.; Kinzhybalo, V.; Zieba, K. *Acta Crystallogr.* **2005**, *E61,* m2382. (i) An, J.; Wang, S.; Yan, B.; Chen, Z. *J. Coord. Chem.* **2002**, *55,* 1223. (j) Gomez-Segura, J.; Lhotel, E.; Paulsen, C.; Luneau, D.; Wurst, K.; Veciana, J.; Ruiz-Molina, D.; Gerbier, P. *New J. Chem.* **2005***, 29*, 499. (i) Baikie, A. R. E.; Hursthouse, M. B.; New, D. B.; Thornton, P. *Chem. Commun.* **1978***,* 62. (j) Parsons, S.; Murrie, M.; Teat, S.; Winpenny, R. Wood, P. *Private Communication*, **2004**. (k) Ribas, J. Albela, B. Stoeckli-Evans, H.; Christou, G. *Inorg. Chem.* **1997**, *36*, 2352. (l) Li, J.; Zhang, F.; Shi, Q.; Wang, J.; Wang, Y.; Zhou, Z. *Inorg. Chem. Commun.* **2002**, *5,* 51. (m) Sari, M.; Poyraz, M.; Buyukgungor, O.; Cannon, R. D. *Acta Crystallogr.* **2006**, *E62,* m3439. (n) Kim, J.; Lim, J.

M.; Do, Y. *Eur. J. Inorg. Chem.* **2003**, 2563. (o) Gerbeleu, N. V.; Timco, G. A.; Manole, O. S.; Struchkov, Y. T.; Batsanov, A. S.; Grebenko, S. V. *Russ. Coord. Chem.* **1994**, *20*, 357. (p) Huang, H.; Wang, T.-W.; Li, Y.-Z.; You, X.-Z. *Chin. J. Inorg. Chem.* **2002**, *18*, 797. (q) Wu, R.; Poyraz, M.; Sowrey, F. E.; Anson, C. E.; Wocadlo, S.; Powell, A. K.; Jayasooriya, U. A.; Cannon, R. D.; Nakamoto, T.; Katada, M.; Sano, H. *Inorg. Chem.* **1998**, *37*, 1913. (r) Zhang, S.-W.; Wei, Y.-G. Liu, Q.; Shao, M.-C.; Zhou, W.-S. *Polyhedron* **1996**, *15*, 1041. (s) Baca, S. G.; Stoeckli-Evans, H.; Ambrus, C.; Malinovskii, S. T.; Malaestean, I.; Gerbeleu, N.; Decurtins, S. *Polyhedron* **2006**, *25*, 3617.

[68] (a) Vincent, J. B.; Chang, H. R.; Folting, K.; Huffman, J. C.; Christou, G.; Hendrickson, D. N. *J. Am. Chem. Soc.* **1987**, *109*, 5703, and references cited therein. (b) McCusker, J. K.; Jang, H. G.; Wang, S.;Christou, G.; Hendrickson, D. N. *Inorg. Chem.* **1992**, *31*, 1874. (c) Jones, L. F.; Rajaraman, G.; Brockman, J.; Murugesu, M.; Raftery, J.; Teat, S. J.; Wernsdorfer, W.; Christou, G.; Brechin, E. K.; Collison, D. *Chem. Eur. J.* **2004**, *10*, 5180. (d) Milios, C. J.; Wood, P. A.; Parsons, S.; Foguet-Albiol, D.; Lampropoulos, C.; Christou, G.; Perlepes, S. P.; Brechin, E. K. *Inorg. Chim. Acta* **2007**, *360*, 3932.

[69] Guils, R. D.; Zimmerman, J. L.; McDerrnott, A. E. ; Yachandra, V. K.; Cole, J. L.; Dexheimer, S. L.; Britt, R. D. ; Weighardt, K.; Bossek, U. Sauer, K.; Klein, M. P. *Biochemistry* **1990**, *29*, 486.

[70] George, G. N.; Prince, R. C.; Cramer, S. P. *Science* **1989**, *243*, 789.

[71] (a) Rüettinger, W. Dismukes, G. C. *Chem. Rev.*, **1997**, *97*, 1. (b) Robblee, J. H.; Cince, R. M. .; Yachandra, V. K.; *Biochim. Biophys. Acta*, **2001**, *1503*, 7. (c) Sproviero, E. M.; Gascón, J. A.; McEvoy, J. P.; Brudvig, G. W.; Batista, V. S. *J. Inorg. Biochem.* **2005**, *100*, 780. (d) Sproviero, E. M.; Gascón, J. A. ; McEvoy, J. P.; Brudvig, G. W.; Batista, V. S. *J. Chem. Theory Comput.* **2006**, *2*, 1119.

[72] (a) Sarneski, J. E.; Thorp, H. H.; Brudvig, G. W.; Crabtree, R. H.; Schulte, G. K. *J.Am.Chem.Soc.* **1990**, *112*, 7255. (b) Auger, N. Girerd, J.-J. Corbella, M.; Gleizes, A.; Zimmermann, J.-L. *J. Am. Chem. Soc.* **1990**, *112***,** 448. (c) Reddy, K. R.; Rajasekharan, M.V.; Arulsamy, N.; Hodgson, D. J. *Inorg. Chem.* **1996**, *35***,** 2283.

[73] Sproviero, E. M.; Gascon, J. A.; McEvoy, J. P.; Brudvig, G. W.; Batista, V. S.; *J. Inorg. Biochem.* **2006**, *100*, 786.

[74] (a) Mikuria, M.; Yamato, Y.; Tokkii, T. *Bull. Chem. Soc. Jpn.* **1992**, *65*, 2624. (b) Mikuria, M.; Yamato, Y.; Tokkii, T. *Chem. Lett*. **1991**. 1429.

[75] (a) Wang, S. Y.; Wemple, M. S.; Yoo, J.; Folting, K.; Huffman, J. C.; Hendrickson, D. N.; Christou, G. *Inorg. Chem*. **2000**, *39*, 1501. (b) Aromi, G.; Bhaduri, S.; Artus, P.; Floting, K.; Christou, G. *Inor. Chem*. **2002**, *41*, 805. (c) Pistilli, J.; Beer, R. H. *Inorg. Chem. Commun*. **2002**, *5*, 206. (d) Wemple, M. W. Coggin, D. K.; Vincent, J. B.; McCusker, J. K.; Sterieb, W. E.; Huffman, J. C.; Hendrickson, D. N.; Christou, G. *J. Chem. Soc. Dalton Trans*. **1998**, 719. (e) Wang, S.; Tsai, H. L.; Folting, K.; Martin, J.

D.; J. C.; Hendrickson, D. N.; Christou, G. *J. Chem. Soc. Chem. Commun*. **1994**. 671. (f) Canada-Vilalta, C.; Huffman, J. C.; Christou, G. Polyhedron **2001**, 20, 1785. (g) Libby, E.; Folting, K.; Huffman, C. J.; Huffman, J. C.; Christou, G. *Inorg. Chem.* **1993**, *32*, 2549.

[76] (a) Vincent, J. B.; Christmas, C.; Chang, H. R.; Li, Q.; Boyd, P. D. W.; Huffman, J. C.; Hendrickson, D. N.; Christou. G. *J. Am. Chem. Soc*. **1989**, *111*, 2086. (b) Vincent, J. B.; Christmas, C.; Huffman, J. C.; Christou. G.; Chang, H. R.; Hendrickson, D. N. *J. Chem. Soc. Chem. Commun*. **1987**, 236. (c) Bouwman, E.; Bolcar, M. A.; Libby, E.; Huffman, J. C.; Folting, K.; Christou, G. *Inorg. Chem*. **1992**, *31*. 5185. (d) Libby, E.; McCusker, J. K.; Schmitt, E. A.; Folting, K; Hendrickson, D. N.; Christou, G. *Inorg. Chem*. **1991**, *30*, 3486. (e) Boskovic, C.; Folting, K; Christou, G. *Polyhedron*, **2000**, *19*, 2111. (f) Wang, S.; Huffman, J. C.; Folting, K.; Streib, W. E.; Lobokovsky, E. B.; Christou, G. *Angew. Chem*. **1991**, 103, 1681.

CHAPTER II

Mononuclear manganese(III) complexes of acetyl acetone, unexpected polymorphs.

2.1 Introduction

The crystal structure determination of $[Mn(acac)_2(H_2O)_2]\ ClO_4$ (acacH = acetylacetone)[1] provided a rare comparison of the coordination polyhedron of a Jahn-Teller active d^4 complex with the analogous, inactive d^5 complex, *viz.*, $[Mn(acac)_2(H_2O)_2]$. With a view to develop this comparison into a college chemistry experiment, we attempted the preparation of the d^4 complex cation as a more student-friendly nitrate salt. Quite unexpectedly, this resulted in four polymorphs of the monohydrate of the nitrate. The phenomenon of polymorphism[2] has generated much interest in recent times due to its importance in biological as well as commercial - to pharmaceutical science. The existence of polymorphism implies that free energy difference between different forms is small and that the kinetic factors are important during crystallization. From enthalpy point of view, the product, which is most likely to form, should be the one with the lowest energy. Kinetically favored crystals form when system tries to relieve the entropy of a super saturated state. Z' is the number of molecules or formula unit per asymmetric unit. Structures with high Z' values continue to interest crystallographers but it is still not properly understood why some categories of structures exhibit a higher frequency of Z'>1.

2.2. Experimental

All chemicals were purchased from Ranbaxy chemicals and used without further purification. IR spectra were obtained with a Shimadzu FT-IR 8000 spectrometer. Elemental analysis was obtained using a FLASH EA 1112 SERIES CHNS analyzer.

2.2.1 Synthesis

Preparation of $[Mn(acac)_2(H_2O)_2]NO_3.H_2O$

Manganese(II) acetate (1.00 g, 4.08 mmol) and acetylacetone (0.800 g, 8.29 mmol) were dissolved in 2.5 mL water. To this solution, solid ceric ammonium nitrate (3.30 g 6.02 mmol) was added slowly while stirring. Green precipitate formed was filtered off and dried (1.30 g). Different polymorphs were obtained by recrystallisation of the precipitate as described below.

Polymorphs **1** and **2**: The precipitate was dissolved in 3 ml of 1:2 acetic acid - water mixture. In order to promote crystallization, 0.5 g of sodium nitrate was added to the above solution. Slight precipitate that formed upon dissolution of sodium nitrate was re-dissolved by adding minimum amount of water. Green crystals formed within one day when the solution was kept at 0 ° C. While checking the crystals on the diffractometer, it was found that there were two types with similar block type morphologies (prominent face with four or five edges) formed in nearly equal amounts. Yield 0.370 g (1.00 mmol, 25%). Anal. calcd. for $MnC_{10}H_{20}NO_{10}$ (M.W. 369.2): C, 32.53; H, 5.46; N, 3.79. Found: C, 32.48; H,

5.44; N, 3.96. Important IR absorptions (KBr disk, cm^{-1}): 3441, 1969, 1753, 1628, 1537, 1426, 1350, 1277, 1030, 941, 810, 689, 633, 492 and 428.

Polymorphs **3** and **4**: The precipitate was dissolved in 5 mL of water and 0.50 g sodium nitrate (0.50 g, 5.88 mmol) was added. Slight precipitate that formed was re-dissolved by adding minimum amount of water. Crystals were formed within a few days when the solution was kept at 5° C. The majority of the crystals (about 60 %) belonged to polymorph **1**. About 40% of the crystals had a different morphology having prominent hexagonal faces. They belong to polymorph **3**. Yet another polymorph, **4** (similar in shape to **1**) was formed as a minor product. When crystallization was repeated several times, form **4** could be isolated only in two experiments. The total yield from crystallization from water was less than 5% due to decomposition of the Mn(III) complex as seen from the slow decolorisation of the solution.

[$Mn(acac)_2(HOMe)_2]_3[Ce(NO_3)_6]$ (5)

In quest for the further polymorphs, whole of the above precipitate (1.30 g) was dissolved in methanol and volume of the methanol was reduced considerably by heating in water bath and kept for crystallization outside at room temperature. Surprisingly compound **5** was formed. Yield 1.26 g (0.861 mmol, 64.6%). Anal. cald. for $Mn_3C_{36}H_{66}N_6O_{36}$ (M.W. 1463.9): C, 29.54; H, 4.54; N, 5.74. Found: C, 29.60; H, 4.50; N, 5.80. Important IR absorptions (KBr disk, cm^{-1}): 3410, 2471, 2357, 1757, 1628, 1521, 1385, 1032, 939, 823, 688 and 490.

Preparation of $[Mn(acac)_2(H_2O)_2]BF_4.2H_2O$ (6)

To a mixture of NH_4BF_4 (1.00 g 9.54 mmol) and manganese(II) acetate in 5 mL water, acetylacetone (0.800 g, 8.29 mmol) was added. Powdered ammonium

ceric sulfate was added slowly while stirring. A mixture of green and white precipitate was formed. Green precipitate was separated immediately by dissolving in minimum amount of acetonitrile and drying on the water bath. Yield 0.576 g (1.36 mmol 34%). Characteristic IR peaks (KBr disk cm^{-1}) 3462, 2484, 2363, 2320, 2137, 2054, 1977, 1543, 1523, 1340, 1032, 935, 694. C, H, N Analysis: Anal. Calcd. for $Mn_1C_{10}H_{22}O_8BF_4$ (MW 412.04): C, 29.15; H, 5.38. Found: C, 30.09; H, 5.12. X-ray quality crystals were obtained when this precipitate was dissolved in a minimum amount of 1:1 acetic acid - water mixture and kept for crystallization at 0° C for several weeks.

2.3 X-ray crystallography

Data were collected on a Bruker SMART APEX CCD X-ray diffractometer using graphite monochromated Mo Kα radiation. The data were reduced using SAINTPLUS[3], and multiscan absorption corrections using SADABS[4] were applied. The structures were solved using SHELXS-97 and refined using SHELXL-97[5]. All ring hydrogen atoms were assigned on the basis of geometrical considerations and were allowed to ride upon the respective carbon atoms. All water hydrogen atoms were located from the difference Fourier maps and bond length constraints were applied. In compound **1**, the acetyl acetonate was located on two positions. Every atom has 50% occupancy and was assigned directly from the Fourier peaks. In compound **6**, BF_4^- was disordered over two inversion related positions. Crystal data are in Table 2.1 and 2.2 and important inter-atomic distances and angles are in Tables 2.3, 2.3, 2.3, 2.6, 2.7 and 2.9.

2.4 Computational methods

DFT calculations along with geometry optimization were done using the B3LYP exchange correlation functional[6] as implemented in the Gaussian-03[7]. The spin-unrestricted version was employed for open shell ions. For both types of calculations, triple-ζ basis sets[8] were used for Mn atom and double-ζ basis sets[9] were used for all other atoms. Lattice energies of polymorphs **1**, **2**, **3** and **4** were computed using 4.8 version of Cerius[2] program by energy minimization of crystal structures with Universal 1.02 force fields[10].

2.5 Crystal structure

2.5.1 Crystal structure of $[Mn(acac)(H_2O)_2]NO_3.H_2O$ 1, 2, 3 and 4 and $[Mn(acac)_2(H_2O)_2]$ BF_4 (6)

Solid state structures of trans-diaquabis(acetylacetonato)manganese(III) cation and nitrate anions are of four types in which **1**, **2** and **3** crystallize in space group $P\bar{1}$ and **4** crystallize in space group $P2_1/c$ (Figure. 2.1-2.4). Compound **6** crystallizes in space group $C2/m$ (Figure. 2.5). All of the manganese centres are six coordinated with four oxygen atoms from two bidentate acetyl acetone ligands in the equatorial plane where as water molecules occupy axial positions. One feature that is common to all the polymorphs is a Z'-number greater than 1. Z' is here defined as the number of crystallographically different cations in the asymmetric unit. Taken together, there are twelve ions in all and all but two are located on crystallographic inversion centers.

Table 2.1 Crystallographic data for **1**, **2, 3** and **4**

	1	**2**	**3**	**4**
Formula	$MnC_{10}H_{20}N\,O_{10}$	$MnC_{10}H_{20}N\,O_{10}$	$Mn\,C_{10}\,H_{20}\,N\,O_{10}$	$MnC_{10}H_{20}\,N\,O_{10}$
Formula weight	369.21	369.21	369.21	369.21
Crystal system	Triclinic	Triclinic	Triclinic	Monoclinic
Space group	$P\bar{1}$	$P\bar{1}$	$P\bar{1}$	$P2_1/c$
a (Å)	7.7085(7)	7.902(4)	7.901(4)	7.8378(5)
b (Å)	7.7158(7)	13.238(7)	13.298(7)	12.9697(8)
c (Å)	15.9918(14)	15.966(8)	16.832(8)	31.268(2)
$\alpha(^o)$	97.8890(10)	86.226(8)	109.655(7)	90
$\beta\,(^o)$	91.533(2)	80.642(8)	94.745(8)	94.6900(10)
$\gamma(^o)$	118.3800(10)	89.990(8)	90.033(8)	90
V ($Å^3$)	824.28(13)	1644.2(14)	1659.0(14)	3167.9(3)
Z	2	4	4	8
T (ºC)	298(2)	298(2)	298(2)	100(2)
D_{calc} (g cm^{-3})	1.488	1.491	1.478	1.548
μ (mm^{-1})	0.847	0.850	0.842	0.882
F(000)	384	768	768	1536
Crystal size (mm)	0.24 x 0.20 x 0.20	0.24 x 0.18 x 0.16	0.24 x 0.22 x 0.18	0.38 x 0.36 x 0.28
θ Range (º)	1.29 -25.93	1.30 - 26.20	1.29 - 26.17	1.31 - 26.05
h/k/l	-9, 9 /-9, 9 /-19, 19	-9,9 /-16, 16 /-19, 19	-9, 9 /-16, 16 /-20, 20	-9, 9 /-6, 16 /-38, 38
Reflection collected	8507	17286	16977	32272
Unique reflect., [R_{int}]	3194 [0.0225]	6520 [0.0282]	6491 [0.0314]	6250 [0.0286]
Goodness of fit	1.039	1.011	1.038	1.125
R_1 [I>2σ(I)]	0.0347	0.0391	0.0371	0.0369
wR_2	0.0970	0.1192	0.1108	0.0980

Only in one case is there a disorder due to the positioning of the acac ligand. In all structures the plane of acac sp^2 carbon atoms deviates from $Mn(O)_4$ equatorial plane. According to the extend of deviation we can categorize the cations into Type-I and Type-II. Type-I ions are having less deviations (1-5°) than that of the type-II ions (21-29º). Further, the axial Mn-O bond distances in the Type-I ions are slightly longer than that of Type-II. The bond distances are in the range, 2.23-2.24 Å for Type-I and 2.20-2.21 Å for Type-II (table. 2.7). The above differences in coordination geometry, seen in all the polymorphs, appear to be imposed by the H-bonding interactions in the lattice. That intermolecular interactions can often extend a significant influence on coordination geometry has been previously noted[11,12].

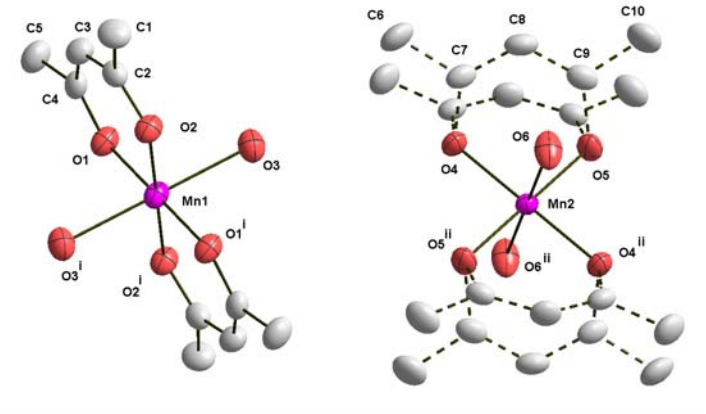

Figure 2.1 Thermal ellipsoid plot of the coordination environment of the complex cations in **1.** Atoms are represented as 50% probability ellipsoids and ring and water hydrogens, nitrate anions have been omitted for clarity. Symmetry code: (i) -*x*, -*y*, -*z*. (ii) -*x*, -*y*, -*z*+1.

Table 2.2. Crystallographic data for **5** and **6**

	5	**6**
Formula	$Mn_3C_{36}H_{66}CeN_6O_{36}$	$Mn\ C_{10}\ H_{22}B_2F_4O_8$
Formula weight	1463.89	422.84
Crystal system	Trigonal	Monoclinic
Space group	$R\bar{3}$	C2/m
a (Å)	16.5842(3)	7.5897(6)
b (Å)	16.5842(3)	11.8987(10)
c (Å)	18.3249(8)	10.2350(8)
α	90	90
β (º)	90	110.5490(10)
γ	120	90
V (Å^3)	4364.8(2)	865.49(12)
Z	3	2
T (K)	100(2)	100(2)
D_{calc} (g cm^{-3})	1.671	1.623
μ (mm^{-1})	1.505	0.838
F(000)	2235	434
Crystal size	0.24 x 0.20 x 0.18	0.32 x 0.23 x 0.20
θ Range (º)	1.80 to 28.25	2.13 to 28.26
h/k/l	-21, 22 / -21, 21/ -24, 24	-10, 9 / -15, 15 / -13, 13
Reflection collected	16956	4915
Unique reflect., [R_{int}]	2362 [0.0265]	1067 [0.0178]
Goodness of fit on F^2	1.118	1.161
R_1 [$I>2\sigma(I)$]	0.0238	0.0608
wR_2 (all data)	0.0585	0.1482

Table 2.3 Selected bond lengths [Å] and angles [º] for (**1**)[a]

Mn(1)-O(2)	1.9073(15)	O(4)#1-Mn(1)-O(6)	89.92(10)
Mn(1)-O(1)	1.9102(15)	O(5)#1-Mn(1)-O(6)	89.78(10)
Mn(1)-O(3)	2.2332(19)	O(2)#2-Mn(2)-O(1)	87.73(8)
Mn(2)-O(4)	1.8980(15)	O(4)-Mn(2)-O(5)	91.86(7)
Mn(2)-O(5)	1.9030(15)	O(4)-Mn(2)-O(6)	90.10(8)
Mn(2)-O(6)	2.197(2)	O(5)-Mn(2)-O(6)	90.21(8)
O(2)-Mn(1)-O(1)	92.30(7)	O(2)-Mn(2)-O(3)#2	89.68(9)
O(2)-Mn(1)-O(3)	90.32(7)	O(2)#2-Mn(2)-O(3)#2	90.32(9)
O(1)-Mn(1)-O(3)	89.42(7)	O(1)-Mn(2)-O(3)#2	90.59(9)
O(4)-Mn(1)-O(5)#1	88.21(8)		

[a] Symmetry transformation used to generate equivalent atoms: (#1) -x,-y,-z+1; (#2) -x,-y,-z.

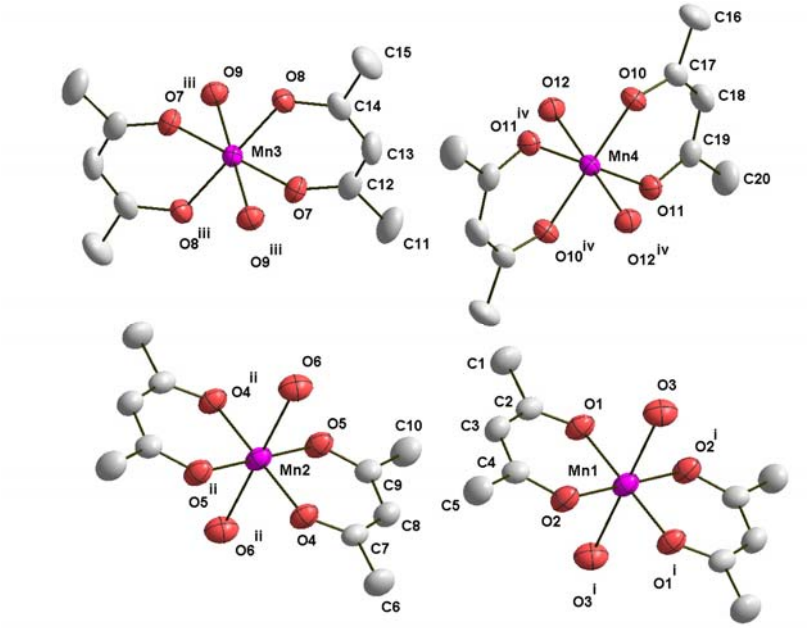

Figure 2.2 1 Thermal ellipsoid plot of the coordination environment of the complex cations in **2**. Symmetry code: (i) -*x*+1, -*y*, -*z* (ii) -*x*, -*y*+1, -*z*, (iii) -*x*, -*y*+1, -*z*+1, (iv) -*x*+1, -*y*, -*z*+1

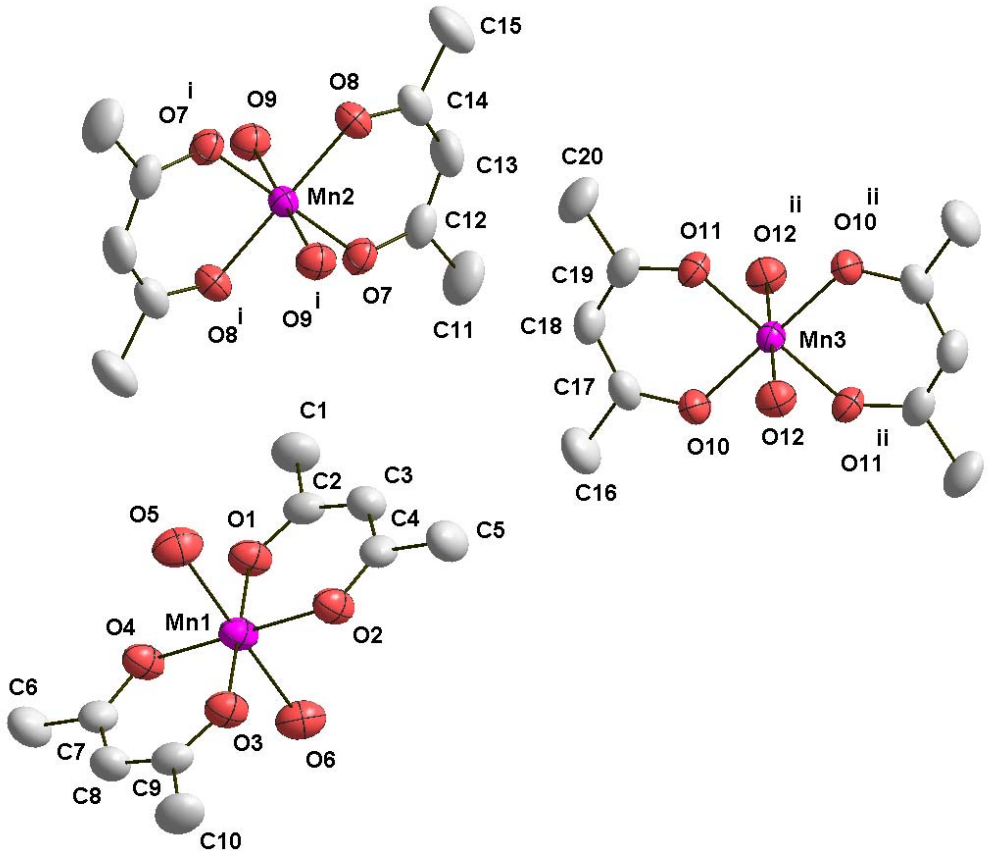

Figure 2.3 Thermal ellipsoid plot of the coordination environment of the complex cations in **3**. Atoms are represented as 50% probability ellipsoids and ring and water hydrogens, nitrate anions have been omitted for clarity. Symmetry code: (i) -*x*+1, -*y*+1, -*z*+1 (ii) -*x*, -*y*, -*z*+1.

Hydrogen bonding plays a very important role in the packing scheme of the polymorphs **1** - **4**. All hydrogen atoms of the coordinated water molecules participate in hydrogen bonding In the Type-I ion, one hydrogen from each coordinated water molecule is bonded to a nitrate oxygen, with the other bonded

to a lattice water oxygen. Type-II complex ion, on the other hand, has all the four hydrogen atoms bonded to nitrate oxygen atoms.

Table 2.4 Selected bond lengths [Å] and angles [º] for $[Mn(acac)_2(H_2O)_2]\ NO_3.H_2O$ (**2**)[a]

Mn(1)-O(1)	1.9091(17)	O(1)#1-Mn(1)-O(3)	90.99(7)
Mn(1)-O(2)	1.8996(17)	O(5)-Mn(2)-O(4)	91.44(8)
Mn(1)-O(3)	2.208(2)	O(5)-Mn(2)-O(6)	88.81(7)
Mn(2)-O(4)	1.9068(17)	O(4)-Mn(2)-O(6)	89.19(7)
Mn(2)-O(5)	1.8996(16)	O(5)#2-Mn(2)-O(4)	88.58(8)
Mn(2)-O(6)	2.208(2)	O(5)-Mn(2)-O(6)#2	91.15(7)
Mn(3)-O(7)	1.9017(18)	O(4)-Mn(2)-O(6)#2	90.78(7)
Mn(3)-O(8)	1.9134(18)	O(4)#2-Mn(2)-O(6)#2	89.22(7)
Mn(3)-O(9)	2.228(2)	O(7)-Mn(3)-O(8)	92.18(8)
Mn(4)-O(10)	1.9186(18)	O(7)-Mn(3)-O(9)	90.75(8)
Mn(4)-O(11)	1.8995(18)	O(8)-Mn(3)-O(9)	89.41(8)
Mn(4)-O(12)	2.231(2)	O(7)#3-Mn(3)-O(8)	87.81(8)
O(2)-Mn(1)-O(1)	91.40(8)	O(7)#3-Mn(3)-O(9)	89.20(8)
O(2)-Mn(1)-O(3)	89.57(7)	O(8)#3-Mn(3)-O(9)	90.57(8)
O(1)-Mn(1)-O(3)	88.97(7)	O(11)#4-Mn(4)-O(10)	87.60(7)
O(2)#1-Mn(1)-O(1)	88.61(8)	O(11)-Mn(4)-O(10)	92.40(8)
O(2)-Mn(1)-O(3)#1	90.39(7)	O(11)-Mn(4)-O(12)	89.86(8)
O(2)#1-Mn(1)-O(3)#1	89.61(7)	O(10)-Mn(4)-O(12)	90.84(8)
O(1)-Mn(1)-O(3)#1	90.99(7)	O(11)#4-Mn(4)-O(10)#4	92.40(7)
O(1)#1-Mn(1)-O(3)#1	89.01(7)	O(11)-Mn(4)-O(12)#4	90.17(8)

[a] Symmetry transformation used to generate equivalent atoms: (#1) -x+1, -y, -z; (#2) -x, -y+1, -z; (#3) -x, -y+1, -z+1; (#4) -x+1, -y, -z+1.

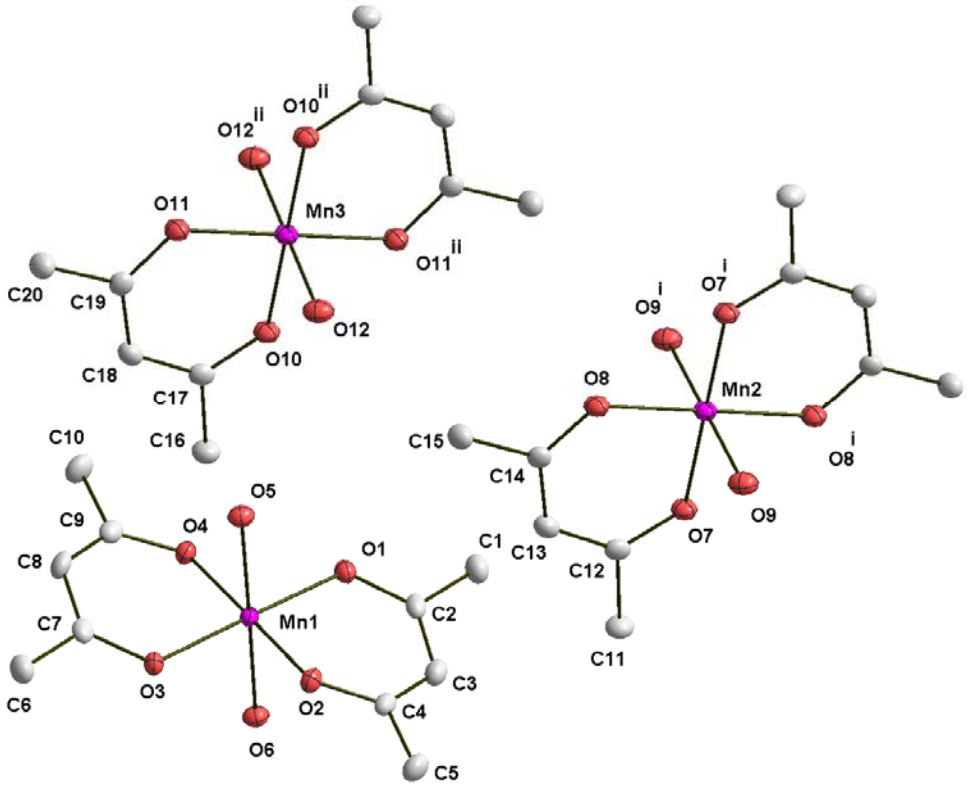

Figure 2.4 Thermal ellipsoid plot of the coordination environment of the complex molecules **4**. Atoms are represented as 50% probability ellipsoids and ring and water hydrogens, nitrate anions have been omitted for clarity. Symmetry code: (i) -*x*+1, -*y*+1, -*z* (ii) -*x*, -*y*, -*z*.

The resulting two-dimensional network, excluding the acac ions is shown in Figure 2.6. This network in which Type-II ions form one-dimensional chains which are then inter-connected by the Type-I ions is present in all the polymorphs. Even though the H-bonded water network shown in Figure 2.6 is present in all the polymorphs, there are certain differences. Saturation with regard to H-bonding is achieved by bonding the free hydrogen of the lattice water with the acac oxygen atom.

Table 2.5 Selected bond lengths [Å] and angles [º] for (**3**)[a]

Mn(1)-O(2)	1.9117(16)	O(3)-Mn(1)-O(6)	89.48(7)
Mn(1)-O(4)	1.9132(16)	O(2)-Mn(1)-O(5)	90.02(8)
Mn(1)-O(1)	1.9135(17)	O(4)-Mn(1)-O(5)	89.97(8)
Mn(1)-O(3)	1.9149(17)	O(1)-Mn(1)-O(5)	89.18(7)
Mn(1)-O(6)	2.234(2)	O(3)-Mn(1)-O(5)	90.55(7)
Mn(1)-O(5)	2.237(2)	O(6)-Mn(1)-O(5)	179.28(6)
Mn(2)-O(7)	1.9128(15)	O(7)-Mn(2)-O(8)	91.38(7)
Mn(2)-O(8)	1.9129(15)	O(7)-Mn(2)-O(9)	89.13(6)
Mn(2)-O(9)	2.2050(19)	O(8)-Mn(2)-O(9)	89.19(6)
Mn(3)-O(10)	1.9116(15)	O(8)#1-Mn(2)-O(7)	88.59(7)
Mn(3)-O(11)	1.9165(15)	O(8)#1-Mn(2)-O(9)	90.83(6)
Mn(3)-O(12)	2.2075(19)	O(7)#1-Mn(2)-O(9)	90.90(6)
O(2)-Mn(1)-O(4)	179.99(8)	O(10)-Mn(3)-O(11)#2	88.58(7)
O(2)-Mn(1)-O(1)	92.14(7)	O(10)-Mn(3)-O(11)	91.41(7)
O(4)-Mn(1)-O(1)	87.86(7)	O(10)-Mn(3)-O(12)	90.57(6)
O(2)-Mn(1)-O(3)	88.00(7)	O(11)-Mn(3)-O(12)	90.82(6)
O(4)-Mn(1)-O(3)	92.00(7)	O(10)#2-Mn(3)-O(11)	88.58(7)
O(1)-Mn(1)-O(3)	179.70(7)	O(10)-Mn(3)-O(12)#2	89.40(6)
O(2)-Mn(1)-O(6)	89.26(8)	O(11)#2-Mn(3)-O(12)#2	90.86(6)
O(4)-Mn(1)-O(6)	90.75(8)	O(11)-Mn(3)-O(12)#2	89.14(6)
O(1)-Mn(1)-O(6)	90.79(7)		

[a] Symmetry transformation used to generate equivalent atoms: (#1) -x+1,-y+1,-z+1; (#2) -x,-y,-z+1.

Table 2.6 Selected bond lengths [Å] and angles [°] for (**4**)[a]

Mn(1)-O(1)	1.9050(14)	O(2)-Mn(1)-O(5)	91.34(6)
Mn(1)-O(2)	1.9089(14)	O(1)-Mn(1)-O(6)	88.98(6)
Mn(1)-O(3)	1.9140(14)	O(2)-Mn(1)-O(6)	89.66(6)
Mn(1)-O(4)	1.9218(14)	O(3)-Mn(1)-O(6)	90.45(6)
Mn(1)-O(5)	2.1979(14)	O(4)-Mn(1)-O(6)	90.57(6)
Mn(1)-O(6)	2.1993(14)	O(5)-Mn(1)-O(6)	178.97(6)
Mn(2)-O(8)	1.9108(14)	O(8)-Mn(2)-O(7)	92.39(6)
Mn(2)-O(7)	1.9148(14)	O(8)-Mn(2)-O(9)	90.63(6)
Mn(2)-O(9)	2.2237(14)	O(7)-Mn(2)-O(9)	89.78(6)
Mn(3)-O(11)	1.9080(14)	O(8)-Mn(2)-O(7)#1	87.61(6)
Mn(3)-O(10)	1.9160(14)	O(7)#1-Mn(2)-O(9)	90.23(6)
Mn(3)-O(12)	2.2284(14)	O(8)#1-Mn(2)-O(9)#1	90.64(6)
O(1)-Mn(1)-O(2)	91.61(6)	O(7)#1-Mn(2)-O(9)#1	89.77(6)
O(1)-Mn(1)-O(3)	179.19(6)	O(7)-Mn(2)-O(9)#1	90.23(6)
O(2)-Mn(1)-O(3)	87.81(6)	O(11)#2-Mn(3)-O(10)	87.63(6)
O(1)-Mn(1)-O(4)	89.10(6)	O(11)-Mn(3)-O(10)	92.36(6)
O(2)-Mn(1)-O(4)	179.26(6)	O(11)-Mn(3)-O(12)	89.63(6)
O(3)-Mn(1)-O(4)	91.48(6)	O(10)-Mn(3)-O(12)	88.93(6)
O(1)-Mn(1)-O(5)	91.22(6)	O(11)-Mn(3)-O(10)#2	87.63(6)
O(3)-Mn(1)-O(5)	89.36(6)	O(10)-Mn(3)-O(12)#2	91.07(6)
O(4)-Mn(1)-O(5)	88.42(6)	O(10)#2-Mn(3)-O(12)#2	88.93(6)

[a] Symmetry transformation used to generate equivalent atoms: (#1) -x+1, -y+1, -z; (#2) -x, -y, -z.

In polymorphs **2** and **3** one of the lattice water hydrogen atoms form H-bond with two acac oxygen atoms. Such H-bonds are not present in polymorph **1** and **4**. H-bond pattern (twelve membered ring) shown by Type-II ions were present in

various reported ($[ML(OH_2)_2](NO_3)_2$) structures[13-20] (CSD refcodes: AHAFEU, DUMBOC, DUMBUI, GIGZEB, HEXMIH, HEXMAZ, IRETUU, KAGMIP, LUFVIR and SUXPAC).

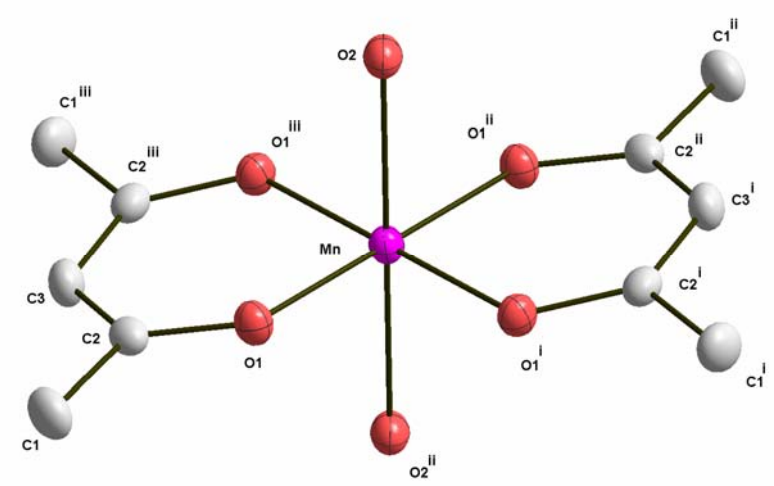

Figure 2.5 Thermal ellipsoid plot of the coordination environment of the complex cation in **6**: Atoms are represented as 50% probability ellipsoids and ring and water hydrogens, nitrate anions have been omitted for clarity (i) -x+1, y,-z (ii) -x+1, -y, -z, (iii) x, -y, z

Table 2.7 Selected bond lengths [Å] and angles [°] for (**6**)[a]

Mn-O(1)	1.910(2)	O(1)-Mn-O(2)	89.03(9)
Mn-O(2)	2.229(3)	O(1)#1-Mn-O(2)	90.99(9)
O(1)-Mn-O(1)#1	87.62(13)	O(1)#2-Mn-O(1)#3	87.62(13)
O(1)-Mn-O(1)#2	92.38(13)	O(1)-Mn-O(2)#2	90.99(9)
O(1)#1-Mn-O(1)#3	180.00(13)		

[a] Symmetry transformation used to generate equivalent atoms: (#1) (i) -x+1, y,-z (#2) -x+1, -y, -z, (#3) x, -y, z

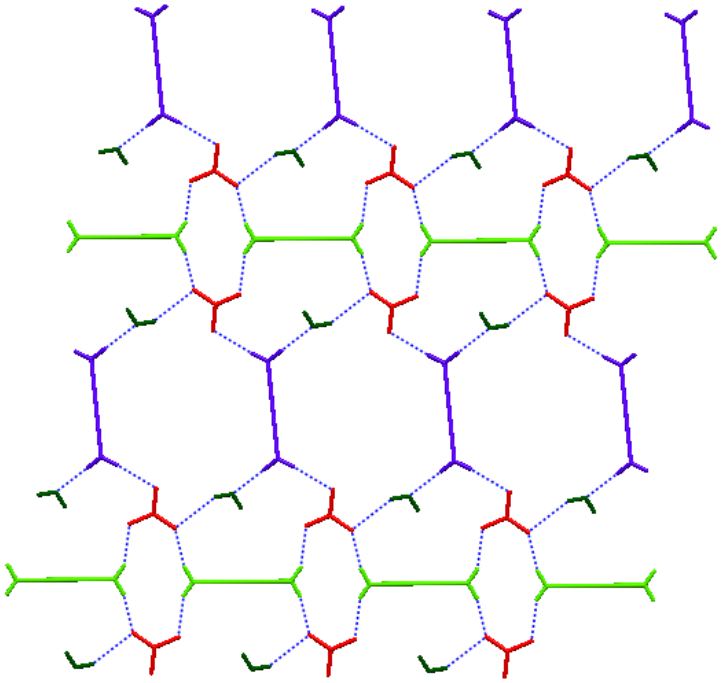

Figure 2.6. Two dimensional network of hydrogen bonds seen in **1**. The acac ligands have been omitted.

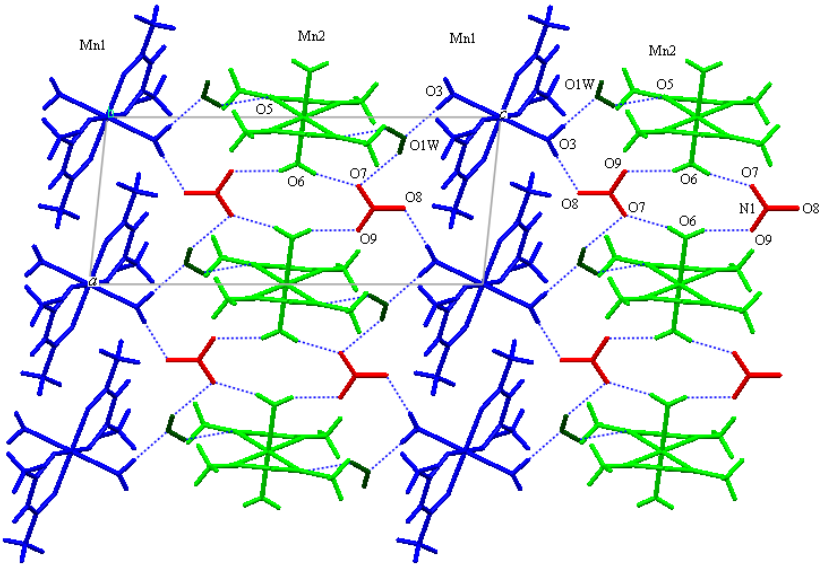

Figure 2.7 View, in the *ac*-plane, of the two-dimensional hydrogen bonded layers of **1**.

Table 2.8 Metric parameters (Å, º) of the $[Mn(acac)_2(H_2O)_2]^+$ ion in various crystals

	Ion (Type)	Mn-$O_{equatorial}$	Mn-O_{axial}	δ^a	Hydrogen bond D…A and D-H…A
1	Mn1 (I)	1.91, 1.91	2.23	3	2.72, 172; 2.90, 175
	Mn2 (II)	1.90, 1.90	2.20	29	2.68, 163; 2.70, 154
2	Mn1 (II)	1.90, 1.91	2.21	22	2.75, 165; 2.75, 159
	Mn2 (II)	1.90, 1.91	2.21	21	2.75, 152; 2.75, 168
	Mn3 (I)	1.90, 1.91	2.23	2	2.91, 174; 2.72, 173
	Mn4 (I)	1.90, 1.91	2.23	3	2.89, 170; 2.74, 177
3	Mn1 (I)	1.91, 1.91,	2.23, 2.24	3, 3	2.90, 173; 2.74, 174
		1.91, 1.91			2.91, 173; 2.72, 172
	Mn2 (II)	1.91, 1.91	2.20	22	2.76, 155; 2.76, 163
	Mn3 (II)	1.91, 1.92	2.21	22	2.76, 164; 2.77, 157
4	Mn1 (II)	1.90, 1.91,	2.20, 2.20	25, 26	2.71, 160; 2.72, 157
		1.91, 1.92			2.71, 157; 2.74, 162
	Mn2 (I)	1.91, 1.91	2.22	1	2.86, 180; 2.71, 177
	Mn3 (I)	1.91, 1.92	2.23	5	2.84, 177; 2.75, 173
5	Mn (I)	1.91, 1.91	2.23	12	2.64, 170; 2.75, 126

[a]Angle between $Mn(O)_4$ mean-plane and the plane of the three sp^2-C atoms of acac.

Water-nitrate interaction in these structures interconnects the discrete units in one-dimension. Some of the reported structures[21-27] (CSD ref code: DAPSCR1O, FELDAB, FODOEH, GAZTOQ, IWOZEB, TEMXIS,TEMXIS01, UGACOU

and VIGDAQ) which contain $[ML(OH_2)_2](NO_3)_2$ and lattice water did not show similar H-bond pattern. Instead, in all of these structures lattice water extensively form H-bonds with coordinated water molecule and resulted in 3-dimensional interconnected units. One structure[28] (CSD refcode: VEJNEE) that was analogues to **1** had different H-bond patterns due to the ligand complexity.

All compounds forms hydrogen bonded extended structures as shows in Figures 2.7–2.11. Packing of **2** and **3** down *a* and *b* axis are similar. But there is an explicit difference in packing along c axis. If two crystal structures contain similar infinite two-dimensional molecular arrangements (layers) then they are termed as two-dimensionally isostructural.

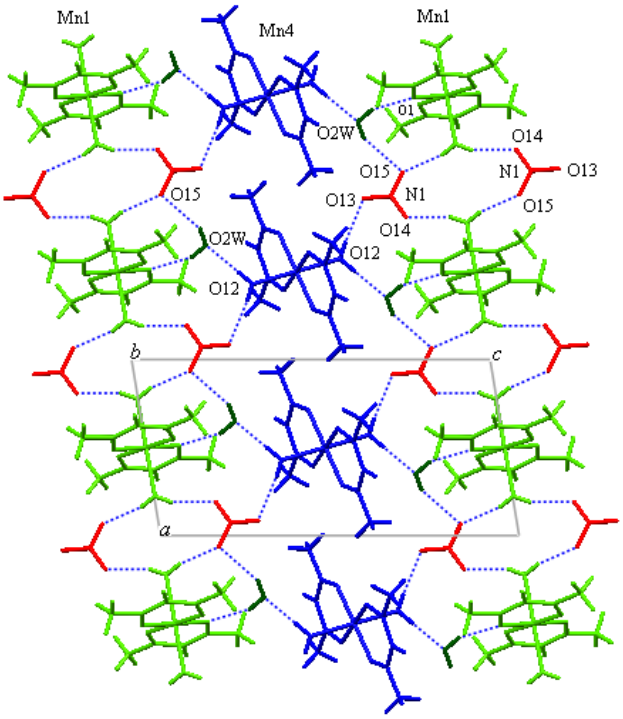

Figure 2.8 View, in the *ac*-plane, of two-dimensional hydrogen bonded layers of Mn1, Mn4 units of **2**.

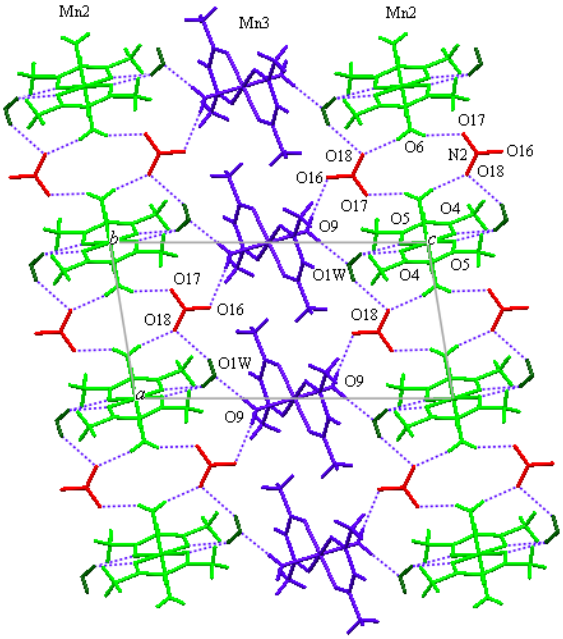

Figure 2.9 View, in the *ac*-plane, of the two-dimensional hydrogen bonded layers of Mn2, Mn3 units of **2**.

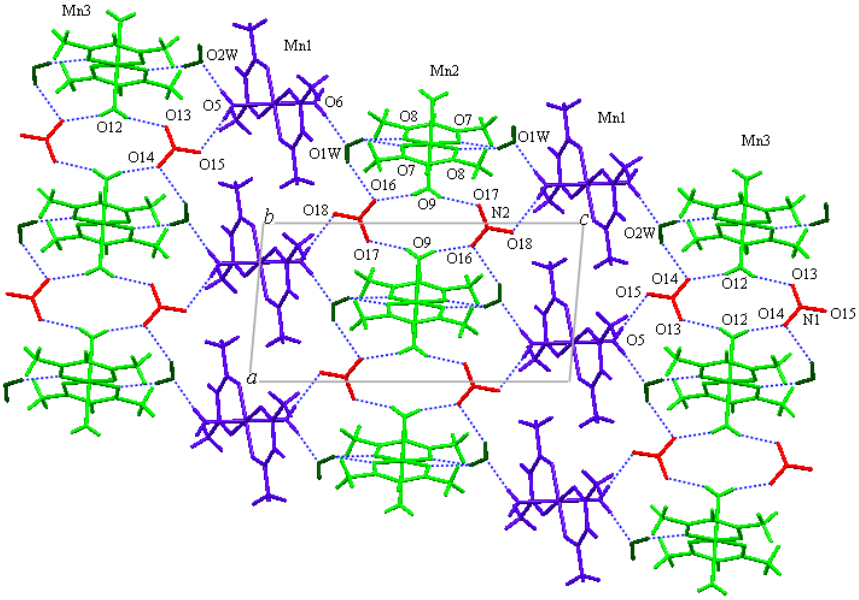

Figure 2.10 View, in the *ac*-plane, of the two-dimensional hydrogen bonded layers of **3**.

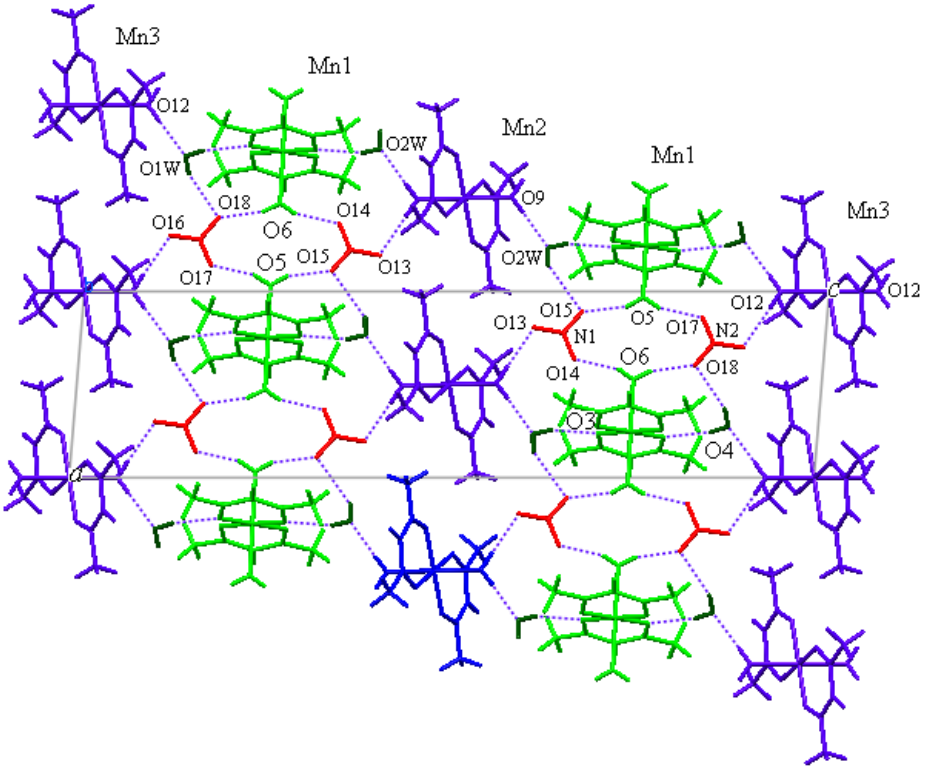

Figure 2.11 View, in the *ac*-plane, of the two-dimensional hydrogen bonded layers of **4**.

Particular packing pattern often leading to one- and two-dimensional isostructural compounds are known in the literature[29]. So **2** and **3** are two-dimensionally isostructural polymorphs. **4** and **3** has similar packing pattern along *b* axis but pack differently along *a* and *c* axis, hence they are also one-dimensionally isostructural. The cation in **6**, $[Mn(acac)_2(H_2O)_2]^+$ forms two dimensional hydrogen bonded structures with the help of lattice water molecule (Figure 12). These hydrogen bonded structures are interconnected into three-dimension by an O-H…F interaction with the BF_4 anion (Figures 13, 14).

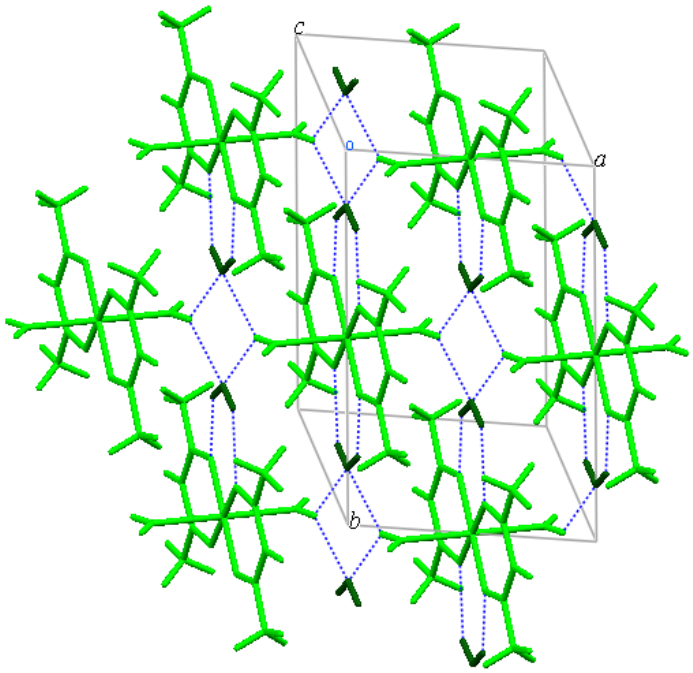

Figure 2.12 View of the two-dimensional hydrogen bonded layers of **6**.

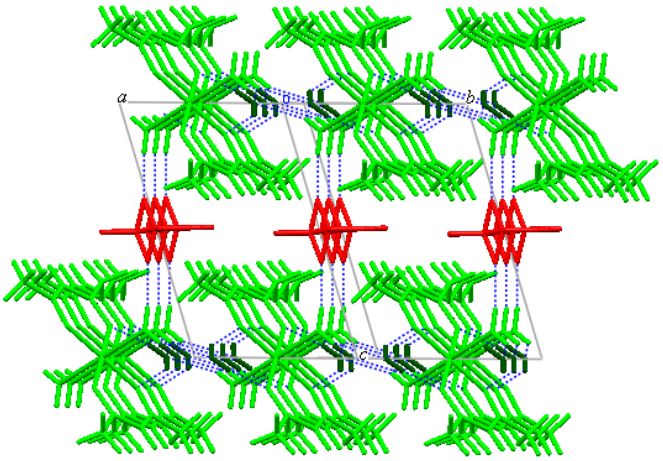

Figure 2.13 Two-dimensional hydrogen bonded layers of **6** are connected by BF_4 (BF_4 was disordered over symmetry related position) anions and form three-dimensional hydrogen bonded networks.

ab plane, *a*-axis horizontal

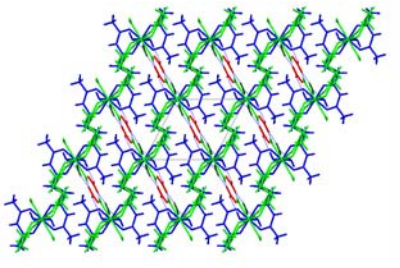

1

ac plane, *a*-axis horizontal

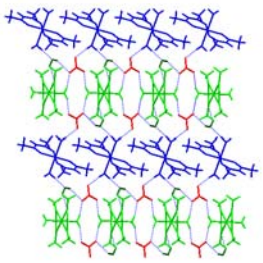

1

bc plane,*b* -axis horizontal

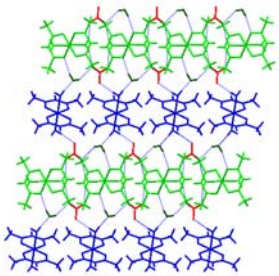

1

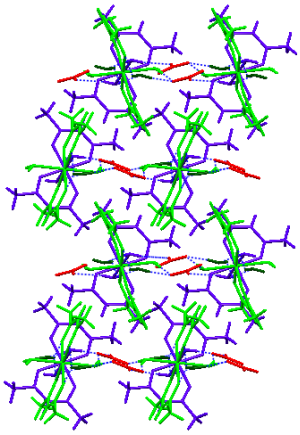

2

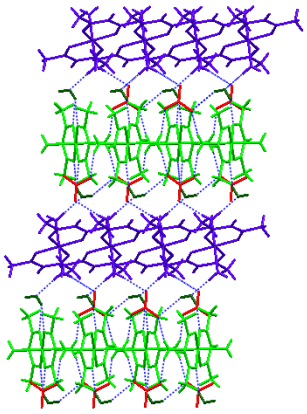

2

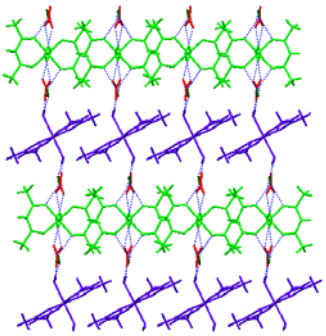

2

ab plane, *a*-axis horizontal

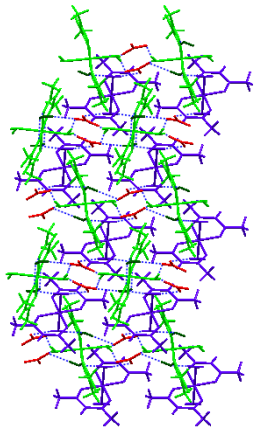

3

ac plane, *a*-axis horizontal

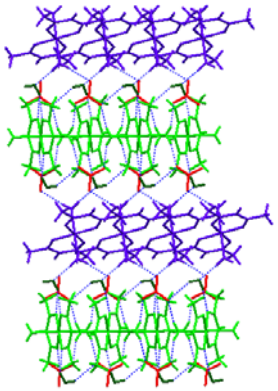

3

bc plane,*b* -axis horizontal

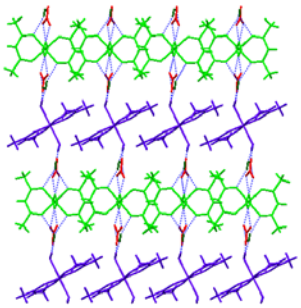

3

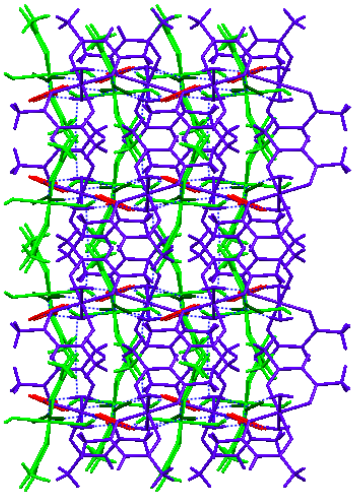

4

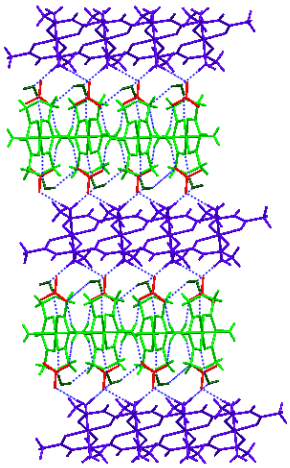

4

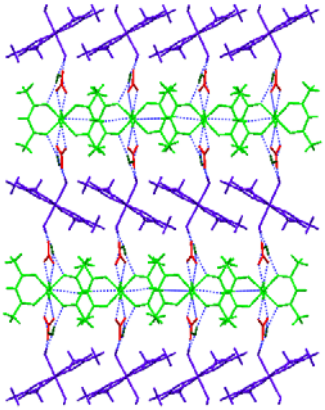

4

2.5.2 Crystal structure of [$Mn(acac)_2(HOMe)_2]_3[Ce(NO_3)_6]$ (5)

In **5** Asymmetric unit contains half $[Mn(acac)(HOCH_3)_2]^+$ cation and 1/6 th of $Ce(NO_3)_6$. Ce(III) ion located at an inversion center is coordinated with six

chelating nitrate anions. One independent NO_3^- ion shows considerable asymmetry in chelation (Ce-O(5) 2.6012(11) Å and Ce-O(4) 2.6647(12) Å). ∠O-Ce-O angle is 48.43(4)°. Manganese is coordinated with two bidentate acetyl acetone ligands on equatorial plane and with two methanol molecule on axial direction in a trans manner. Average Mn-O equatorial distance is 1.9091(11) Å and axial Mn-O distance is 2.2197(13) Å. Distance between manganese(III) and cerium(III) centers are found to be 7.760 Å.

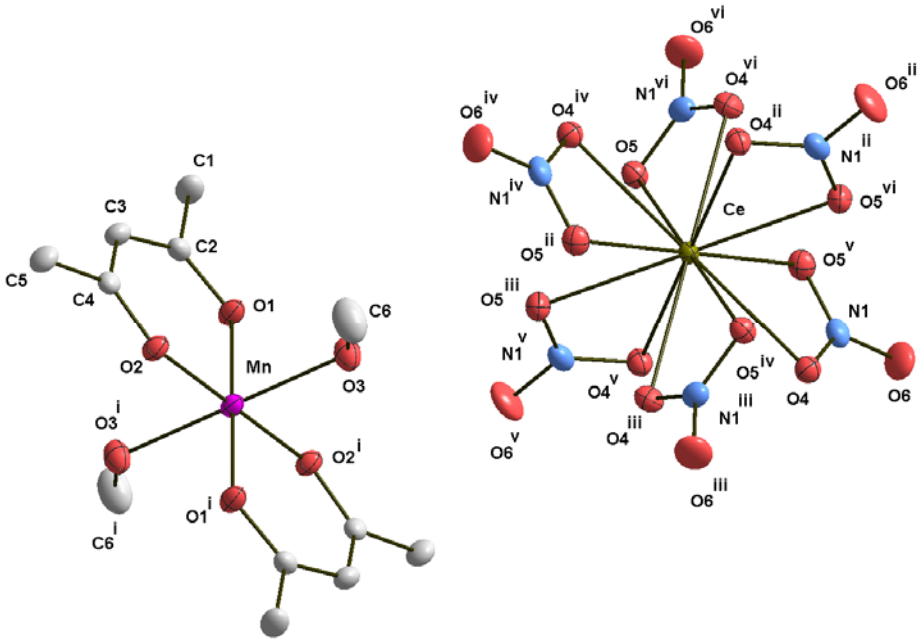

Figure 2.15 Thermal ellipsoid plot of the coordination environment of the complex molecules **5**: Atoms are represented as 50% probability ellipsoids and ring and water hydrogens, nitrate anions have been omitted for clarity**6**. Symmetry code: (i) -x, -y,-z (ii) x-y, -y, z, (iii) -x+y, -x, z (iv) -x+1/3, -y+2/3, -z+2/3 (v) y+1/3, -x+y+2/3, -z+2/3 (vi) x-y+1/3, x+2/3, -z+2/3.

Table 2.9 Selected bond lengths [A] and angles [deg] for **5**

Ce-O(5)	2.6012(11)	O(5)-Ce-O(4)	110.99(4)
Ce-O(4)	2.6647(12)	O(2)-Mn-O(1)	91.91(5)
Mn-O(2)	1.9068(11)	O(2)-Mn-O(3)	88.74(5)
Mn-O(1)	1.9113(11)	O(1)-Mn-O(3)	86.87(5)
Mn-O(3)	2.2197(13)		

Coming to crystal packing of **5**, methanol molecules coordinated with manganese and all uncoordinated oxygen atom of the nitrate anions coordinated with cerium, participate in hydrogen bonding. Hence each $Ce(NO_3)_6^{3-}$ anion is hydrogen bonded with six $[Mn(acac)_2(HOCH_3)_2]^+$ cations (O3…O6, 2.931(2) Å) and forms three-dimensional hydrogen bonded (4,4) networks with rectangular voids along *a* and *b* axes (Figure 2.16). Interestingly these voids are blocked by a two fold parallel interpenetration of identical networks (Figure. 2.17). Of late, interpenetrating networks[30] are studied more extensively in crystal engineering of coordination polymers and metal organic frameworks. Topology of interpenetration in general and its establishment of useful relationship between structure and properties in particular is now more or less an unexplored field of chemical topology.

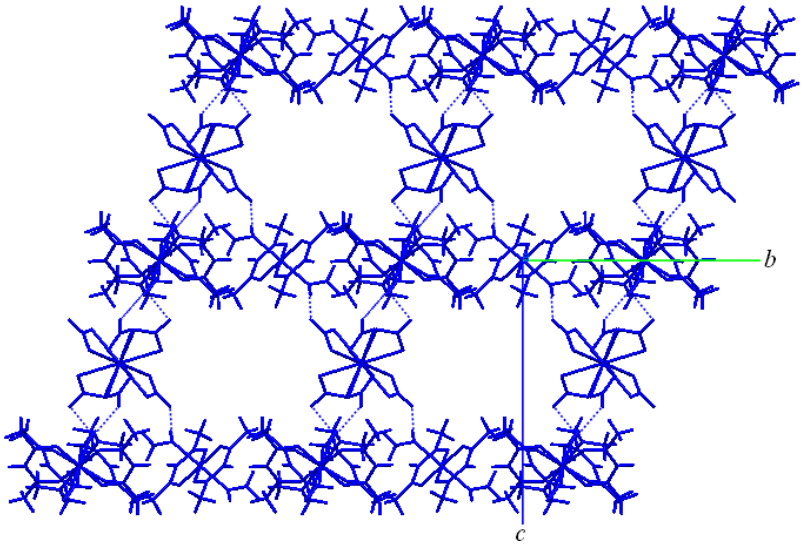

Figure 2.16 View of hydrogen bonded (4,4) networks of **5** with rectangular voids down the *a* axis.

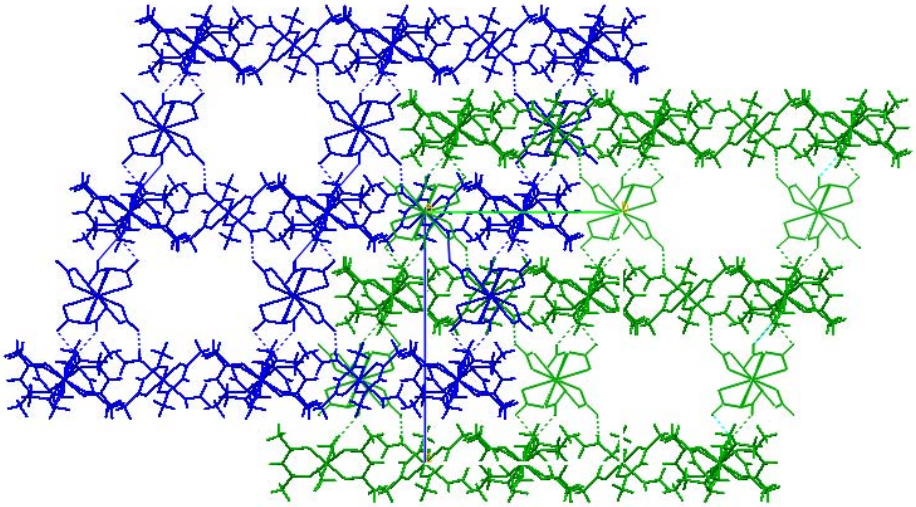

Figure 2.17 Two-fold parallel interpenetrating (4,4) networks of **5**.

2.6 Lattice energy calculations

The crystal lattice energies U_{latt} of polymorph **1-4** were computed using Cerius[2] (Table 2.10). Form **4** is the most stable crystal structure (-131.31 kcal mol^{-1}, Polymorph **1** excluded because of disorder) and forms **2** and **3** are less stable 8.81 kcal mol^{-1} and 10.32 kcal mol^{-1} respectively. So the observed stability is found to be **4** > **2** > **3**.

Table 2.10 Lattice energies[U_{latt} kcal mol^{-1}] of forms **1-4** compounds in Cerius[2], corrected per molecule

U_{latt}	**1**	**2**	**3**	**4**
Total	-147.14	-122.50	-120.99	-131.31
Van der waals	-25.83	-29.58	-27.95	-28.78
Coulombic	-121.31	-92.52	-93.04	-102.53

2.7 Geometry optimization

The geometry optimization of the cationic part of **3** (Mn1) was done without any constraints. The optimized structure of the isolated cation is superimposed on a crystallographic structure (Type-II complex chosen for illustration) in Figure 2.18. The bond distances in the optimized geometry are within 0.06Å of the crystallographic values. Since the acetylacetonate group (excluding methyl hydrogen atoms) are coplanar with the Mn-O(4) equatorial plane in the optimized structure, the deviation of it from the Mn-O(4) plane can be considered as criteria for stability. The structure, which is having less deviation, will be more stable. So

empirically by counting average deviation per molecule, we can predict the stability of different forms of the polymorphs.

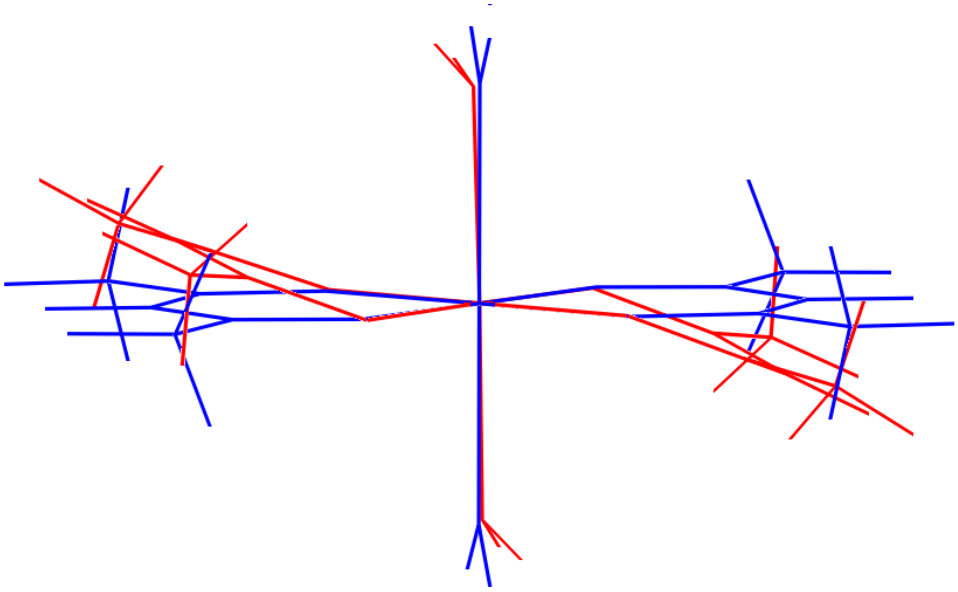

Figure 2.18 Optimized structure of the cation (planar chelate) superimposed on crystallographic structure (Mn1 of structure **3**, chair chelate).

Deviation (°) per molecules for form **1**, **2**, **3** and **4** were calculated and found to be 32.13, 24.72, 30.85 and 21.10. Because of the disorder the value for **1** doesn't come accordance with the calculated lattice energy but for other forms empirically predicted stability are in order of density (**4** > **2** > **3**) and which is in accordance with the calculated lattice energy.

2.8 Conclusion

All four forms of $[Mn(acac)_2(H_2O)_2]NO_3$. H_2O are packing polymorphs. Since $[Mn(acac)_2(H_2O)_2]ClO_4.H_2O$[1] and $[Mn(acac)_2(H_2O)_2]BF_4.2H_2O$ (**5**) did not show any polymorphism, the nitrate anion has an inevitable role in the formation of above packing polymorphs. Since form **4** exhibit the highest density of all four forms, it is possible that this form is thermodynamically stable form. Also the lattice energy calculations suggest that the most stable form is **4**. The order of calculated stability of different forms is found to be **4** > **2** > **3.** Kinetically driven products will be crystallizing first to relieve the entropy of the saturated system. Thermodynamically controlled form **4** will be crystallizing last, by that time manganese(III) ions will not be stable and that could be the reason for the absence of form **4** in several repeated batches of experiments. By simply counting the deviations of acac from equatorial plane per molecule, empirically it is possible to predict which form will be stable. The compensation of conformer stabilization by crystal environment increases the likelihood of polymorphism.

2.9 References

1. Swarnabala, G.; Reddy, K. R.; Tirunagar, J.; Rajasekharan, M. V. *Transition Met. Chem.* **1994**, *19*, 506.
2. Bernstein, J.; *Polymorphism in Molecular Crystals;* Oxford University Press: New York, **2002**.
3. *SAINTPLUS*, Bruker AXS Inc. Madison, Wisconsin, USA.
4. Sheldrick, G. M. *SADABS*, *Program for Empirical Absorption Correction*, University of Gottingen, Germany, **1996**.
5. M. Sheldrick, *SHELXS* and *SHELXL-97*, University of Gottingen, Gottingen, Germany, **1997**.
6. Becke, A. D. *J. Chem. Phys*. **1993**, *98*, 5648.
7. Frisch, M. J.; Trucks, G. W.; Schlegel, H. B.; Scuseria, G. E.; Robb, M. A.; Cheeseman, J. R.; Montgomery, J. A.; Vreven, T., Jr.; Kudin, K. N.; Burant, J. C.; Millam, J. M.; Iyengar, S. S.; Tomasi, J.; Barone, V.; Mennucci, B.; Cossi, M.; Scalmani, G.; Rega, N.; Petersson, G. A.; Nakatsuji, H.; Hada, M.; Ehara, M.; Toyota, K.; Fukuda, R.; Hasegawa, J.; Ishida, M.; Nakajima, T.; Honda, Y.; Kitao, O.; Nakai, H.; Klene, M.; Li, X.; Knox, J. E.; Hratchian, H.P.; Cross, J. B.; Adamo, C.; Jaramillo, J.; Gomperts, R.; Stratmann, R. E.; Yazyev, O.; Austin, A. J.; Cammi, R.; Pomelli,C.; Ochterski, J. W.; Ayala, P. Y.; Morokuma, K.; Voth, G. A.;Salvador, P.; Dannenberg, J. J.; Zakrzewski, V. G.; Dapprich, S.;Daniels, A. D.; Strain, M. C.; Farkas, O. D.; Malick, K.; Rabuck,A.D.; Raghavachari, K.; Foresman, J. B.; Ortiz, J. V.; Cui, Q.;Baboul, A. G.;

Clifford, S.; Cioslowski, J.; Stefanov, B. B.; Liu, G.; Liashenko, A.; Piskorz, P.; Komaromi, I.; Martin, R. L.; Fox, D. J.; Keith, T.; Al-Laham, M. A.; Peng, C. Y.; Nanayakkara, A.; Challacombe, M.; Gill, P. M. W.; Johnson, B.; Chen, W.; Wong, M. W.; Gonzalez, C.; Pople, J. A. *Gaussian 03*, revision C.01; Gaussian, Inc.: Pittsburgh, PA, **2003**.

8. Schaefer, A.; Huber, C.; Ahlrichs, R. *J. Chem. Phys.* **1994**, *100*, 5829.
9. Schaefer, A.; Horn, H.; Ahlrichs, R. *J. Chem. Phys.* **1992**, *97*, 2571.
10. Crystal packer of the Cerius^2 suit software was used for crystal lattice energy calculaton: see www.accelrys.com.
11. Swarnabala, G.; Rajasekharan, M. V. *Polyhedron* **1996**, *15*, 3197.
12. Steed, J. W.; Junk, P. C.; Johnson, K.; Legido, C. *Polyhedron* **2003**, 22,769.
13. Gómez-Saiz, P.; Garcia-Tojal, J.; Maestro, M. A.; Mahía, J.;Arnáiz, F. J; Rojo, T. *Polyhedron* **2002**, *21*, 2257.
14. Ianelli, S.; Nardelli, M.; Pelizzi, C. *Gazz. Chim. Ital.* **1985**, *115*, 715.
15. Romanenko, G. V.; Sheludyakova, L. A.; Vasiléva, L. I. Podberezskaya, N. V.; Varand, V. L. *Russ. J. Struct. Chem.* **1987**, *28*, 78.
16. Li, C. Y.; Liu, C. S.; Li, J. R.; Bu, X. H. *Cryst. Growth Des.* **2007**, *7*, 286.
17. Van Langenberg, K. A.; Moubaraki, B.; Murray, K. S.; Tiekink, E. R. T. *Z. Kristallogr. New Cryst. Struct.* **2003**, *218*, 345.
18. Zhang, R. L.; Zhao, J. S.; Shi, Q. Z.; Ng, S.W. *Acta Cryst*. **2003**, *E59*, 476.

19. Bushuev, M. B.; Virovets, A. V. Garcia, Y.; Christine Gieck, Sheludyakova, L. A.; Ikorskii, V. N.; Tremel, W.; Gütlich, P. Lavrenova, L. G. *Polyhedron* **2002**, *21*, 797.

20. Chen, Z.-F.; Xiong, R.-G.; Zhang, J., Chen, X.-T.; Xue, Z.-L.; You, X.-Z. *Inorg. Chem.* **2001**, *40*, 4075.

21. Palenik, G. J.; Wester, D. W.; Rychlewska, U.; Palenik, R. C. *Inorg. Chem.* **1976**, *15*, 1814.

22. Bino, A. Frim, R. Genderen, M. V. *Inorg. Chim. Acta* **1987**, *127*, 95.

23. Pappalardo, S.; Bottino, F.; Finocchiaro, P.; Mamo, A. Fronczek, F. R. *J. Inclusion Phenom. Macrocyclic Chem.* **1987**, *5*, 153.

24. Hueso-Ureña, F.; Jiménez-Pulido, S. B.; Moreno-Carretero, M. N.; Quirós-Olozábal. M.; Salas-Peregrín, J. M. *Inorg. Chim. Acta* **1998**, *277*, 103.

25. Nordell, K. J.; Schultz, K. N.; Smith, M. D. *Acta Cryst*. **2004**, *E60*, m857.

26. Bacchi, A.; Pelizzi, G.; Minardi, G.; Pistuddi, A. M.; Solinas, C.; Chelucci, G. *Transition Met. Chem.* **2002**, *27*, 274.

27. Virovets, A. V.; Bushuev, M. B.; Lavrenev, L. G. *Russ. J. Struct. Chem*. **2000**, *41*, 871.

28. Wang, J.-G.; Du, Q.-Y.; Li, P.-Y. *Chinese J. Struct. Chem.* **2006**, *25*, 747.

29. Fabian, L.; Kalman, A. *Acta Cryst.* **2004**, *B60*, 547.

30. Batten, S. R.; Robson, R. *Angew. Chem., Int. Ed*. **1998,** *37*, 1461.

CHAPTER III

DFT and TDDFT studies of mononuclear fluoro manganese(III) complexes.

3.1. Introduction

Superoxide dismutases are important antioxidant enzymes widely distributed in prokaryotic and eukaryotic cells[1,2]. Mononuclear Mn(III) sites are known to be present in superoxide dismutase enzymes (Mn-SOD) which catalyse the disproportionation of O_2^- ion. Crystallographic and spectroscopic studies show that the site is five coordinate[3]. Nevertheless, manganese(III) compounds are attractive systems for studying optical properties associates with Jahn-Teller distortion. These complexes are of interest in view of the vibronic instability of Mn^{3+} in octahedral ligand fields and its effect on structure and optical absorption of crystals. Mn^{3+} in aqueous solution readily undergoes disproportionation in presence of diimine ligands, *viz*., 2,2'-bipyridine (bpy) and 1,10-phenanthroline (phen) and their derivatives, leading to mixed valent complexes containing the dioxobridged core, $[Mn_2O_2]^{3+}$ [4-10]. Mononuclear Mn(III) complexes containing diimine ligands are, therefore, relatively small in number. The structurally characterized complexes are $[Mn(phen)_2Cl_2]NO_3.2.5CH_3COOH$[11], $Mn(phen)(OH_2)Cl_3$[12] and $Mn(bpy)F_3(OH_2)$[13]. Detailed assignments of the optical transitions based on polarized absorption studies have been made for the fluoro manganese complex of bpy. In this chapter we report various mononuclear flouro manganese complexes of

phen and bpy. Calculations based on density functional theory (DFT) have also been performed to check its usefulness for the assignment of electronic transition energies of this d^4 system.

3.2. Experimental

3.2.1. Reagents

All chemicals were purchased from Ranbaxy chemicals and used without further purification. $Mn(OAc)_3.2H_2O$ was prepared using a reported procedure[15].

3.2.2 Synthesis

Preparation of $[Mn(bpy)F_2(H_2O)_2]NO_3.H_2O$ (1). Manganese(III) acetate (1.608 g, 6.00 mmol) was added to 10 mL of 1.6N HNO_3 containing 2,2'-bipyridine (0.936 g, 6.00 mmol) and stirred for 10-15 minutes, the dark green solution was filtered and 10.0 mL of HF (48%) was added to it. This solution was kept aside at room temperature for 3-4 days over which period dark green crystals were deposited. Yield 1.525 g (4.18 mmol, 69.7%). Anal. Calcd. for $MnC_{10}H_{14}N_3O_6F_2$ (M.W, 365.17) C, 32.89; H, 3.86; N, 11.51. Found: C, 33.28; H, 3.89; N, 11.51. Important IR absorptions (KBr disk, cm^{-1}): 3395, 1604, 1564, 1504, 1450, 1385, 1039, 775, 727 and 601.

Preparation of $Mn(bpy)F_2(H_2O)Cl$ (2) Manganese(III) acetate (0.402 g, 1.50 mmol) was added to a 5.0 mL of 1.1 N HCl containing 2,2'-bipyridine (0.234 g, 1.50 mmol) and stirred for 10-15 minutes, the dark green solution was filtered and 2.5 mL of HF(48%) was added to it. This solution was kept aside at room temperature for 3-4 days over which period dark green crystals were deposited. Yield 0.193 g (0.638 mmol 42.5%). Anal. Calcd. for $MnC_{10}H_{10}N_2OClF_2$ (M.W,

302.6) C, 39.69; H, 3.30; N, 9.26. Found: C, 39.00; H, 3.39; N, 9.81. Important IR absorptions (KBr disk, cm^{-1}): 3342, 1602, 1498, 1450, 1311, 1251, 1165, 1107, 1037, 779, 725, 659 and 604.

Preparation of $[Mn(phen)F_3(H_2O)].H_2O$ (3) $[Mn(phen)F_3(H_2O)]$ (4) Manganese(II) acetate (0.735 g, 3.00 mmol) and 1,10-phenanthroline monohydrate (0.960 g, 4.84 mmol) were dissolved in 24 mL 1:1 glacial acetic acid / water mixture. To this solution, $KMnO_4$ (0.120 g 0.759 mmol) dissolved in minimum amount of water was added slowly, stirred for 10 minutes and filtered. To the above dark brown solution, 6mL of 48% hydrofluoric acid was added and allowed to stand. Brown crystals were deposited within 24h. Yield 0.568 g (1.73 mmol, 57.6%). Anal. cald. for $MnC_{12}H_{12}N_2O_2F_3$ (M.W. 328.17): C, 43.92; H, 3.69; N, 8.54. Found: C, 44.04; H, 3.53; N, 8.92. Important IR absorptions (KBr disk, cm^{-1}): 3339, 3076, 2355, 1649, 1626, 1579, 1518, 1425, 1342, 1104, 1101, 850, 723, 576, and 420. Close examination of the sample revealed the presence of two types of crystals. The vast majority of the crystals having rough surfaces were found to be the monohydrate (**3)** while the minor component, which were more lustrous and free of surface defects are found to be the anhydrous form (**4**).

Preparation of $[Mn(phen)F_2(H_2O)_2]NO_3.(H_2O)_{1/2}$ (**5**). 1,10-Phenanthroline monohydrate (0.300 g, 1.514 mmol) and manganese(III) acetate (0.402 g, 1.50 mmol) were dissolved in 5 mL of 1.6 N HNO_3 and stirred for 5-10 minutes. To the dark brown solution 0.60 mL of 48 % HF was added and filtered. The solution was kept aside at room temperature for 3-4 days over which period dark brown crystals were deposited. Yield 0.232 g (0.61 mmol, 40.8%) Anal. cald. for $MnC_{12}H_{13}N_3F_2O_6$ (M.W. 388.18): C, 37.13; H, 3.36; N, 10.82. Found: C, 37.52;

3.28; N, 10.92. Important IR absorptions (KBr disk,cm^{-1}): 3302, 3069 1635, 1581, 1521, 1491, 1413, 1361 1315, 1145, 1109, 1033, 877, 850, 748, 719 and 621.

Preparation of Mn(phen)F_2(H_2O)Cl (**6**). 1,10-phenanthroline monohydrate and manganese(III) acetate (0.268 g, 1.00 mmol) were dissolved in 10 mL of 1:1 of 1.1 N HCl / glacial acetic acid mixture and stirred. To the dark brown solution 5 mL of 48 % HF was added. The solution was filtered and allowed to stand. Brown crystals were formed with in few days. Yield 0.102 g (0.46 mmol, 46 %) Anal. cald. For $MnC_{12}H_{10}N_2O_1ClF2$ (M.W. 326.61): C, 44.13, H, 3.09; N, 8.58. Found: 44.62; 3.02; 8.74. Important IR absorptions (KBr disk, cm^{-1}): 3348, 3234, 1950, 1647, 1626, 1583, 1516, 1425, 848, 723, 642, 424.

3.3. Computational methods

DFT and time dependent DFT (TDDFT) calculations were done using the B3LYP exchange correlation functional[16] as implemented in the Gaussian-03[17]. The spin-unrestricted version was employed for open shell ions. For both types of calculations, triple-ζ basis sets[18] were used for Mn atom and double-ζ basis sets[19] were used for all other atoms. Other basis sets in the Gaussian-03 suite were also used for comparison.

3.4. Measurements

IR spectra were obtained with a Shimadzu FT-IR 8000 spectrometer. Elemental analysis was obtained using a FLASH EA 1112 SERIES CHNS analyzer. Diffuse reflectance spectra were measured by using a Shimadzu UV-3100 spectrometer equipped with an ISR-3100 integrating sphere attachment.

3.4.1. Crystallographic data collection and structure determination

Data were collected on a Brucker SMART APEX CCD X-ray diffractometer using graphite monochromated Mo Kα radiation. The data were reduced using SAINTPLUS[20], and multiscan absorption corrections using SADABS[21] were applied. The structures were solved using SHELXS-97 and refined using SHELXL-97[22]. All ring hydrogen atoms were assigned on the basis of geometrical considerations and were allowed to ride upon the respective carbon atoms. All water hydrogen atoms were located from the difference Fourier maps and bond length constraints were applied. Crystal data are in Table 3.1, 3.5 and important interatomic distances and angles in Table 3.2, 3.3, 3.6 and 3.8.

3.5. Crystal structure.

3.5.1 Crystal structures of $[Mn(bpy)F_2(H_2O)_2]NO_3.H_2O$ (1) and $Mn(bpy)F_2(H_2O)Cl$ (2). Both $[Mn(bpy)F_2(H_2O)_2]^+$ (Figure 3.1) and $Mn(bpy)F_2(H_2O)Cl$ (Figure 3.2) have distorted octahedral geometry with bpy and the two F^- ions in the equatorial plane and OH_2 and Cl^- along the axial positions. The in-plane bond distances (Å) are in the range, Mn-N 2.023 - 2.029 and Mn-F 1.798 - 1.871, while the axial bond distances are 2.172 - 2.253 for Mn-OH_2 and 2.559 for Mn-Cl. The axial elongation is typical of Mn^{3+} which has the Jahn-Teller active d^4 configuration. In both structures the Mn atom and the equatorial coordinating atoms are almost exactly coplanar (mean deviation 0.0152 Å for **1** and 0.0463 Å for **2**). However the two trans angles are greatly different due to small bite angle of the bpy ligand. The axial bonds are approximately perpendicular to the

equatorial plane, the angle between the mean plane and axial bonds (˚) being 88.91 (0.05) and 87.47 (0.04) (**1**), 89.74 (0.05) and 83.47 (0.03) (**2**).

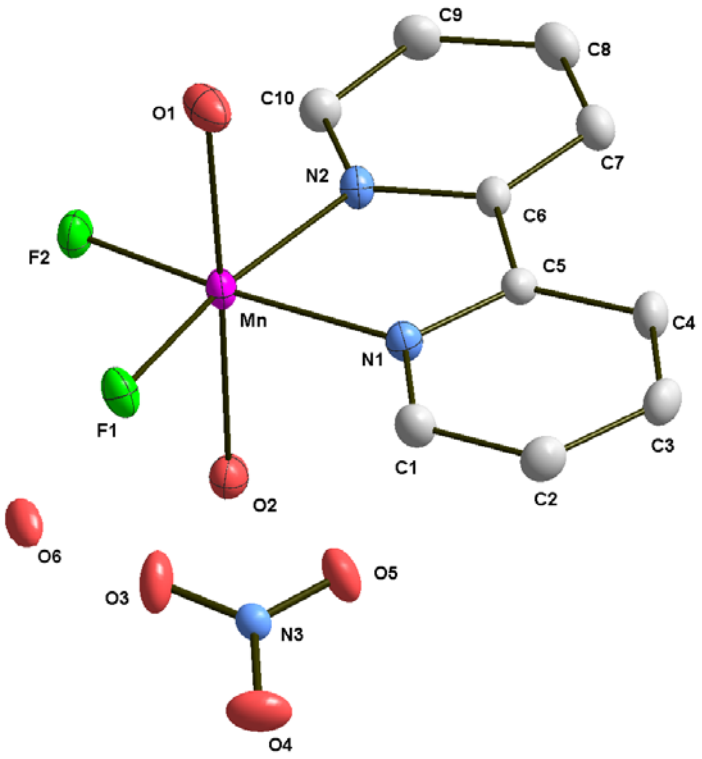

Figure 3.1. Thermal ellipsoid plot of the coordination environment of the complex molecules **1**. Atoms are represented as 50% probability ellipsoids and ring and water hydrogens have been omitted for clarity.

Coming to the crystal packing, both structures exhibit network formation through hydrogen bonding. One-dimensional chains are formed through the intermolecular interaction of the coordinated water molecules in **1** (Figure 3.3) and the coordinated water molecules and Cl^- ion in **2** (Figure 3.4). These chains are further linked by hydrogen bonding with F^- ion. In **1**, lattice water molecule and NO_3^- ion also

participate in hydrogen bonding. Important hydrogen bonding contacts are in Table. 3.4

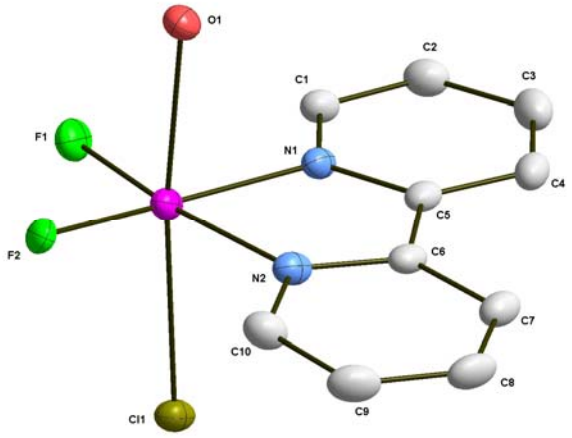

Figure 3.2. Thermal ellipsoid plot of the coordination environment of the complex molecules **2**. Atoms are represented as 50% probability ellipsoids and ring and water hydrogens have been omitted for clarity.

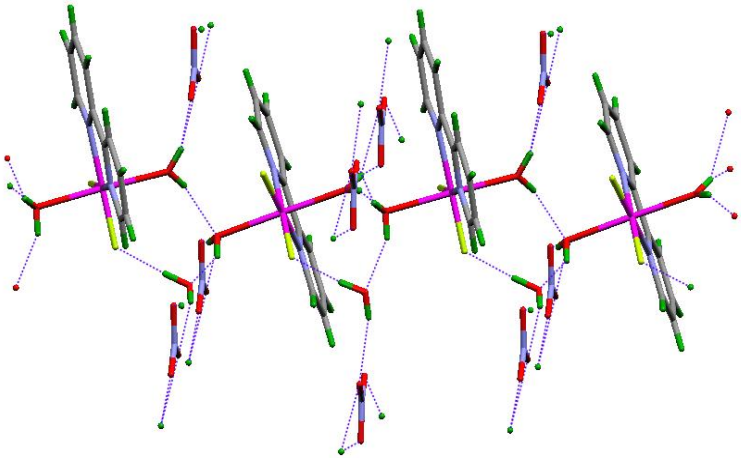

Figure 3.3 Crystal packing of **1**, which exhibits a network formation through intermolecular interactions of coordinated water molecules and through the interactions of lattice water and NO_3^-.

Table 3.1. Crystallographic data for **1**, **2** and **3**

	1	**2**	**3**
Formula	$MnC_{10}H_{14}N_3O_6F_2$	$MnC_{10}H_{10}N_2OClF_2$	$MnC_{12}H_{12}F_3N_2O_2$
Formula weight	365.17	302.6	328.18
Crystal system	monoclinic	monoclinic	Monoclinic
Space group	C*c*	$P2_1/c$	$P2_1/c$
a (Å)	8.9329(6)	9.7203(9)	8.580(3)
b (Å)	14.0864(6)	9.3549(9)	7.302(3)
c (Å)	11.1791(6)	13.1337(12)	21.667(7)
β (^{o})	91.772(10)	110.416(10)	110.354(12)
V (Å^3)	1406.02(13)	1119.26(18)	1272.7(8)
Z	4	4	4
T (ºC)	100 (2)	100 (2)	298(2)
λ (Å)	0.71073	0.71073	0.71073
D_{calc} (g cm^{-3})	1.725	1.796	1.713
μ (mm^{-1})	1.0	1.427	1.076
F(000)	744	608	664
Crystal size (mm)	0.47 x 0.35 x 0.33	0.48 x 0.36 x 0.27	0.31 x 0.17 x 0.13
θ Range (º)	2.70-28.25	2.24-28.26	2.01-28.23
h/k/l	-11, 11 / -18, 18 / 14, 14	-12, 12 / -11, 12 / 17 -17	-11, 11 /-9, 9, / -28, 28
Reflection collected	7970	12144	13890
Unique reflect.,[R_{int}]	3268 [0.0264]	2669 [0.0264]	3019 [0.0305]
Goodness of fit on F^2	1.042	1.062	1.161
R_1 [I>2σ(I)]	0.0250	0.0346	0.0526
wR_2 (all data)	0.0670	0.0940	0.1169

Table 3.2. Selected bond lengths [Å] and angles [°] for **1**.

Mn-F(1)	1.8382(11)	F(2)-Mn-O(1)	92.41(6)
Mn-F(2)	1.7982(11)	N(1)-Mn-N(2)	79.24(6)
Mn-N(1)	2.0265(15)	F(1)-Mn-O(1)	90.81(6)
Mn-N(2)	2.0290(15)	N(1)-Mn-O(1)	90.01(7)
Mn-O(1)	2.1725(12)	N(2)-Mn-O(1)	90.34(6)
Mn-O(2)	2.2154(12)	F(2)-Mn-O(2)	86.94(6)
F(2)-Mn-F(1)	95.80(5)	F(1)-Mn-O(2)	87.41(6)
F(2)-Mn-N(1)	171.26(6)	N(1)-Mn-O(2)	90.90(6)
F(1)-Mn-N(1)	92.56(6)	N(2)-Mn-O(2)	91.54(6)
F(2)-Mn-N(2	92.34(6)	O(1)-Mn-O(2)	178.03(7)
F(1)-Mn-N(2)	171.72(6)		

The most striking feature of the two structures is the large difference (0.04 - 0.05 Å) in the two Mn-F distances. In the only other known difluoro complex Mn^{3+}, the distances are equal within experimental error and in trifluoro complex the equatorial Mn-F distances are very similar. In both **1** and **2**, the F^- ion, which participates as a hydrogen bond acceptor, has the larger Mn-F bond distance. Therefore, in both crystals, the differential Mn-F interaction within the chromophore correlates well with the differential intermolecular interactions. It may be noted that the axial bond distances also show differences. These are however, bonds rendered particularly labile by vibronic interactions and they are often subject to perturbation by lattice effects. In the anisotropy of the in-plane Mn-F bonds, representing a hard base-hard acid interaction, one witnesses a true competition between two non-covalent forces, one weak (hydrogen bond) and another strong (coordinate bond).

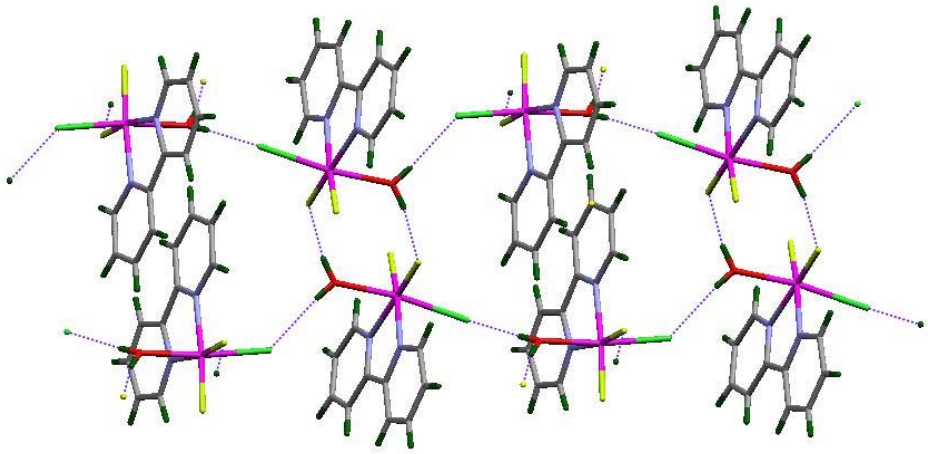

Figure 3.4 Crystal packing of **2**, which exhibit a network formation through coordinated water and chlorine molecules.

Table 3.3 Selected bond lengths [Å] and angles [°] for compound **2**

Mn-F(1)	1.8172(13)	N(1)-Mn-N(2)	78.86(7)
Mn-F(2)	1.8711(12)	F(1)-Mn-O(1)	90.09(6)
Mn-N(1)	2.0228(17)	F(2)-Mn-O(1)	87.37(6)
Mn-N(2)	2.0260(17)	N(1)-Mn-O(1)	87.00(6)
Mn-O(1)	2.2534(15)	N(2)-Mn-O(1)	89.80(6)
Mn-Cl(1)	2.5594(6)	F(1)-Mn-Cl(1)	95.92(4)
F(1)-Mn-F(2)	95.75(6)	F(2)-Mn-Cl(1)	95.55(4)
F(1)-Mn-N(1)	92.23(6)	N(1)-Mn-Cl(1)	89.20(5)
F(2)-Mn-N(1)	170.24(6	N(2)-Mn-Cl(1)	83.70(5)
F(1)-Mn-N(2)	171.07(7)	O(1)-Mn-Cl(1)	173.01(4)
F(2)-Mn-N(2)	93.16(7)		

Table. 3.4 Intermolecular interactions in **1** and **2**

D-H…A	D-H (Å)	D-H….A (Å)	D….A (Å)	∠DHA (º)
		1		
O6-H62… F1	0.854	1.833	2.683	173.71
O2-H21… O6	0.791	1.955	2.653	146.88
O2-H22… O5	0.762	2.059	2.760	160.82
O6-H61… O3	0.795	2.068	2.827	159.63
O1-H11… O2	0.807	2.062	2.843	162.84
O1-H12… O4	0.810	2.204	2.912	146.14
O1-H12… O3	0.810	2.290	3.009	148.22
		2		
O-H12… Cl	0.751	2.387	3.135	174.13
O-H11… F2	0.878	1.876	2.736	169.89

3.5.2. Crystal structures of [Mn(phen)F_3(H_2O)].H_2O (3) [Mn(phen)F_3(H_2O)] (4)

[Mn(phen)F_3(H_2O)].H_2O complex has been previously reported[14], but structure was not characterized. The molecular structures of the complexes (Fig. 3.5 and Fig. 3.6) in both crystals are grossly similar and comparable to that of the bpy analogue[13]. They consist of a Mn(III) ion coordinated to three fluoride ions, a water molecule and a phen ligand. The octahedron around Mn(III) is highly distorted, the Jahn-Teller effect leading to elongated axial bonds.

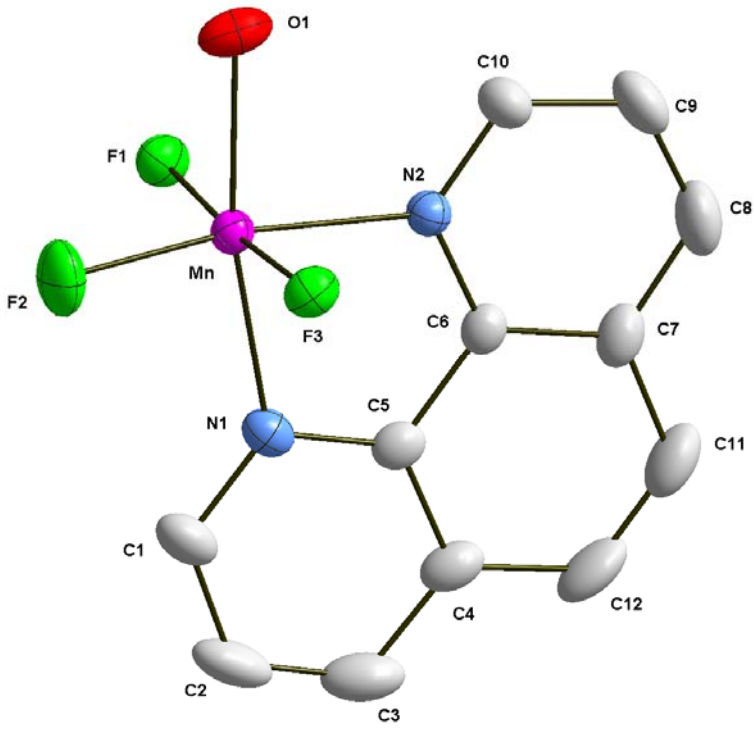

Figure 3.5 Thermal ellipsoid plot of the coordination environment of the complex molecules **3** Atoms are represented as 50% probability ellipsoids and ring and water hydrogens have been omitted for clarity.

One imine N atom and the water oxygen atom are situated on the distortion axis: Mn-N1 2.238(3), Mn-O1 2.148(2) Å for **3**; Mn-N1, 2.255(2), Mn-O 2.162(2) Å for **4**. Coming to the crystal packing (Figure. 3.7), in both **3** and **4** H-bonding between coordinated fluoride ions and water molecule assembles the complex molecules into a chain along the *b* axis (F1…O1 2.651(3) Å, F3…O1 2.634(3) Å in **3** and F3…O 2.659(2) Å, F1…O 2.609(2) Å in **4**).

Table 3.5. Crystallographic data for **4, 5** and **6**

	4	**5**	**6**
Formula	$MnC_{12}H_{10}F_3N_2O$	$MnC_{12}H_{10}N_2OClF_2$	$Mn_4C_{48}H_{48}N_{12}O_{21}F_8$
Formula weight	310.16	326.61	1500.74
Crystal system	Monoclinic	monoclinic	monoclinic
Space group	$P2_1/c$	C2/*c*	C2/*c*
a (Å)	8.3505(7)	21.012(11)	12.5686(6)
b (Å)	7.2723(6)	7.324(4)	29.9081(15)
c (Å)	19.1759(17)	17.030(9)	15.2227(7)
β (º)	101.7890(10)	106.702	93.2120(10)
V (Å^3)	1139.94(17)	2510(2)	5713.3(5)
Z	4	8	4
T (K)	100(2)	298(2)	100 (2)
λ (Å)	0.71073	0.71073	0.71073
D_{calc} (g cm^{-3})	1.807	1.729	1.745
μ (mm^{-1})	1.190	1.280	0.980
F(000)	624	1312	3040
Crystal size	0.21 x 0.16 x 0.15	0.37 x 0.31 x 0.22	0.2 x 0.16 x 0.15
θ Range (º)	2.17-28.09	2.02-25.00	1.36-24.99
h/k/l	-10, 10, / -9, 9 / -25 25	-24, 24 / -8, 8 / -20 20	-14, 14 / -35, 35 / -18 18
Reflection collectec	12662	11155	27351
Unique reflect., [R_{int}]	2708 [0.0361]	2211 [0.0336]	5035 [0.0449]
Goodness of fit on F^2	1.082	1.113	1.361
R_1 [$I>2\sigma(I)$]	0.0354	0.0663	0.0684
wR_2 (all data)	0.0831	0.1746	0.1373

Table 3.6. Selected bond lengths [Å] and angles [°]

		3	
Mn-F(1)	1.8163(17)	O(1)-Mn-N(1)	169.88(10)
Mn-F(2)	1.8559(18)	F(1)-Mn-N(2)	90.25(9)
Mn-F(3)	1.8230(17)	F(3)-Mn-N(2)	86.79(8)
Mn-N(1)	2.238(3)	F(2)-Mn-N(2)	170.80(9)
Mn-N(2)	2.090(2)	F(1)-Mn-O(1)	89.06(8)
Mn-O(1)	2.148(2)	F(3)-Mn-O(1)	87.62(8)
F(1)-Mn-F(3)	175.43(7)	F(2)-Mn-O(1)	95.84(11)
F(1)-Mn-F(2)	92.23(9)	N(2)-Mn-O(1)	93.05(10)
F(3)-Mn-F(2)	91.23(9)	F(1)-Mn-N(1)	92.40(8)
F(2)-Mn-N(1)	94.11(10)	F(3)-Mn-N(1)	90.33(8)
N(2)-Mn-(1)	76.93(9)		
		4	
Mn-F(1)	1.8465(12)	F(1)-Mn-N(2)	86.22(6)
Mn-F(2)	1.8071(12)	F(2)-Mn-O	96.68(6)
Mn-F(3)	1.8379(12)	F(3)-Mn-O	90.85(6)
Mn-N(1)	2.2554(17)	F(1)-Mn-O	86.25(6)
Mn-N(2)	2.0750(17)	N(2)-Mn-O	91.23(6)
Mn-O	2.1621(16)	F(2)-Mn-N(1)	95.33(6)
F(2)-Mn-F(3)	93.52(6)	F(3)-Mn-N(1)	93.63(6)
F(2)-Mn-F(1)	92.09(6)	F(1)-Mn-N(1)	88.10(6)
F(3)-Mn-F(1)	173.95(5)	N(2)-Mn-N(1)	76.59(6)
F(2)-Mn-N(2)	171.79(6)	O-Mn-N(1)	166.89(6)
F(3)-Mn-N(2)	88.54(6)		

In **3** there is an additional hydrogen bond between fluoride ion and lattice water molecule (F2…O2, 2.397(5) Å). The adjacent H-bonded chains interact through π-stacking leading to an interdigitized packing. The stacking distances are in the range 3.448(5) - 3.599(5) Å for **3** and 3.374(3) - 3.563(3) Å for **4**. The above arrangement produces channels along the *a*-axis in both crystals. The slight differences in the

relative orientation of the molecules in adjacent chains lead to differences in the channel width such that in **3** it can accommodate water molecules while in **4** it remains empty.

Table 3.7. Correlation between H-bonded donor-acceptor (F…O) distances and Mn-F bond distances.

		[Mn(phen)F_3(H_2O)]. H_2O (**3**)		
Donor (D)	<DHA (°)	D…A (Å)	Acceptor (A)	Mn-A (Å)
O2	128(7)	2.397(5)	F2	1.856(2)
O1	173(6)	2.634(3)	F3	1.822(2)
O1	173(10)	2.651(3)	F1	1.817(2)
		Mn(phen)F_3(H_2O) (**4**)		
O	176(3)	2.609(2)	F1	1.8465(12)
O	176(3)	2.659(2)	F3	1.8379(12)
		Mn(bpy)F_3(H_2O)[13]		
O1		2.633(3)	F1	1.8386(14)
O1		2.649(3)	F3	1.835(2)

The complex molecule in **3** and **4** may be regarded as distortion isomers of Mn(phen)(OH_2)F_3. There are subtle differences between their geometries brought about by the interplay of intramolecular and intermolecular interactions. As seen from Table 3.7, there is a negative correlation between Mn-F bond distances and the H- bond donor - acceptor distances.

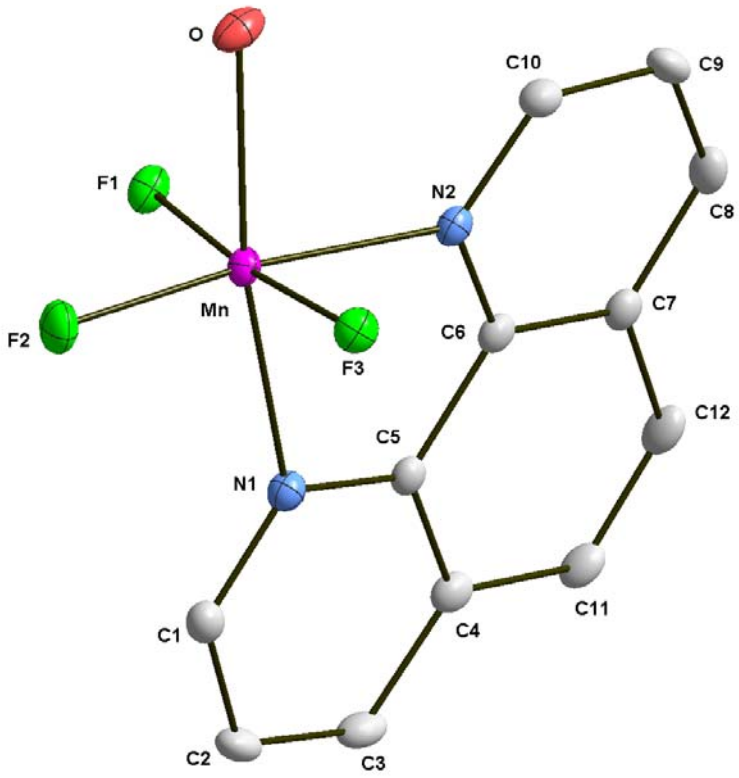

Figure 3.6 Thermal ellipsoid plot of the coordination environment of the complex molecules **4**. Atoms are represented as 50% probability ellipsoids and ring and water hydrogens have been omitted for clarity.

In spite of significant deviation between individual Mn-F distances, their average value is same in the two compounds (1.832(2) Å in **3** and 1.830(1) Å in **4**). The two isomers differ in the extend of Jahn-Teller distortion. The average axial bond length is 2.193(2) Å in **3** compared to 2.209(2) Å in **4**. The increased axial elongation in **4** is accompanied by a concomitant reduction in the two trans bond distances, Mn-N2 and Mn-F2. However, the other two trans Mn-F bonds which are influenced by H-bonding remain significantly longer. The intermolecular interactions therefore, lead

to the unusual situation of equatorial *trans* bonds getting simultaneously elongated or shortened. That intermolecular interactions can often extend a significant influence on coordination geometry has been previously noted[23-24]. In the present case, the equatorial bond distances of the Mn(III) complex are greatly perturbed by H-bonding interaction in both crystals.

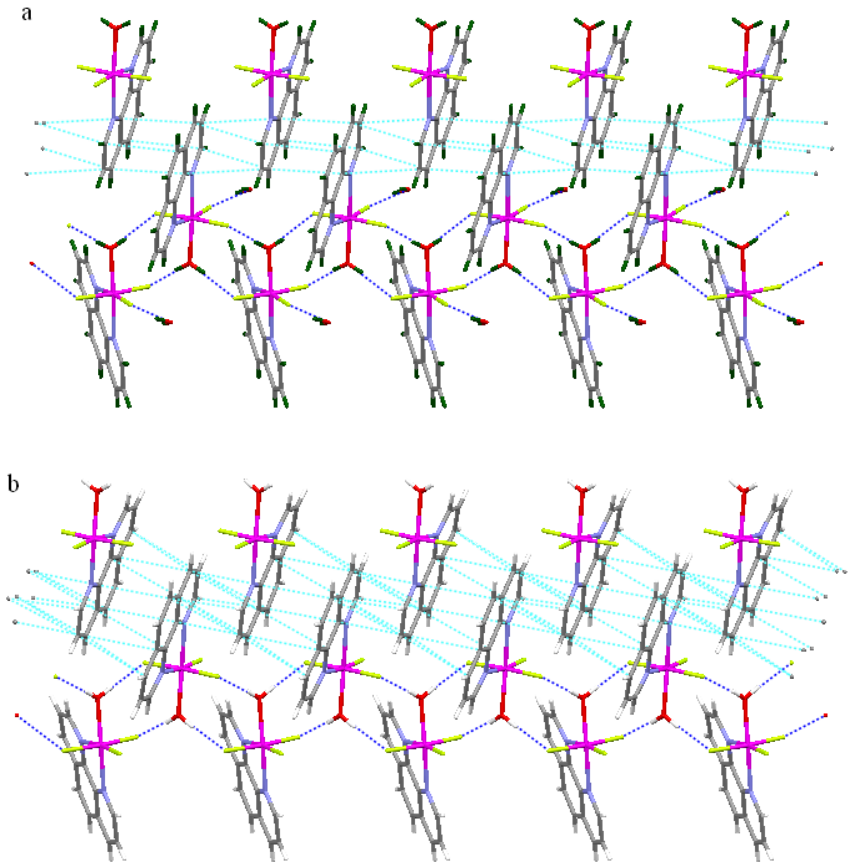

Figure 3.7 Crystal packing showing hydrogen bonding (blue) and π-stacking (light blue) networks: **(a) 3**; **(b) 4**.

The distortions are then compensated by adjusting the axial interactions, the process being facilitated by the Jahn-Teller plasticity of the coordination polyhedron. It may be noted that the bond valance sum remains identical in both the structures at 3.2 (expected value 3).

3.5.3. Crystal structures of $[Mn(phen)F_2(H_2O)_2]NO_3.(H_2O)_{1/2}$ (**5**) and $Mn(phen)F_2(H_2O)Cl$ (**6**).

Both complexes have distorted octahedral geometry. There are two crystallographically independent, but chemically similar $[Mn(phen)F_2(H_2O)_2]^+$ cations in the unit cell of **5**. Coordination mode of **5** is grossly similar to that of **1**, where both OH_2 molecules are on distortion axis. But coordination mode of **6** is similar to that of **4**, where one imine N atom and the water oxygen atom are situated on the distortion axis (Mn-N(1) 2.123(4) Å, Mn-O 2.148(4) Å) (Figure 3.8 and Figure 3.9). The in-plane bond distances (Å) are in the range, Mn-F 1.786(3) – 1.834(3) and Mn-N 2.029(4) – 2.123(4). The Mn-Cl distance in **6** is 2.292(2) Å. In **5** the Mn atoms and the equatorial coordinating atoms are almost exactly coplanar (mean deviation 0.0265 Å for Mn1 and 0.0415 Å for Mn2) but it deviate considerably in **6** (0.1270 Å). The cation $[Mn(phen)F_2(H_2O)_2]^+$ in **5** form two-dimensional hydrogen bonded networks on *ac* plane (Figure 3.10). Mn2 form ladder like double chain by O-H…O and O-H…F hydrogen bonds along *c* axis. Mn1 cations itself form hydrogen bonded chain along *c* axis. Interestingly O-H…O and O-H...F interactions interconnect these Mn1 and Mn2 chains into two-dimension to form a hydrogen bonded networks with shortest Mn…Mn distance of 5.105 Å (Figure. 3.11). Intermolecular interaction perturbs the equatorial Mn-F

bonds. The Mn1-F1, Mn2-F3 and Mn2-F4 bonds, which have significant hydrogen bond interactions, are longer than the Mn1-F2 bond.

Table 3.8. Selected bond lengths [Å] and angles [°] for **5**

Mn(1)-F(2)	1.786(3)	N(2)-Mn(1)-O(1)	85.30(14)
Mn(1)-F(1)	1.834(3)	F(2)-Mn(1)-O(2)	88.44(13)
Mn(1)-N(1)	2.030(4)	F(1)-Mn(1)-O(2)	94.47(14)
Mn(1)-N(2)	2.042(4)	N(1)-Mn(1)-O(2)	91.07(15)
Mn(1)-O(1)	2.180(3)	N(2)-Mn(1)-O(2)	88.82(15)
Mn(1)-O(2)	2.184(4)	O(1)-Mn(1)-O(2)	173.88(14)
Mn(2)-F(4)	1.820(3)	F(4)-Mn(2)-F(3)	96.90(13)
Mn(2)-F(3)	1.828(3)	F(4)-Mn(2)-N(4)	170.66(14)
Mn(2)-N(4)	2.029(4)	F(3)-Mn(2)-N(4)	91.51(14)
Mn(2)-N(3)	2.052(4)	F(4)-Mn(2)-N(3)	91.16(14)
Mn(2)-O(3)	2.155(4)	F(3)-Mn(2)-N(3)	171.89(14)
Mn(2)-O(4)	2.190(3)	N(4)-Mn(2)-N(3)	80.52(14)
F(2)-Mn(1)-F(1)	95.57(12)	F(4)-Mn(2)-O(3)	94.63(14)
F(2)-Mn(1)-N(1)	173.71(14)	F(3)-Mn(2)-O(3)	90.22(13)
F(1)-Mn(1)-N(1)	90.72(14)	N(4)-Mn(2)-O(3)	89.37(15)
F(2)-Mn(1)-N(2)	93.12(14)	N(3)-Mn(2)-O(3)	88.20(14)
F(1)-Mn(1)-N(2)	170.78(14)	F(4)-Mn(2)-O(4)	89.49(13)
N(1)-Mn(1)-N(2)	80.60(15)	F(3)-Mn(2)-O(4)	87.95(13)
F(2)-Mn(1)-O(1)	93.55(13)	N(4)-Mn(2)-O(4)	86.74(14)
F(1)-Mn(1)-O(1)	91.09(13)	N(3)-Mn(2)-O(4)	93.07(13)
N(1)-Mn(1)-O(1)	86.32(14)	O(3)-Mn(2)-O(4)	175.66(15)

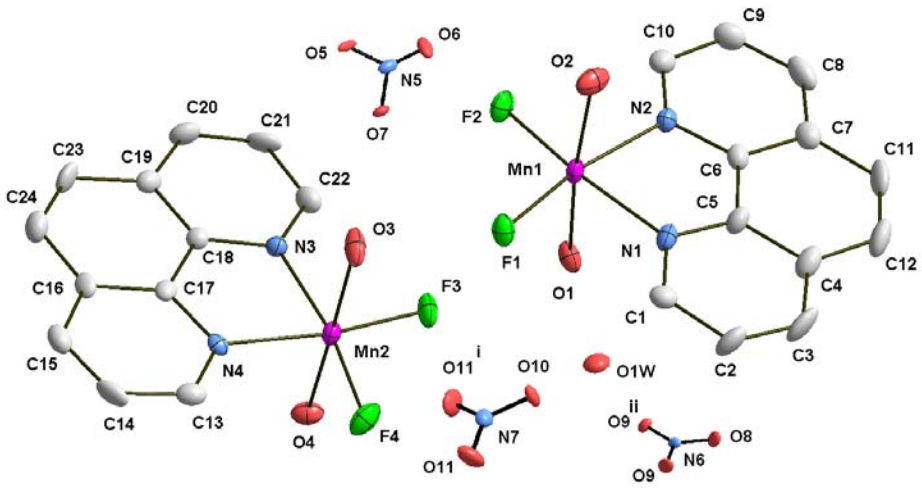

Figure 3.8. Thermal ellipsoid plot of the coordination environment of the complex molecules in **5** Atoms are represented as 50% probability ellipsoids and ring and water hydrogens have been omitted for clarity. symmetry code: (i) -x+1, y, -z+1/2; (ii) -x, y, -z+1/2.

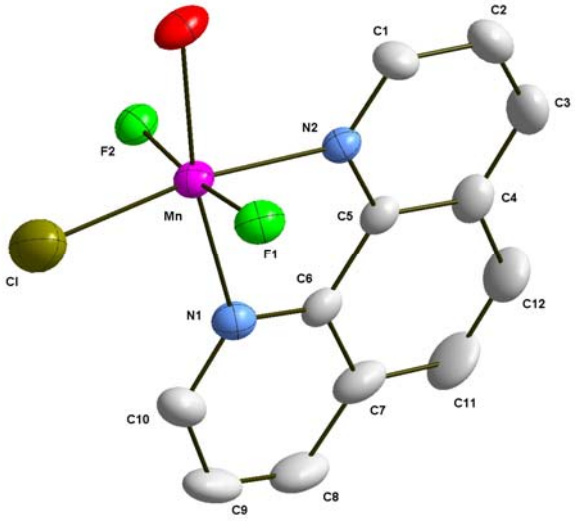

Figure 3.9 Thermal ellipsoid plot of the coordination environment of the complex molecule in **6**. Atoms are represented as 50% probability ellipsoids and ring and water hydrogens have been omitted for clarity.

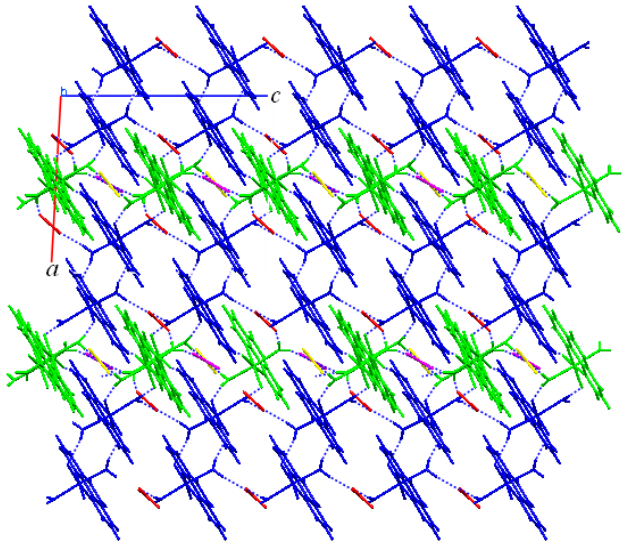

Figure 3.10. Crystal packing of compound **5** showing hydrogen bonding interaction between Mn1 (green) and Mn2 (blue) chains.

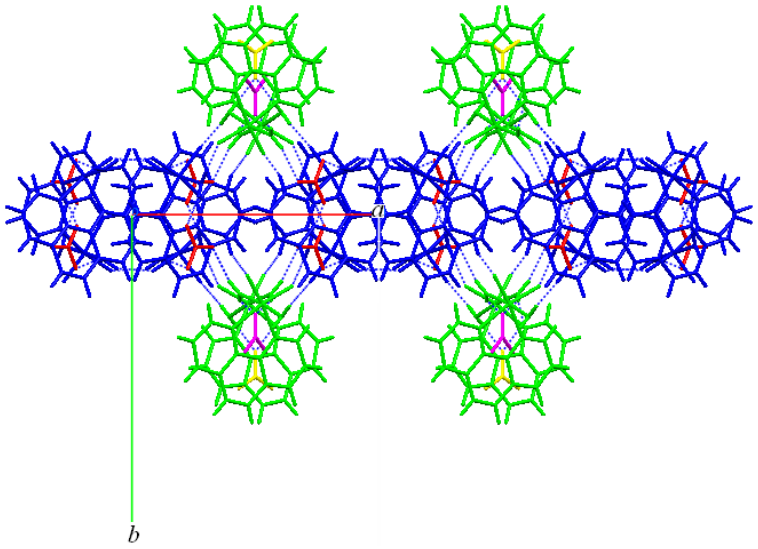

Figure 3.11 View of the Mn1chain (green) and Mn2 chain (blue) down the *c* axis for **5**.

Table. 3.9 Intermolecular interactions in **5** and **6**

D-H…A	D-H (Å)	D-H…A (Å)	D…A (Å)	∠DHA (º)
		5		
O1-H1A…F3	0.80(5)	1.82(5)	2.608(4)	169(5)
O1-H1B…O8	0.83(5)	1.88(5)	2.709(4)	178(6)
O2-H2A…O11	0.81(5)	1.93(5)	2.718(7)	166(5)
O2-H2B…O7	0.83(5)	1.97(5)	2.780(5)	165(4)
O3-H3A…F1	0.82(5)	1.83(5)	2.645(4)	177(7)
O3-H3B…O5	0.80(4)	1.94(4)	2.740(5)	172(5)
O4-H4A…O6	0.83(5)	1.94(5)	2.762(5)	170(6)
O4-H4B…F4	0.82(5)	2.05(5)	2.771(4)	146(5)
O4-H4B…O1W	0.82(5)	2.48(6)	3.080(16)	131(5)
		6		
O-H1A…F2	0.85(6)	1.80(6)	2.628(6)	164(6)
O-H1B…F1	0.80(5)	1.87(4)	2.675(6)	176(7)

$Mn(phen)F_2(H_2O)Cl$ form one-dimensional zig-zag chain by O-H…F and C-H…Cl interaction along *b* axis. Detailed analysis of crystal structure reveals that C-H…Cl interaction form a two-fold helical structure along *b* axis (Figure 3.12). The helical repeat distance is 7.324 Å which is *b* axis translation. There are four enantiomeric helices running through the unit cell. Here the metal coordinated chlorine act as hydrogen bond acceptor while C-H moiety (C1) of the phen ring act as the hydrogen bond donor. The C-H…Cl bond parameters are quite comparable to

those of the reported C-H…Cl systems[25]. In D-H…Cl–M interaction, the intermolecular contacts are categorized as 'short' (2.52 Å) 'intermediate' (2.52-2.95 Å) and long (2.95-3.15 Å) based on the H…Cl distance[26]. The present case belongs to 'intermediate' category according to this classification. It has been shown recently that halogens act as strong hydrogen bond acceptor when bound to transition metals, in contrast to their limited ability to serve as a weak hydrogen bond acceptor when bound to carbon[25, 27].

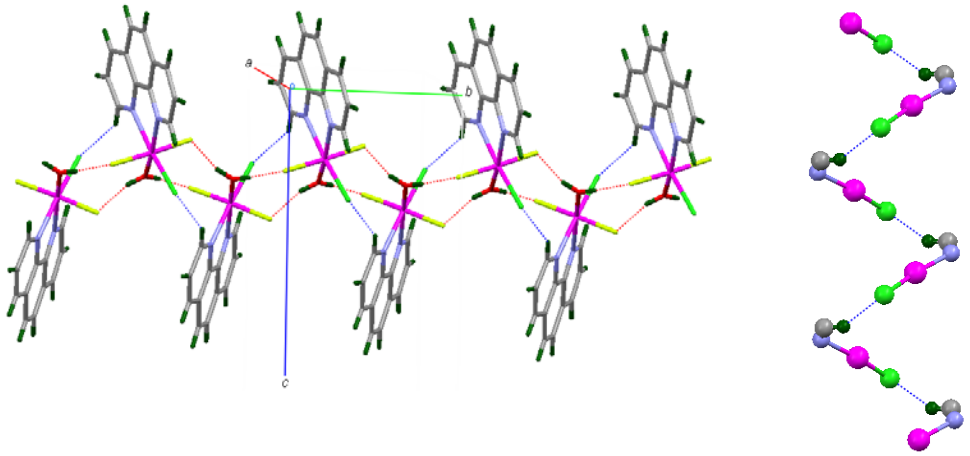

a

b

Figure 3.12 (a) Crystal packing showing O-H…F (red) and C-H…Cl (blue) interactions in **6**. **(b)** C-H…Cl interactions in **6** which lead to a helical structure.

3.6 Electronic spectra

3.6.1. $[Mn(bpy)F_2(H_2O)_2]NO_3 . H_2O$

Diffuse reflectance spectrum of **1** is shown in Figure 3.13 Assuming complex **1** presents an elongation distortion that develops perpendicular to the equatorial plane, the four broad bands below 26000 cm^{-1} may be assigned to *d-d* transitions between the split components of the ^5E and $^5T_2$ states of the d^4 ion as follows: 14310 cm^{-1} ($d_z^2 \rightarrow d_{xy}$); 20330 cm^{-1} ($d_{x^2-y^2} \rightarrow d_{xy}$); 22520 cm^{-1} ($d_{yz} \rightarrow d_{xy}$) and 24100 cm^{-1} ($d_{xz} \rightarrow d_{xy}$). The one electron labels refer to a coordinate system in which the *z*-axis is perpendicular to the mean plane containing Mn, F1, F2, N1 and N2 and the *x*-axis symmetric about the F1-Mn-F2 angle. These assignments are consistent with those published for $[MnF_6]^{3-}$ (ref. 28) and $Mn(bpy)F_3(H_2O)$[13].

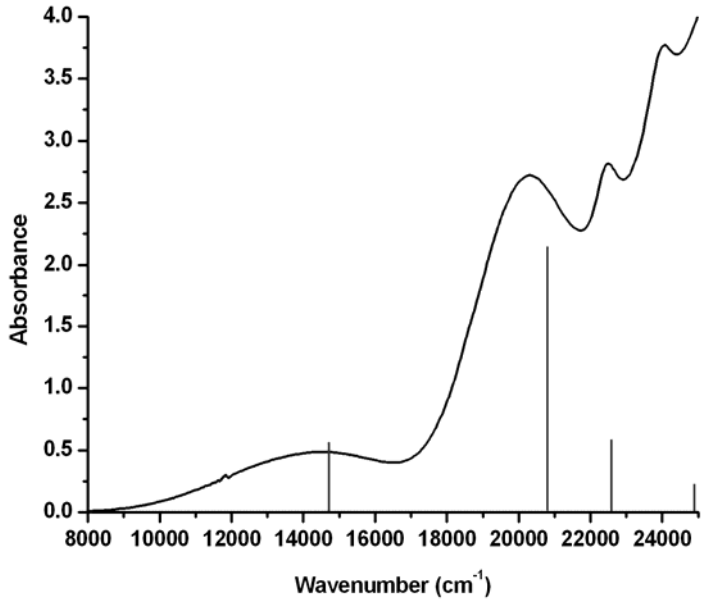

Figure 3.13 Diffuse reflectance spectrum of **1**. The vertical lines indicate the positions of *d-d* absorption maxima calculated using TDDFT.

In recent times, DFT calculations have been used to assign bands in Mn(III) complexes[28]. In order to check the agreement between DFT theory and observed spectra, DFT calculations have been performed on **1** at experimental geometry. The three t_{2g} and one e_g orbital make up the set of *single occupied molecular orbitals* (SOMO'S). The highest energy SOMO was mainly composed of d_z^2 orbital of the manganese ion, whereas the *lowest unoccupied molecular orbital* (LUMO) possessed a manganese d_{xy} character.

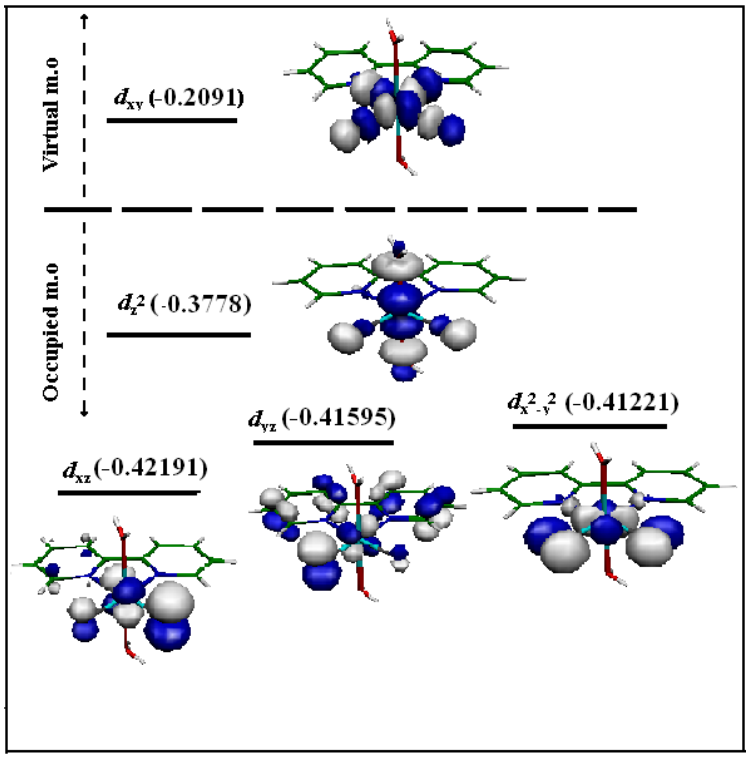

Figure 3.14 The molecular orbitals of $[Mn(bpy)F_2(H_2O)_2]^+$ which have predominantly 3*d* contributions in the spin quintet ground state. Orbital energies (Hartree) are given following the orbital labels.

The molecular orbitals which have predominantly 3*d* contributions in the spin quintet ground state are shown in Figure 3.14 The band positions (cm^{-1}) along with dominant orbital contributions calculated using TDDFT are 14830 ($d_z^2 \rightarrow d_{xy}$), 20877 ($d_x^2{}_{-y}^2 \rightarrow d_{xy}$), 22665 ($d_{yz} \rightarrow d_{xy}$), 24975 ($d_{xz} \rightarrow d_{xy}$). Calculation of the lowest triplet state gave energy of 7571 cm^{-1} for this state.

3.6.2. $Mn(bpy)F_2(H_2O)Cl$

Diffuse reflectance spectrum of **2** is shown in Fig. 3.15. The four broad bands, 13160 cm^{-1}, 20370 cm^{-1}; 22270 cm^{-1} and 23810 cm^{-1} may be assigned to *d-d* transitions between the split components of the ^5E and $^5T_2$ states of the d^4 ion. In order to check the agreement between DFT theory and observed spectra, DFT calculations have been performed on **2** at experimental geometry. The one electron labels refer to a coordinate system in which the *z*-axis is perpendicular to the mean plane containing Mn, F1, F2, N1 and N2 and the *x*-axis symmetric about the F1-Mn-F2 angle.

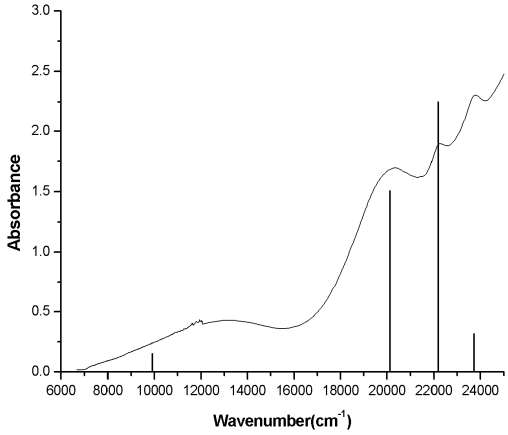

Figure 3.15 Diffuse reflectance spectrum of **2**. The vertical lines indicate the positions of *d-d* absorption maxima calculated using TDDFT.

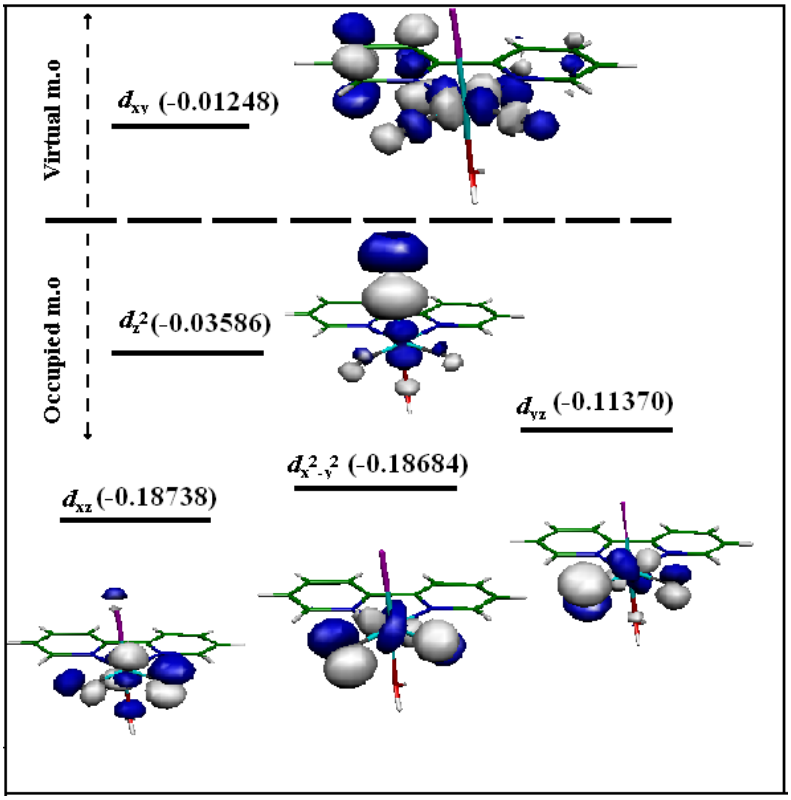

Figure 3.16 The molecular orbitals of $Mn(bpy)F_2(H_2O)Cl$ which have predominantly 3*d* contributions in the spin quintet ground state. Orbital energies (Hartree) are given following the orbital labels.

The molecular orbitals which have predominantly 3*d* contributions in the spin quintet ground state are shown in Figure 3.16 The band positions (cm^{-1}) along with dominant orbital contributions calculated using TDDFT are 9500 ($d_z^2 \rightarrow d_{xy}$), 20100 ($d_{yz} \rightarrow d_{xy}$), 22500 ($d_{x2-y}^2 \rightarrow d_{xy}$), 23500 ($d_{xz} \rightarrow d_{xy}$). Calculation of the lowest triplet state gave energy of 6380 cm^{-1} for this state. It turns out that the energy of the lowest energy spin allowed transition is in poor agreement with experiment. While the spin forbidden transition as well as spin-orbit coupling involving the lowest

triplet state can influence the lowest energy band, these are probably not sufficient to account for the observed difference of 3660 cm^{-1}. In all likelihood, perturbation by lattice strain on the vibronically sensitive $d_z^2 \rightarrow d_{xy}$ transition may be responsible for the discrepancy in this case.

3.6.3. [Mn(phen)F_3(H_2O)] H_2O

Diffuse reflectance spectrum of **3** is shown in Figure 3.17. The three broad bands below 26000 cm^{-1} may be assigned to *d-d* transitions between the split components of the ^5E and $^5T_2$ states of the d^4 ion as follows: 10810 cm^{-1} ($d_z^2 \rightarrow d_{xy}$); 18650 cm^{-1} ($d_{x^2-y^2} \rightarrow d_{xy}$); 22321 cm^{-1} (d_{xz}, $d_{yz} \rightarrow d_{xy}$). The one electron labels refer to a coordinate system in which the *z*-axis is perpendicular to the mean plane containing Mn, F1, F2, F3 and N2 and the *x*-axis symmetric about the F2-Mn-F3 angle. The corresponding transitions in the bpy complex[13] are at 11000 cm^{-1}, 18500 cm^{-1} and (21500, 23000) cm^{-1}. The close similarity between the spectra of two structurally very similar compounds lend support to the above assignment, because the bands in the bpy complex were assigned based on single crystal polarized absorption studies.

In order to check the agreement between DFT theory and observed spectra, DFT calculations have been performed on **3** at experimental geometry. The molecular orbitals which have predominantly 3*d* contributions in the spin quintet ground state are shown in Figure 3.18 The band positions (cm^{-1}) along with dominant orbital contributions calculated using TDDFT are 14447 ($d_z^2 \rightarrow d_{xy}$), 19763 ($d_{x2-y^2} \rightarrow d_{xy}$), 21882 ($d_{xz} \rightarrow d_{xy}$), 24137 ($d_{yz} \rightarrow d_{xy}$). It turns out that the energy of the lowest energy transition is in poor agreement with experiment. Calculation of the lowest triplet state gave an energy of 8820 cm^{-1} for this state.

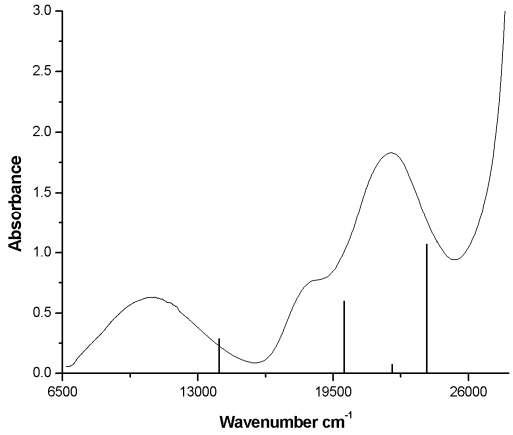

Figure 3.17. Diffuse reflectance spectrum of **3**. The vertical lines indicate the positions of *d*-*d* absorption maxima calculated using TDDFT.

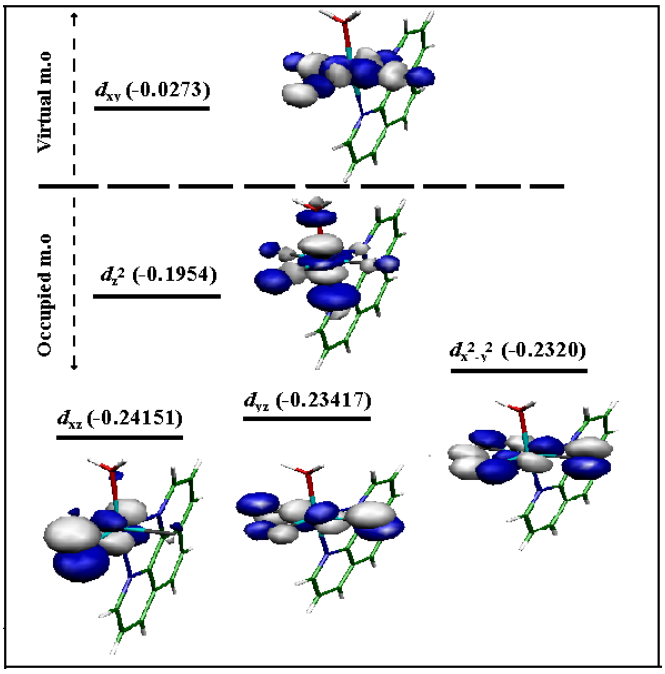

Figure 3.18 The molecular orbitals of **[**Mn(phen)F_3(H_2O)], which have predominantly 3*d* contributions in the spin quintet ground state. Orbital energies (Hartree) are given following the orbital labels.

While the spin forbidden transition as well as spin-orbit coupling involving the lowest triplet state can influence the lowest energy band, these are probably not sufficient to account for the observed difference of 3600 cm^{-1}. In all likelihood, perturbation by lattice strain on the vibronically sensitive $d_z^2 \rightarrow d_{xy}$ transition may be responsible for the discrepancy in this case. In the case of Cu(II) compounds, the effect of lattice strain on EPR parameters which are influenced by the axial ligand field are well documented[29].

3.6.4 $[Mn(phen)F_2(H_2O)_2]NO_3.(H_2O)_{1/2}$

Diffuse reflectance spectrum of **5** is shown in Figure 3.19. The three broad bands below 26000 cm^{-1} may be assigned to *d-d* transitions between the split components of the ^5E and $^5T_2$ states of the d^4 ion as follows: 13477 cm^{-1} ($d_z^2 \rightarrow d_{xy}$); 20325 cm^{-1} ($d_{x^2-y^2} \rightarrow d_{xy}$); 22522 cm^{-1} ($d_{yz} \rightarrow d_{xy}$); 23584 cm^{-1} ($d_{xz} \rightarrow d_{xy}$).

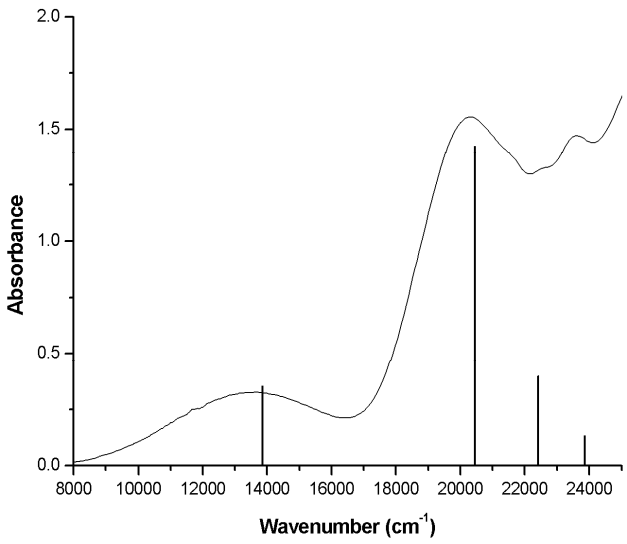

Figure 3.19 Diffuse reflectance spectrum of **5**. The vertical lines indicate the positions of *d-d* absorption maxima calculated using TDDFT.

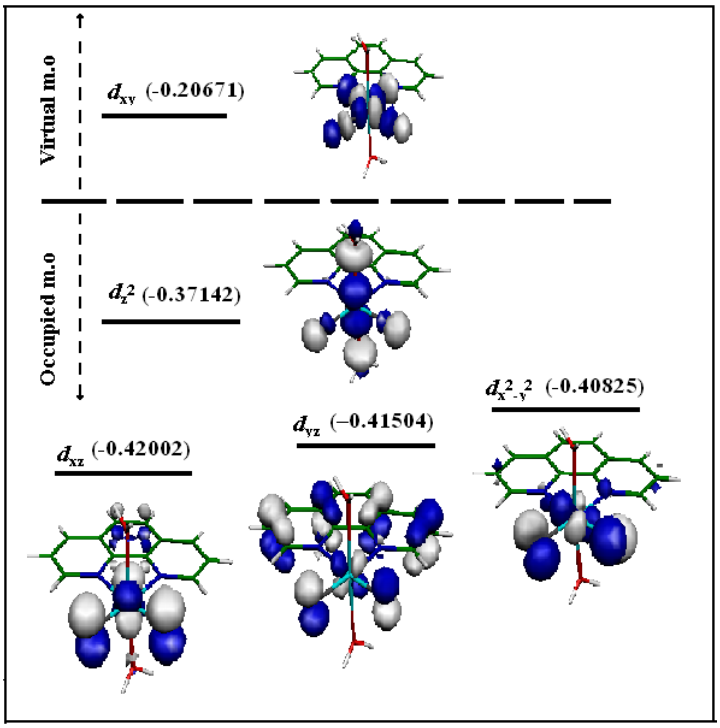

Figure 3.20 Diffuse reflectance spectrum of $[Mn(phen)F_2(H_2O)_2]^+$. The vertical lines indicate the positions of *d-d* absorption maxima calculated using TDDFT.

The one electron labels refer to a coordinate system in which the *z*-axis is perpendicular to the mean plane containing Mn1, F1, F2, N1 and N2 and the *x*-axis symmetric about the F1-Mn-F2 angle. In order to check the agreement between DFT theory and observed spectra, DFT calculations have been performed on **5** at experimental geometry. The molecular orbitals which have predominantly 3*d* contributions in the spin quintet ground state are shown in Figure 3.20 The band positions (cm^{-1}) along with dominant orbital contributions calculated using TDDFT are 13800 ($d_z^2 \rightarrow d_{xy}$), 20400 ($d_{x^2-y^2} \rightarrow d_{xy}$), 22300 ($d_{xz} \rightarrow d_{xy}$), 23900 ($d_{yz} \rightarrow d_{xy}$). Calculation of the lowest triplet state gave energy of 7766 cm^{-1} for this state.

3.6.5 Mn(phen)$F_2(H_2O)Cl$

Diffuse reflectance spectrum of **6** is shown in Figure 3.21. The three broad bands : 9980 cm^{-1}, 18248 cm^{-1} and 21008 cm^{-1} may be assigned to *d-d* transitions between the split components of the ^5E and $^5T_2$ states of the d^4 ion.

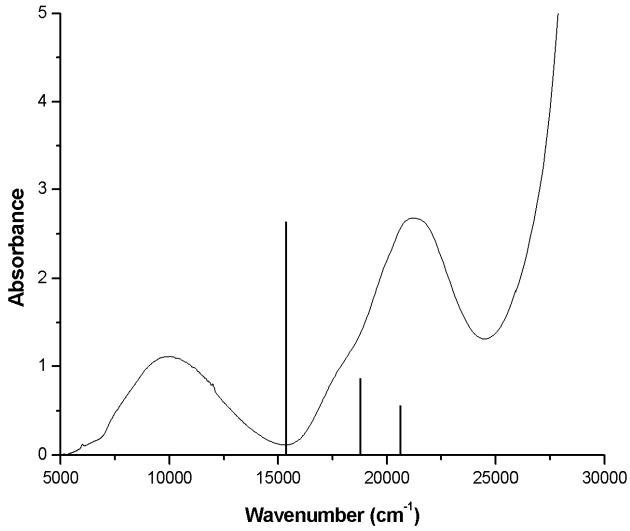

Figure 3.21 Diffuse reflectance spectrum of **6**. The vertical lines indicate the positions of *d-d* absorption maxima calculated using TDDFT

The band positions (cm^{-1}) along with dominant orbital contributions calculated using TDDFT are 15401 ($d_z^2 \rightarrow d_{xy}$); 18261 cm^{-1}; ($d_{xz} \rightarrow d_{xy}$); 21276 ($d_{x^2-y^2} \rightarrow d_{xy}$). The $d_{yz} \rightarrow d_{xy}$ transition was not observed in the calculation (Figure 3.22). The one electron labels refer to a coordinate system in which the *z*-axis is perpendicular to the mean plane containing Mn1, F1, F2, N1 and N2 and the *x*-axis symmetric about the F1-Mn-F2 angle. The Calculation of the lowest triplet state gave energy of 7970 cm^{-1} for this state.

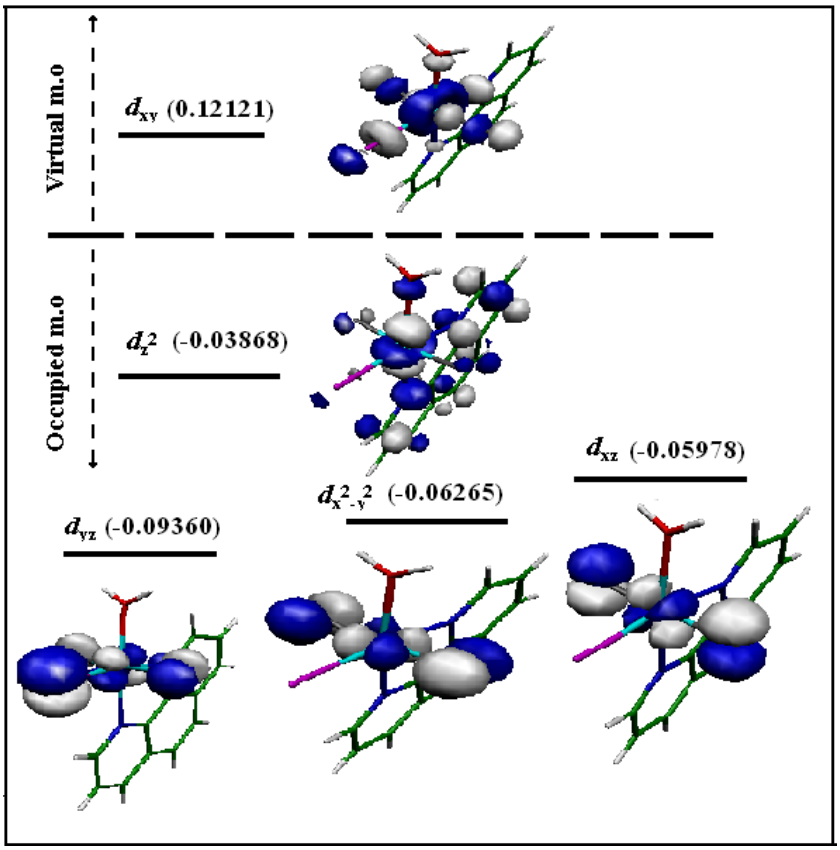

Figure 3.22. The molecular orbitals of $Mn(phen)F_2(H_2O)Cl$ which have predominantly 3*d* contributions in the spin quintet ground state. Orbital energies (Hartree) are given following the orbital labels.

3.7 Conclusion

Six higher valent fluoro manganese complexes have been synthesized and structurally characterized. All of them are Jan-Teller active d^4 systems. DFT and TDDFT calculations were performed for all of these complexes to correlate the observed electronic spectra. Except for the lower energy $d_z^2 \rightarrow d_{xy}$ transitions of the complexes **2**, **3** and **6** all other transitions showed a reasonably good correlation with the observed spectra. Use of different basis sets did not significantly alter the

band positions. Although we cannot rule out the role of particular function employed, there may be other reasons as well like spin forbidden transitions as well as spin-orbit coupling involving lowest triplet state influence the lowest energy band. Interestingly in all cases the triplet states were close to the lowest energy absorption maxima. Perturbation by the lattice strains on the vibronically sensitive $d_z^2 \rightarrow d_{xy}$ may have influence on the lower energy transitions may be responsible for the discrepancy in these cases.

3.8 References

1. Ludwig, M. L.; Metzger, A. L.; Pattridge, K. A.; Stallings, W. C. *J. Mol. Biol*. **1991**, *219*, 335.
2. Lah, M. S.; Dixon, M. M.; Pattridge, K. A.; Stallings, W. C.; Fee, J. A.; Ludwig, M. L. *Biochemistry* **1995**, *34*, 1646.
3. Liu, P.; Ewis, H. E.; Huang, Y.-J.; Lu, C.-D.; Tai, P. C.; Weber, I. T. *Acta*. *Cryst*. **2007**, *F63*, 1003.
4 Chen, H.; Tagore, R.; Das, S.; Incarvito, C.; Faller, J. W.; Crabtree, R. H.; Brudvig, G.W. *Inorg. Chem.* **2005**, *44*, 7661.
5. Mukhopadhyay, S.; Armstrong, W. H. *J. Am. Chem. Soc*. **2003**, *125*, 13010.
6. Baffert, C.; Collomb, M.-N.; Deronzier, A.; Pecaut, J.; Limburg, J.; Crabtree, R. H.; Brudvig, G. W. *Inorg. Chem.* **2002**, *41*, 1404.
7. Bashkin, J. S.; Schake, A. R.; Vincent, J. B.; Chang, H.-R.; Li, Q.; Huffman, J. C.; Christou, G.; Hendrickson, D. N. *J. Chem. Soc., Chem. Commun.* **1988**, 700.

8. Ramalakshmi, D.; Rajasekharan, M. V. *Acta Cryst.* **1999**, *B55*, 186.

9. Swarnabala, G.; Rajasekharan, M. V. *Inorg. Chim. Acta* **1990**, *168*, 167.

10. Plaksin, P. M.; Stoufer, R. C.; Matthew, M.; Palenik, G. J. *J. Am. Chem. Soc.* **1972**, *94*, 212.

11. Reddy, K. R.; Rajasekharan, M. V.; *Polyhedron* **1994**, *13***,** 765.

12. Swarnabala, G.; Reddy, K. R.; Tirunagar, J.; Rajasekharan, M.V. *Transition Met. Chem.* **1994**, *19*, 506.

13. Nunez, P.; Elias, C.; Fuentes, J.; Solans, X.; Tressaud, A.; de Lucas, M. C. M.; Rodriguez, F. *J. Chem. Soc., Dalton Trans.* **1997**, 4335.

14. Bhattacharjee, M. N.; Chaudhuri, M. K.; Purkayastha, R. N. D. *Inorg. Chem*. **1989**, *28*, 3747.

15. Brauer, G. Ed. *Handbook of Preparative Inorganic Chemistry*: Academic Press: New York. 2, **1965**, 1469.

16. Becke, A.D. *J. Chem. Phys*. **1993**, *98*, 5648.

17 Frisch, M. J.; Trucks, G. W.; Schlegel, H. B.; Scuseria, G. E.; Robb, M. A.; Cheeseman, J. R.; Montgomery, J. A.; Vreven, T., Jr.; Kudin, K. N.; Burant, J. C.; Millam, J. M.; Iyengar, S. S.; Tomasi, J.; Barone, V.; Mennucci, B.; Cossi, M.; Scalmani, G.; Rega, N.; Petersson, G. A.; Nakatsuji, H.; Hada, M.; Ehara, M.; Toyota, K.; Fukuda, R.; Hasegawa, J.; Ishida, M.; Nakajima, T.; Honda, Y.; Kitao, O.; Nakai, H.; Klene, M.; Li, X.; Knox, J. E.; Hratchian, H. P.; Cross, J. B.; Adamo, C.; Jaramillo, J.;

Gomperts, R.; Stratmann, R. E.; Yazyev, O.; Austin, A. J.; Cammi, R.; Pomelli, C.; Ochterski, J. W.; Ayala, P. Y.; Morokuma, K.; Voth, G. A.; Salvador, P.; Dannenberg, J. J.; Zakrzewski, V. G.; Dapprich, S.;Daniels, A. D.; Strain, M. C.; Farkas, O. D.; Malick, K.; Rabuck, A.D.; Raghavachari, K.; Foresman, J. B.; Ortiz, J. V.; Cui, Q.; Baboul, A. G.; Clifford, S.; Cioslowski, J.; Stefanov, B. B.; Liu, G.; Liashenko, A.; Piskorz, P.; Komaromi, I.; Martin, R. L.; Fox, D. J.; Keith, T.; Al-Laham, M. A.; Peng, C. Y.; Nanayakkara, A.; Challacombe, M.; Gill, P. M. W.; Johnson, B.; Chen, W.; Wong, M. W.; Gonzalez, C.; Pople, J. A. *Gaussian 03*, revision C.01; Gaussian, Inc.: Pittsburgh, PA, **2003**.

17. Schaefer, A.; Huber, C.; Ahlrichs, R. *J. Chem. Phys.* **1994**, *100*, 5829.

18. Schaefer, A.; Horn, H.; Ahlrichs, R. *J. Chem. Phys.* **1992**, *97*, 2571.

19. SAINTPLUS, Bruker AXS Inc. Madison, Wisconsin, USA.

20. Sheldrick, G.M. SADABS Programm for Empirical Absorption Correction, University of Gottingen, Germany, **1996**.

21. Sheldrick, M. SHELXS and SHELXL-97, University of Gottingen, Gottingen, Germany, **1997**.

22. Swarnabala, G.; Rajasekharan, M. V. *Polyhedron* **1996**, *15*, 3197.

24. Steed, J. W.; Junk, P. C.; Johnson, K.; Legido, C. *Polyhedron* **2003**, *22*,769.

25. (a) Balamurugan, V.; Hundal, M. S.; Mukherjee. R.; *Chem. Eur. J*

2004, *10*, 1683. (b) Banerjee, R.; Desiraju, G. R.; Mondal, R.; Howard, J. A. K.; *Chem. Eur. J.* **2004**, *10*, 3373. (c) Kooistra, T. M.; Hekking, K. F. W.; Knijnenburg, Q.; de Bruin, B.; Budzelaar, P. H. M.; de Gelder, R.; Smits, J. M. M.; Gal, A. W. *Eur. J. Chem*. **2003**, 648.

26. Aullón, G.; Bellamy, D. Brammer, L.; Bruton, E. A.; Orpen, A. G. *Chem. Commun*. **1998**, 635.

27. (a) Brammer, L. Chem. Soc. Rev. **2004**, *33*, 476; (b) Brammer, L.; Bruton, E. A.; Sherwood, P. *Cryst. Growth Des.* **2001**, *1*, 277.

28. Allen, G. C.; El-Sharkawy, G. A. M.; Warren, K. D. *Inorg. Chem.* **1971**, *10*, 2538.

29. Albela, B.; Carina, R.; Policar, C.; Poussereau, S.; Cano, J.; Guilhem, J.; Tchertanov, L.; Blondin, G.; Delroisse, M.; Girerd, J.-J. *Inorg. Chem*. **2005**, *44*, 6959.

30. Menon, S.; Rajasekharan, M. V. *Polyhedron* **1998**, *17*, 2463.

CHAPTER IV

Dinuclear manganese complexes

4.1 Introduction

Manganese is required in living systems to perform diverse redox functions including water splitting by photosynthetic enzymes[1-3]. In recent years there has been considerable interest in coordination chemistry of manganese(III) especially dimanganese complexes with μ-oxo-bis-μ-carboxylato unit since it has been proposed as the active site in the ribonucleotide reductase[4]. Similar unit is present in some metalloenzymes such as the Mn-catalases. This enzyme, responsible for the disproportion of H_2O_2 into H_2O and O_2, has been found in some bacteria such as *Thermus thermophilus* and *Lactobacillus plantarum*[5,6]. The crystal structure of the enzymes from the above bacteria shows binuclear manganese(III) sites with one carboxylate bridge and one or two oxygen ligand from the solvent (oxo, hydroxo, or aqua). With the aim of obtaining good model compounds for the above active sites $[Mn_2(\mu\text{-}RCOO)_2(\mu\text{-}O)]^{2+}$ core have been reported in literature[7]. The use of different varieties of carboxylate ligand has become increasingly popular in the synthesis of high nuclearity clusters as well as other complexes. There have been very few reported structures[7t,7u] with halogenated carboxylic acid as bridging ligand.

4.2 Experimental

4.2.1. Reagents

All chemicals were purchased from Ranbaxy chemicals and used without further purification. $Mn(OAc)_3.2H_2O$ was prepared using a reported procedure[8]. 2,6-Diformyl-4-methylphenol was prepared by using a reported procedure[9].

4.2.2 Synthesis

$[Mn_2(bpy)_2O(Cl_3CCOO)_4]Cl_3CCOOH$ (1)

Trichloroacetic acid (0.500 g, 3.61 mmol) and 2,2'-bipyridine (0.170 g, 1.09 mmol) were dissolved in 50 mL dichloromethane. Manganese(III) acetate (0.268 g, 1.00 mmol) was added to the above mixture and stirred for about one hour. It was filtered and kept at room temperature for crystallization. Within one day dark brown crystals separated out. Yield 0.469 g (0.38 mmol, 76 %). Anal. calcd. For. $Mn_2C_{30}H_{17}N_4O_{11}Cl_{15}$ (M.W 1251.15): C, 28.30; H, 1.37; N, 4.48. Found: C, 28.9; H, 1.34; N, 4.81. Important IR absorptions (KBr, cm^{-1}): 3115, 3084, 3055, 2556, 1884, 1749, 1685, 1666, 1602, 1568, 1498, 1471, 1447, 1350, 1313, 1248, 1176, 1159, 1105, 1059, 1033, 831, 767, 727, 680, 532, 480 and 441.

$[Mn_2(phen)_2O(Cl_3CCOO)_4]$ (2)

Trichloroacetic acid (0.500 g, 3.61 mmol) and 1,10-phenanthroline monohydrate (0.200 g, 1.04 mmol) were dissolved in 50 mL dichloromethane. Manganese(III) acetate (0.268 g, 1.00 mmol) was added to the above mixture and stirred for about 30 minutes. It was filtered and kept at room temperature for crystallization. Within one day dark brown crystals separated out. Yield 0.469 g (0.30 mmol, 60

%). Anal. calcd. For. $Mn_2C_{32}H_{16}Cl_{12}N_4O_9$ (M.W. 1135.77): C, 34.87; H, 1.43; N, 5.11. Found: C, 34.84, H, 1.42; N, 4.93. Important IR absorptions (KBr, cm^{-1}): 3070, 1761, 1684, 1666, 1588, 1518, 1427, 1342, 1302, 1147, 1107, 848, 719, 673 and 430.

$[Mn_2(phen)_2O(Cl_2HCCOO)_4]H_2O$ (3)

Dichloroacetic acid (0.166 mL, 2.01 mmol) and 1,10-phenanthroline monohydrate (0.217 g, 1.10 mmol) were dissolved in dichloromethane (100 mL). Manganese(III) acetate (0.268 g, 1.00 mmol) was added to the above mixture and stirred until a clear brown solution was formed. It was filtered and kept at room temperature. Within one a day dark brown precipitate was deposited. The precipitate was dissolved in dichloromethane (25 mL) by adding dichloroacetic acid (0.166 mL, 2.01 mmol). Diethyl ether was diffused into the solution in closed beaker at 5°C. Dark brown crystals were deposited within two days. Yield 0.285 g (0.28 mmol, 56 %). Anal. calcd. For. $Mn_2C_{32}H_{22}C1_8N_4O_{10}$ (M.W. 1016.02): 37.82; H, 2.18; N, 5.51. Found: 37.77, H, 2.12; N, 5.53. Important IR absorptions (KBr, cm^{-1}): 3501, 3063, 2999, 1634, 1585, 1518, 1427, 1377, 1205, 1145, 1105, 873, 850, 818, 779, 721 and 431.

$[Mn_2(bpy)O(OAc)_2(OH_2)_2]$ $(NO_3)_2$ $(H_2O)_5$ (4)

Manganese(III) acetate (0.750g, 2.80 mmol) was dissolved in 5 mL of 1.6 N HNO_3. 2,2'-bipyridine (0.500 g, 3.20 mmol) was added to the above solution and stirred for few minutes. The resulting dark brown solution was filtered and kept in desiccator when brown rectangular crystals of **1** deposited within a few hours.

Yield 0.650 g (0.806 mmol 50 %).Anal. Calc. for $Mn_2C_{24}H_{36}N_6O_{18}$ (M.W. 806.47): C, 35.92; H, 3.09; N, 10.78. Found: C, 35.74, H, 3.50; N, 10.42. Important IR absorptions (KBr, cm^{-1}): 3368, 1578, 1497, 1472, 1352, 1157, 1103, 1057, 1032, 829, 776, 731, 664 and 417.

$[Mn_2(4,4'\text{-}Me_2bpy)_2O(Cl_3CCOO)_4]$ CH_3OH (5)

Trichloroacetic acid (0.50 g, 3.61 mmol) and 4,4'-dimethyl-2,2'-bipyridine (0.185 g, 1.00 mmol) were dissolved in methanol (15 mL). Manganese(III) acetate (0.268 g, 1.00 mmol) was added to the above mixture and stirred. After five minutes it was filtered and kept at room temperature for crystallization. Within two days dark brown crystals separated. Yield 0.15 g (0.13 mmol, 26 %). Anal. calcd. For. $Mn_2C_{33}H_{28}Cl_{12}N_4O_{10}$ (M.W. 1175.87): C, 33.71; H, 2.4; N, 4.76. Found: C, 33.12; H, 2.43; N, 4.95. Important IR absorptions (KBr, cm^{-1}): 3057, 2928, 1649, 1591, 1539, 1456, 1371, 823, 777, 717, 663 and 515.

$[Mn_2(5,5'\text{-}Me_2bpy)_2O(Cl_2HCCOO)_4]$ CH_2Cl_2. H_2O (6)

Dichloroacetic acid (0.166 mL, 2.01 mmol) and 5,5'-dimethyl-2,2'-bipyridine were dissolved in dichloromethane (75 mL). Manganese(III) acetate (0.268 g, 1.00 mmol) was added to the above mixture and stirred until a clear brown solution was formed. It was kept at room temperature for two days by which time a crystalline precipitate was formed. X-ray quality crystals were obtained by the following procedure. Above precipitate was dissolved in dichloromethane (5 mL) and layered with 1:1 hexane, diethyl ether mixture (10 mL) within few days dark brown crystals deposited. Yield 0.294 g (0.27 mmol, 54 %). Anal. calcd. For.

$Mn_2C_{33}H_{32}Cl_{10}N_4O_{10}$ (M.W. 1109.01): C, 33.74; H, 2.91; N, 5.01. Found: C, 33.73; H, 2.88; N, 5.05. Important IR absorptions (KBr disk, cm^{-1}): 3551, 3497, 3115, 3049, 1651, 1508, 1476, 1383, 1207, 1161, 1051, 951, 823, 777, 717, 663, 557 and 418.

$Mn_2(OMe)_2(dbm)_2(Cl_2HCOO)_2$ (7)

Manganese(III) acetate and dichloroacetic acid were added to dichloromethane (30 mL) with constant stirring. Dibenzoylmethane was added to the above dark brown mixture, followed by 5 mL of methanol. Solution was filtered immediately after a clear dark solution was formed. It was filtered and kept at room temperature for crystallization. Within few days micro crystalline precipitate was formed. Yiled 0.273 g (0.31 mmol, 62 %). X-ray quality crystals were obtained by the diffusion of the diethyl ether to dark brown solution. Anal. calcd. For $Mn_2C_{36}H_{30}Cl_4O_{10}$ (M.W. 874.28): C, 49.45, H, 3.46. Found: C, 49.83; H, 3.24. Important IR absorptions (KBr disk, cm^{-1}): 3059, 2924, 1628, 1587, 1516, 1487, 1437, 1361, 1321, 1219, 1161, 1120, 1097, 1068, 1043, 1024, 941, 825, 769, 713, 679, 596, 551 and 478.

$Mn_2(dfppn)(OAc)_3$ (8)

2,6-Diformyl-4-methylphenol (0.082 0.50 mmol) was dissolved in methanol (30 mL) by heating. 1,3-diaminopropane (0.042 mL, 0.503 mmol) was added to the above solution with constant stirring. Manganese(III) acetate (0.134 g, 0.50 mmol) was added to the above solution and volume of the solution was reduced considerably by heating. Green precipitate was formed when the solution was

dried under vacuum. The precipitate was dissolved in acetonitrile and kept for crystallization at room temperature. Within few days dark green crystals separated. Yield 0.066 g (0.096 mmol, 38 %). Anal. calcd. For $Mn_2C_{30}H_{35}N_4O_8$ (M. W. 689.5): C, 52.26; H, 5.12; N, 8.13. Found: C, 52.26; H, 5.12; N, 8.07. Important IR absorptions (KBr disk, cm^{-1}): 3441, 2920, 2845, 1633, 1601, 1564, 1413, 1367, 1317, 1275, 1238, 1128, 1103, 1064, 985, 923, 883, 821, 767, 661, 613, 551, 493, 447 and 414.

Mn_2(dfppn)$(OAc)_2$(NCS) (9)

2,6-Diformyl-4-methylphenol (0.082, 0.50 mmol) was dissolved in 40 mL methanol and 1,3-diaminopropane (0.042 mL, 0.503 mmol) was added, stirred for about 30 minutes. Manganese(III) acetate (0.134 g, 0.50 mmol) was added and volume of the solution was reduced considerably by heating. KSCN (0.097 g, 1.0 mmol) was added to the above solution by dissolving in minimum amount of methanol. Green precipitate was formed when the solution was dried under vacuum. The precipitate was dissolved in acetonitrile and kept for crystallization at room temperature. Within few days dark green crystals deposited. Yield 0.063 g (0.92 mmol, 36 %). Anal. calcd. for $Mn_2C_{29}H_{32}N_5O_6S$ (M.W. 688.54): C, 50.59; H, 4.68; N, 10.17. Found: C, 50.14; H, 4.92; N, 10.28. Important IR absorptions (KBr disk, cm^{-1}): 3431, 2050, 1637, 1564, 1410, 1317, 1277, 1238, 1126, 1059, 927, 823, 765, 667, 615, 551, 495, and 449.

Mn(terp)($Cl_3CCOO)_3$ (10)

Trichloroacetic acid (0.536 g, 3.28 mmol) and 2,2',6,6'-terpyridine (0.234 g, 1.00 mmol) were dissolved in 100 mL dichloromethane. Manganese(III) acetate (0.268 g, 1.00 mmol) was added to the above solution and stirred until a clear brown solution was formed. It was filtered and kept for crystallization at room temperature to yield brown colored crystals for X-ray data collection. Yield 0.498 g (0.64 mmol, 64 %). Anal. calcd. For $MnC_{21}H_{11}Cl_9N_3O_6$ (M.W. 775.32): C, 32.53; N, 1.43; H, 5.42. Found C, 32.52; N; 1.82; H; 5.82. Important IR absorptions (KBr disk, cm^{-1}): 3086, 1720, 1699, 1597, 1479, 1450, 1275, 1161, 1018, 947, 827, 777, 733, 675 and 584.

Mn(terp)($F_3CCOO)_3$ (11)

Trifluoroacetic acid (0.308 mL, 4.00 mmol) and 2,2',6,6'-terpyridine (0.234 g, 1.00 mmol) were dissolved in 120 mL dichloromethane. Manganese(III) acetate (0.268 g, 1.00 mmol) was added to the above solution and stirred until a clear brown solution was formed. It was filtered and kept for crystallization at room temperature to yield brown crystals for X-ray data collection. Yiled 0.434 g (0.69 mmol, 69 %). Anal. calcd. For $MnC_{21}H_{11}F_9N_3O_6$ (M.W. 627.27): C, 40.21; H, 1.77, N; 6.70. Found: C, 40.37; H, 1.73; N, 6.85. Important IR absorptions (KBr disk, cm^{-1}): 3097, 2924; 1736, 1718, 1684, 1597, 1576, 1481, 1456, 1408, 1385, 1317, 1190, 1018, 837, 775, 723, 633, 540 and 443.

$Mn(terp)(Cl_2HCCOO)_3$ (12)

Dichloroacetic acid (0.165 mL, 2.00 mmol) and 2,2',6,6'-terpyridine (0.117 g, 0.500 mmol) were dissolved in 100 mL dichloromethane. Manganese(III) acetate (0.134 g, 0.500 mmol) was added to the above solution and stirred until a clear brown solution was formed. It was filtered and kept for crystallization at room temperature to yield brown colored crystals for X-ray data collection. Yield 0.258 g (0.38 mmol, 76 %). Anal. calcd. For $MnC_{21}H_{11}Cl_9N_3O_6$ (M.W. 671.99): C, 37.53; H, 2.10; N, 6.25. Found: 37.83, H, 2.42, N, 6.58. Important IR absorptions (KBr disk, cm^{-1}): 3115, 3084, 3055, 2989, 1711, 1685, 1597, 1575, 1477, 1454, 1402, 1315, 1194, 1016, 933, 812, 773, 713, 665, 584 and 443.

4.3 Measurements

IR spectra were obtained with a Shimadzu FT-IR 8000 spectrometer. Elemental analysis was obtained using a FLASH EA 1112 SERIES CHNS analyzer. The magnetic susceptibility was measured for compound **1** and **3** in the 1.98 – 300 K temperature range using Quantum Design MPMS SQID susceptometer. The samples were pressed into pellets to avoid orientation effects of the microcrystals during magnetic measurements. Diamagnetic corrections were applied using Pascal's constants[10]. Fitting of the susceptibility data was done using the program SUSEP[11] based on dimer equation[12] for **1** and modified dimer equation[7u] for **3**. ESR spectra were recorded for compounds **8** and **9** on JEOL JES–FA 200 spectrometer. X-ray data was collected on BRUKER-AXS SMART APEX CCD diffractometer.

4.3.1. Crystallographic data collection and structure determination

Data were collected on a Bruker SMART APEX CCD X-ray diffractometer using graphite monochromated Mo Kα radiation. The data were reduced using SAINTPLUS[13], and multiscan absorption corrections using SADABS[14] were applied. The structures were solved using SHELXS-97 and refined using SHELXL-97[15]. All ring hydrogen atoms were assigned on the basis of geometrical considerations and were allowed to ride upon the respective carbon atoms. All water hydrogen atoms were located from the difference Fourier maps and bond length constraints were applied. Crystal data are in Table 4.1, 4.5, 4.10 and 4.14 and important interatomic distances and angles in Table 4.2, 4.3 4.4, 4.6, 4.7, 4.8, 4.9, 4.11, 4.12, 4.13, 4.15, 4.16, and 4.17.

4.4 Crystal structure

4.4.1 Crystal structures of $[Mn_2(bpy)_2O(Cl_3CCOO)_4]Cl_3CCOOH$ (1), $Mn_2(phen)_2O(Cl_3CCOO)_4$ (2) and $[Mn_2(phen)_2O(Cl_2HCCOO)_4]H_2O$ (3)

Three compounds reported here display similar structural features (Figure 4.1, 4.2 and 4.3). The neutral complex molecules consist of a dinuclear unit with two carboxylate bridging ligand Cl3CCOO$^-$ for **1** and **2** and Cl_2HCCOO^- for **3**. Each manganese ion is chelated by a bpy ligand in **1** and phen ligand in **2** and **3**. The coordination sphere is completed by two monodentate Cl_3CCOO^- for **1** and **2** and by two Cl_2HCCOO^- for **3** along Jahn-Teller axis. An important asymmetry in the carboxylate bridges is observed. In all cases Mn-O bond is larger for the carboxylate oxygen atom trans to the monodentate ligand. The structural

parameters of these complexes are comparable with the previously reported complexes[7]. Asymmetric unit in **1** and **3** have two crystallographically independent manganese atoms but complex **2**, which lies on crystallographic imposed two fold axis passing through O3 (Mn1-O3 1.775 Å) contains only one independent Mn atom. Mn…Mn distances are in the range 3.219 - 3.194 Å.

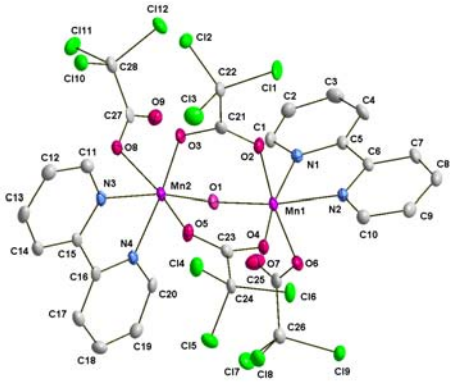

Figure 4.1. Thermal ellipsoid plot of the coordination environment of the complex molecules **1**. Atoms are represented as 50% probability ellipsoids. Lattice trichloroacetic acid and ring hydrogens have been omitted for clarity.

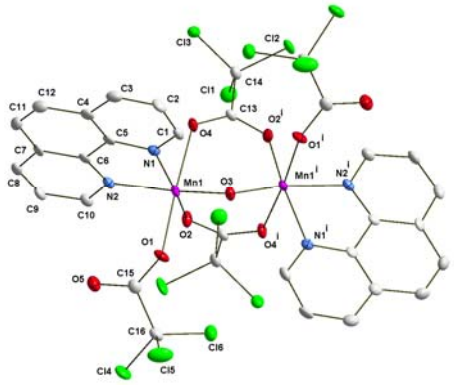

Figure 4.2. Thermal ellipsoid plot of the coordination environment of the complex molecules **2**. Atoms are represented as 50% probability ellipsoids and ring hydrogens have been omitted for clarity. Symmetry code. (i) -x, y, -z+1/2.

Table 4.1. Crystallographic data for **1**, **2** and **3**

	1	**2**	**3**
Formula	$Mn_2C_{30}H_{17}Cl_{15}N_4O_{11}$	$Mn_2C_{32}H_{16}Cl_{12}N_4O_9$	$Mn_2C_{32}H_{22}C1_8N_4O_{10}$
Formula weight	1251.11	1135.77	1016.02
Crystal system	Triclinic	Monoclinic	Triclinic
Space group	$P\bar{1}$	$C2/c$	$P\bar{1}$
a (Å)	11.2726(14)	23.735(2)	8.8033(18)
b (Å)	12.5232(16)	9.6974(10)	11.155(3)
c (Å)	16.181(2)	20.371(2)	19.825(4)
a (°)	87.021(2)	90	83.13(2)
β (°)	89.457(2)	121.3680(10)	84.59(3)
γ (°)	74.946(2)	90	78.89(2)
V (Å^3)	2202.9(5)	4003.4(7)	1891.6(8)
Z	2	4	2
T (°C)	100(2)	100(2)	100(2)
D_{calc} (g cm^{-3})	1.886	1.884	1.784
μ (mm^{-1})	1.544	1.491	1.295
F(000)	1236	2248	1016
Crystal size (mm)	0.24 x 0.20 x 0.18	0.20 x 0.10 x 0.08	0.20 x 0.12 x 0.06
θ Range (°)	1.26 to 26.03	2.01 to 26.06	1.87 to 26.05
h/k/l	-13<=h<=13, -15<=k<=15, -19<=l<=19	-29<=h<=29, -11<=k<=11, -25<=l<=25	-10<=h<=10, -13<=k<=13, -24<=l<=24
Reflection collected	22692	19992	19878
Unique reflect.,[R_{int}]	8606 [0.0349]	3947 [0.0877]	7424 [0.0650]
Goodness of fit on F^2	1.027	1.019	1.012
R_1 [I>2σ(I)]	0.0399	0.0483	0.0555
wR_2 (all data)	0.1101	0.1176	0.1210

Table.4.2. Selected bond lengths [Å] and angles [°] for **1**.

Mn(1)-O(1)	1.783(2)	N(1)-Mn(1)-O(6)	97.49(8)
Mn(1)-O(4)	1.974(2)	N(2)-Mn(1)-O(6)	83.69(8)
Mn(1)-N(1)	2.063(2)	O(2)-Mn(1)-O(6)	161.19(8)
Mn(1)-N(2)	2.070(2)	O(1)-Mn(2)-O(8)	98.89(8)
Mn(1)-O(2)	2.191(2)	O(3)-Mn(2)-O(8)	88.32(8)
Mn(1)-O(6)	2.211(2)	N(4)-Mn(2)-O(8)	93.56(9)
Mn(1)-Mn(2)	3.2186(6)	N(3)-Mn(2)-O(8)	86.52(9)
Mn(2)-O(1)	1.8030(19)	O(1)-Mn(2)-O(5)	91.32(8)
Mn(2)-O(3)	1.989(2)	O(3)-Mn(2)-O(5)	85.13(8)
Mn(2)-N(4)	2.054(2)	N(4)-Mn(2)-O(5)	90.86(9)
Mn(2)-N(3)	2.072(2)	N(3)-Mn(2)-O(5)	84.07(8)
Mn(2)-O(8)	2.131(2)	O(8)-Mn(2)-O(5)	168.59(8)
Mn(2)-O(5)	2.256(2)	O(1)-Mn(1)-Mn(2)	26.32(6)
O(1)-Mn(1)-O(4)	97.07(9)	O(4)-Mn(1)-Mn(2)	81.34(6)
O(1)-Mn(1)-N(1)	93.10(9)	N(1)-Mn(1)-Mn(2)	105.86(7)
O(4)-Mn(1)-N(1)	168.27(9)	N(2)-Mn(1)-Mn(2)	150.89(7)
O(1)-Mn(1)-N(2)	169.36(10)	O(2)-Mn(1)-Mn(2)	72.59(5)
O(4)-Mn(1)-N(2)	90.94(9)	O(6)-Mn(1)-Mn(2)	123.26(5)
N(1)-Mn(1)-N(2)	78.28(10)	O(1)-Mn(2)-Mn(1)	26.01(6)
O(1)-Mn(1)-O(2)	94.32(8)	O(3)-Mn(2)-Mn(1)	80.07(6)
O(4)-Mn(1)-O(2)	87.09(8)	N(4)-Mn(2)-Mn(1)	109.99(7)
N(1)-Mn(1)-O(2)	86.33(9)	N(3)-Mn(2)-Mn(1)	154.06(7)
N(2)-Mn(1)-O(2)	79.05(8)	O(8)-Mn(2)-Mn(1)	116.45(6)
O(1)-Mn(1)-O(6)	103.81(8)	O(5)-Mn(2)-Mn(1)	71.58(5)
O(4)-Mn(1)-O(6)	85.76(8)		

The relative orientation of the two coordination octahedra is readily perpendicular with torsions angles (º) (Monodentate carboxylate-O-Mn-Mn-Monodentate carboxylate-O) 98.20, 112.2 and 96.72 respectively for **1**, **2** and **3**. The Mn-O-Mn angles are quite large (127.4-128.9 º) when compared with the previous reports (120.9-124.7 º)[7].

Table.4.3. Selected bond lengths [Å] and angles [°] for **2**.

Mn(1)-O(3)	1.7745(17)	O(3)-Mn(1)-O(1)	89.60(10)
Mn(1)-O(2)	1.981(3)	O(2)-Mn(1)-O(1)	88.21(11)
Mn(1)-N(2)	2.065(3)	N(2)-Mn(1)-O(1)	90.77(12)
Mn(1)-N(1)	2.066(3)	N(1)-Mn(1)-O(1)	102.01(12)
Mn(1)-O(1)	2.107(3)	O(3)-Mn(1)-O(4)	91.23(10)
Mn(1)-O(4)	2.313(3)	O(2)-Mn(1)-O(4)	84.29(11)
Mn(1)-Mn(1)#1	3.2014(11)	N(2)-Mn(1)-O(4)	89.67(11)
O(3)-Mn(1)-O(2)	100.10(11)	N(1)-Mn(1)-O(4)	85.45(11)
O(3)-Mn(1)-N(2)	170.26(12)	O(1)-Mn(1)-O(4)	172.48(11)
O(2)-Mn(1)-N(2)	89.64(12)	O(3)-Mn(1)-Mn(1)#1	25.57(11)
O(3)-Mn(1)-N(1)	90.71(11)	O(2)-Mn(1)-Mn(1)#1	79.93(8)
O(2)-Mn(1)-N(1)	165.23(12)	N(2)-Mn(1)-Mn(1)#1	161.08(9)
O(3)-Mn(1)-N(1)	90.71(11)	N(1)-Mn(1)-Mn(1)#1	107.29(9)
O(2)-Mn(1)-N(1)	165.23(12)	O(1)-Mn(1)-Mn(1)#1	104.51(8)
N(2)-Mn(1)-N(1)	79.69(13)	O(4)-Mn(1)-Mn(1)#1	73.72(7)

a .Symmetry code (# 1). -x, y, -z+1/2

Table.4.4. Selected bond lengths [Å] and angles [°] for **3**.

Mn(1)-O(1)	1.775(3)	O(2)-Mn(1)-O(4)	171.67(11)
Mn(1)-O(6)	.957(3)	O(1)-Mn(1)-Mn(2)	26.42(9)
Mn(1)-N(2)	2.088(3)	O(6)-Mn(1)-Mn(2)	79.22(9)
Mn(1)-N(1)	2.094(4)	N(2)-Mn(1)-Mn(2)	160.79(10)
Mn(1)-O(2)	2.104(3)	N(1)-Mn(1)-Mn(2)	108.09(10)
Mn(1)-O(4)	2.333(3)	O(2)-Mn(1)-Mn(2)	113.09(8)
Mn(1)-Mn(2)	3.1938(11)	O(4)-Mn(1)-Mn(2)	74.92(8)
Mn(2)-O(1)	1.788(3)	O(1)-Mn(2)-O(5)	99.24(13)
Mn(2)-O(5)	1.936(3)	O(1)-Mn(2)-N(4)	173.71(13)
Mn(2)-N(4)	2.071(4)	O(5)-Mn(2)-N(4)	86.98(13)
Mn(2)-N(3)	2.077(4)	O(1)-Mn(2)-N(3)	94.88(13)
Mn(2)-O(8)	2.175(3)	N(4)-Mn(2)-N(3)	79.07(14)
Mn(2)-O(7)	2.309(3)	O(1)-Mn(2)-O(8)	85.56(13)
O(1)-Mn(1)-O(6)	98.22(13)	O(5)-Mn(2)-O(8)	93.72(12)
O(1)-Mn(1)-N(2)	172.20(13)	N(4)-Mn(2)-O(8)	93.12(13)
O(6)-Mn(1)-N(2)	88.86(13)	N(3)-Mn(2)-O(8)	94.36(13)
O(1)-Mn(1)-N(1)	95.18(14)	O(1)-Mn(2)-O(7)	90.38(12)
O(6)-Mn(1)-N(1)	160.31(13)	O(5)-Mn(2)-O(7)	89.84(12)
N(2)-Mn(1)-N(1)	78.84(14)	N(4)-Mn(2)-O(7)	90.60(12)
O(1)-Mn(1)-O(2)	93.98(13)	N(3)-Mn(2)-O(7)	83.03(12)
O(6)-Mn(1)-O(2)	93.06(12)	O(8)-Mn(2)-O(7)	174.98(11)
N(2)-Mn(1)-O(2)	82.29(12)	O(1)-Mn(2)-Mn(1)	26.22(9)
N(1)-Mn(1)-O(2)	100.35(13)	O(5)-Mn(2)-Mn(1)	78.54(9)
O(1)-Mn(1)-O(4)	94.34(12)	N(4)-Mn(2)-Mn(1)	159.05(10)
O(6)-Mn(1)-O(4)	86.10(12)	N(3)-Mn(2)-Mn(1)	112.71(10)
N(2)-Mn(1)-O(4)	89.40(12)	O(8)-Mn(2)-Mn(1)	102.77(9)
N(1)-Mn(1)-O(4)	78.54(12)	O(7)-Mn(2)-Mn(1)	74.45(8)

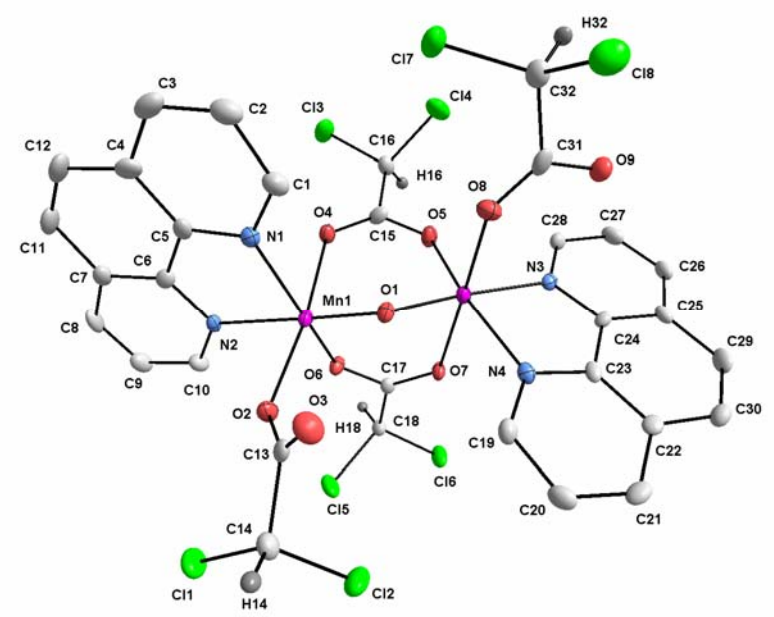

Figure 4.3. Thermal ellipsoid plot of the coordination environment of the complex molecules **3**. Atoms are represented as 50% probability ellipsoids and lattice water and ring hydrogens have been omitted for clarity.

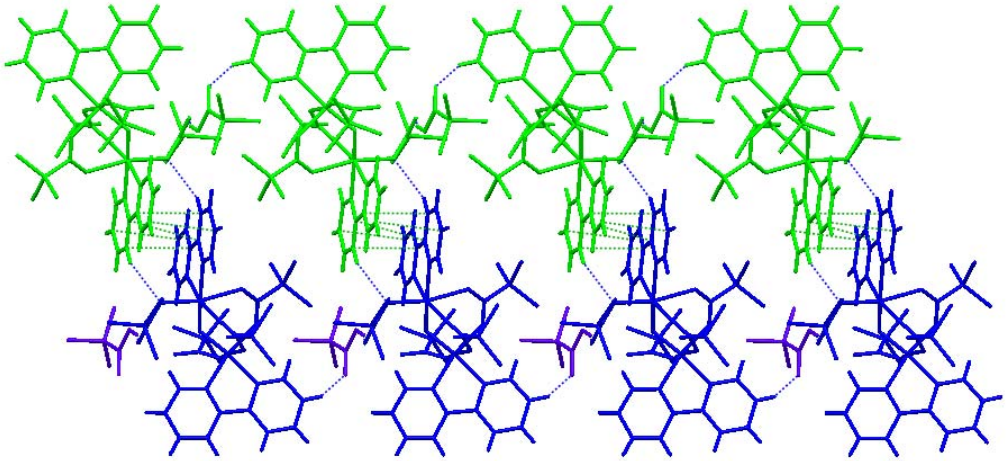

Figure 4.4. π-stacking interactions of two zig-zag chains of **1**.

Lattice trichloroacetic acid plays a major role in the crystal packing of compound **1**. Its C12-H12…O10 and O11-H11…O7 interactions pack the molecules into zig-zag one-dimensional chain. Two such zig-zag chains are interconnected by a C7-H7…O6 interaction as well as by π-π stacking between bpy rings from Mn1 (3.303-3.494 Å) (Figure 4.4). Another π-π stacking interactions from the bpy rings of Mn2 interconnects these double chains into a 2-dimensional network. Compound **2** form a chain along *c* axis by C3-H3…O3 (2.414 Å) and π-π stacking (3.429-3.391 Å) interactions. Interdigitized stacking interaction interconnects these chains into a 2-dimensional network (Figure 4.5).

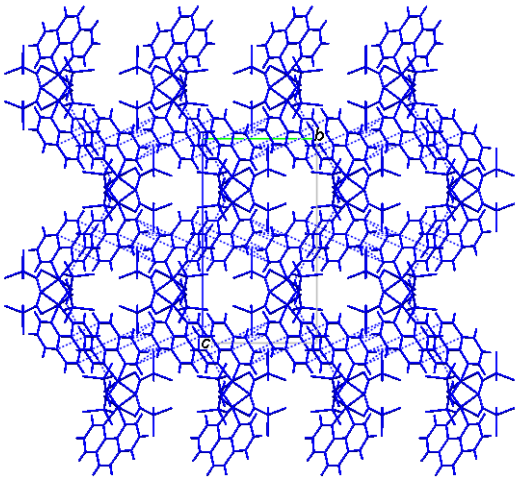

Figure 4.5. 2-dimensional network of compound **2** which shows π-stacking interactions when viewed down the *a* axis

Compound **3** form 2-dimensional hydrogen bonded networks with C-H…O interaction (Figure 4.6). The free lattice water forms intramolecular hydrogen bonds. C-H…Cl interactions and π-π stacking interactions interconnect the 2-dimensional networks into 3-dimensional networks.

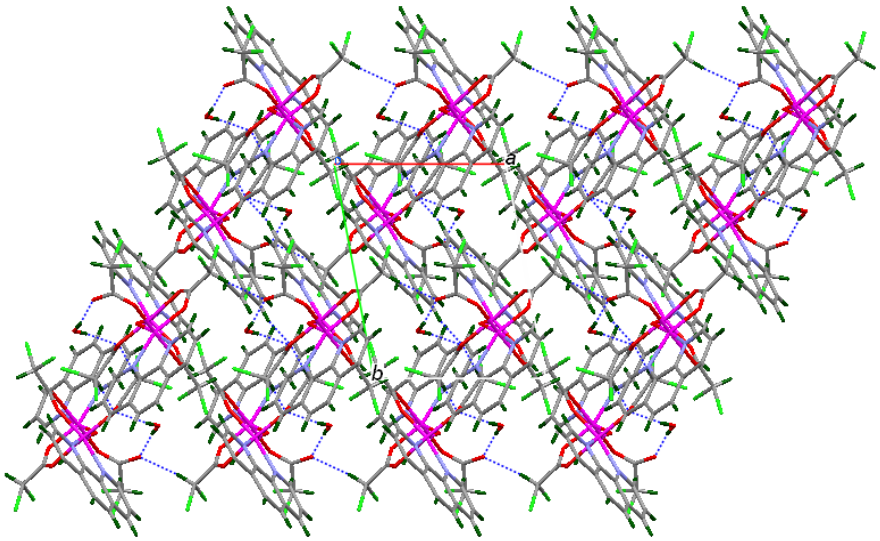

Figure 4.6. 2-dimensional network of compound **3** formed by C-H…O interactions.

4.4.2 Crystal structure of $[Mn_2O(bpy)_2(OAc)_2(OH_2)_2]$ $(NO3)_2$ $(H_2O)_5$ (4)

The molecular structure of the **4** is shown in Figure 4.7. Complex consists of binuclear Mn(III) ions bridged with an oxide anion and two asymmetric acetate groups with an inter metallic separation of 3.1454(4)Å. A chelating bipyridine acts as a terminal ligand and one water molecule completes the octahedral geometry on each manganese atom. Asymmetry in acetate groups owes to its elongated bonds which are trans to the coordinated water molecules along the Jahn-Teller axes. (Mn(1)-O(3), 2.1750(14) and Mn(2)-O(4), 2.2083(14)). The compression of equatorial oxo bonds (Mn(1)-O(1), 1.7908(13)and Mn(2)-O(1), 1.7883(13)) and Mn(1)-O(1)-Mn(2) angle (122.99(7)°) are very much comparable with that of the reported similar structures[7]. Complex has five lattice

water molecules which are connected by intermolecular hydrogen bonds. Complex forms hydrogen bonded extended structure along the *c* axis (Figure 4.8).

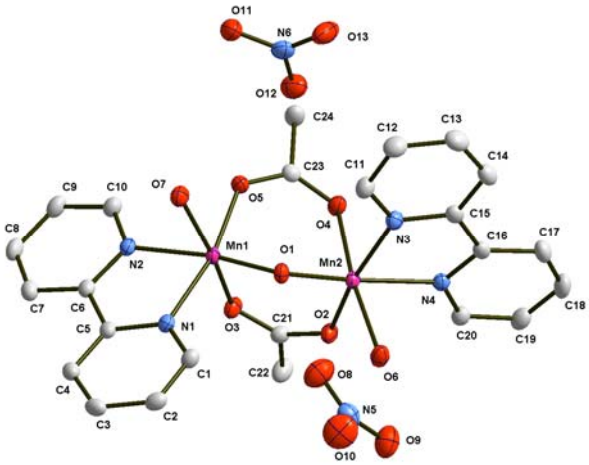

Figure 4.7. Thermal ellipsoid plot of the coordination environment of the complex molecules **4**. Atoms are represented as 50% probability ellipsoids and lattice waters, ring and water hydrogens have been omitted for clarity.

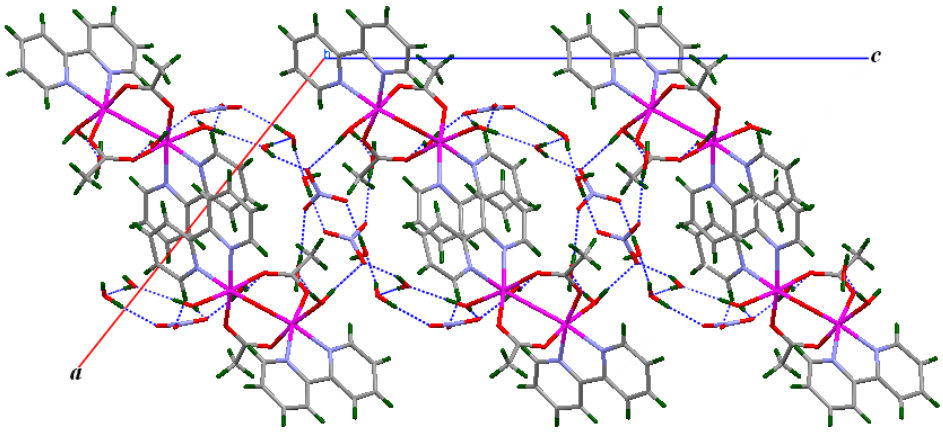

Figure 4.8. The molecular packing of **4** viewed down the *b* axis.

Table 4.5. Crystallographic data for **4**, **5** and **6**

	4	**5**	**6**
Formula	$Mn_2C_{24}H_{36}N_6O_{18}$	$Mn_2C_{33}H_{28}Cl_{12}N_4O_{10}$	$Mn_2C_{33}H_{32}Cl_{10}N_4O_{10}$
Formula weight	806.47	1175.87	1109.01
Crystal system	Monoclinic	Triclinic	Monoclinic
Space group	$P2_1/c$	$P\bar{1}$	$C2/c$
a (Å)	17.7959(10)	9.0981(12)	20.7282(14)
b (Å)	9.9158(6)	15.093(3)	11.6872(8)
c (Å)	24.0325(10)	18.249(4)	18.8749(13)
α (°)	90	85.276(14)	90
β (°)	128.371(3)	75.58(2)	104.7060(10)
γ (°)	90	72.541(11)	90
V (Å^3)	3324.8(3)	2315.1(8)	4422.7(5)
Z	4	2	4
T (ºC)	100(2)	100(2)	100(2)
D_{calc} (g cm^{-3})	1.611	1.687	1.666
μ (mm^{-1})	0.847	1.294	1.232
F(000)	1664	1176	2232
Crystal size (mm)	0.47 x 0.33 x 0.24	0.38 x 0.16 x 0.14	0.38 x 0.24 x 0.20
θ Range (º)	1.46 to 26.04	1.15 to 26.04	2.02 to 24.99
h/k/l	-21<=h<=21, -12<=k<=12, -29<=l<=29	-11<=h<=11, -18<=k<=18, -22<=l<=22	-24<=h<=24, -13<=k<=13, -22<=l<=22
Reflection collected	33626	24271	20773
Unique reflect.,[R_{int}]	6547 [0.0235]	9075 [0.0293]	3889 [0.0351]
Goodness of fit on F^2	1.047	1.045	1.049
R_1 [I>2σ(I)]	0.0334	0.0387	0.0310
wR_2 (all data)	0.0930	0.0957	0.0793

Table 4.6. Selected bond lengths [A] and angles [deg] for **4**

Mn(1)-O(1)	1.7908(13)	N(2)-Mn(1)-O(3)	84.71(6)
Mn(1)-O(5	1.9509(14)	O(1)-Mn(1)-O(7)	93.51(6)
Mn(1)-N(1)	2.0597(17)	O(5)-Mn(1)-O(7)	87.21(6)
Mn(1)-N(2)	2.0727(16)	N(1)-Mn(1)-O(7)	87.15(6)
Mn(1)-O(3)	2.1750(14)	N(2)-Mn(1)-O(7)	86.33(6)
Mn(1)-O(7)	2.2328(14)	O(3)-Mn(1)-O(7)	170.37(5)
Mn(1)-Mn(2)	3.1454(4)	O(1)-Mn(2)-O(2)	99.30(6)
Mn(2)-O(1)	1.7883(13)	O(1)-Mn(2)-N(4)	170.14(6)
Mn(2)-O(2)	1.9535(14)	O(2)-Mn(2)-N(4)	90.14(6)
Mn(2)-N(4)	2.0671(16)	O(1)-Mn(2)-N(3)	93.13(6)
Mn(2)-N(3)	2.0759(16)	O(2)-Mn(2)-N(3)	167.04(6)
Mn(2)-O(6)	2.1797(14)	N(4)-Mn(2)-N(3)	77.66(7)
Mn(2)-O(4)	2.2083(14)	O(1)-Mn(2)-O(6)	92.97(6)
O(1)-Mn(1)-O(5)	98.68(6)	O(2)-Mn(2)-O(6)	90.71(6)
O(1)-Mn(1)-N(1)	92.37(6)	N(4)-Mn(2)-O(6)	84.01(6)
O(5)-Mn(1)-N(1)	167.87(6)	N(3)-Mn(2)-O(6)	92.31(6)
O(1)-Mn(1)-N(2)	170.68(7)	O(1)-Mn(2)-O(4)	95.05(6)
O(5)-Mn(1)-N(2)	90.62(6)	O(2)-Mn(2)-O(4)	87.26(6)
N(1)-Mn(1)-N(2)	78.31(6)	N(4)-Mn(2)-O(4)	88.20(6)
O(1)-Mn(1)-O(3)	95.90(6)	N(3)-Mn(2)-O(4)	88.01(6)
O(5)-Mn(1)-O(3)	89.37(6)	O(6)-Mn(2)-O(4)	171.95(5)
N(1)-Mn(1)-O(3)	94.46(6)		

Table.4.7. Intermolecular contacts of compound **4**

D-H	d(D-H)	d(H..A)	<DHA	d(D..A)	A	
O7-H72	0.808	1.912	166.44	2.704	O18	
O15-H152	0.940	1.821	155.54	2.705	O9	
O6-H62	0.850	1.881	178.25	2.731	O14	
O7-H71	0.821	1.931	172.55	2.747	O13	-x+1, y-1/2, -z+3/2
O15-H151	0.892	1.902	169.12	2.783	O17	
O16-H161	0.967	1.860	161.89	2.795	O8	
O17-H172	0.853	1.973	176.35	2.825	O11	x, -y+3/2, z-1/2
O14-H141	0.806	2.023	177.45	2.829	O15	
O14-H142	0.799	2.085	165.08	2.864	O13	-x+1, -y+1, -z+1
O6-H61	0.821	2.062	177.94	2.883	O8	
O18-H181	0.806	2.156	157.57	2.917	O12	
O16-H162	0.830	2.277	143.28	2.984	O4	x, y+1, z

4.4.3 $Mn_2(4,4'\text{-}Me_2bpy)_2O(Cl_3CCOO)_4]\ CH_3OH$ (5) and $[Mn_2(5,5'\text{-}Me_2\ bpy)_2O(Cl_2HCCOO)_4]\ CH_2Cl_2.\ H_2O$ (6)

The molecular structures of the complexes are shown in Figure 4.9 and 4.11. Complexes involve bridging by two carboxylate groups (Cl_3CCOO in **5** and Cl_2HCCOO in **6**) and an oxide ion. Each metal centre has a distorted octahedral environment. The other three coordination sites are occupied by the two nitrogen atoms of the ligand. Sixth coordination is completed by a monodentate trichloro acetate group in **5** and dichloro acetate group in **6** along the Jahn-Teller axis. The Mn-Mn distance is 3.220 Å in **5** and 3.173 Å in **6** are comparable with the values reported for the other complexes. The Mn-O-Mn angle is 130.15 for **5** and 125.13

for **6**. The Mn-O-Mn angle of **5** is quite large when compared with the previous reports (120.9-124.7 º).

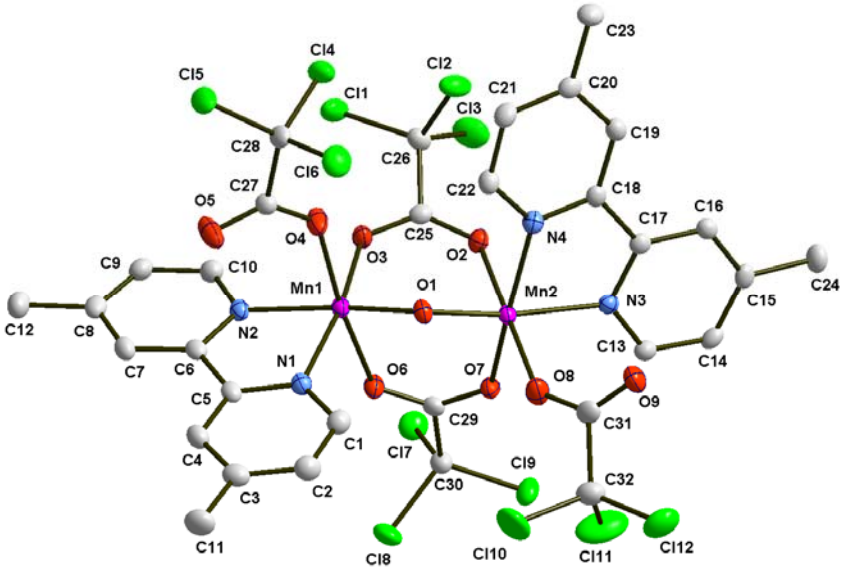

Figure 4.9. Thermal ellipsoid plot of the coordination environment of the complex molecules **5**. Atoms are represented as 50% probability ellipsoids. Methanol and ring hydrogens have been omitted for clarity.

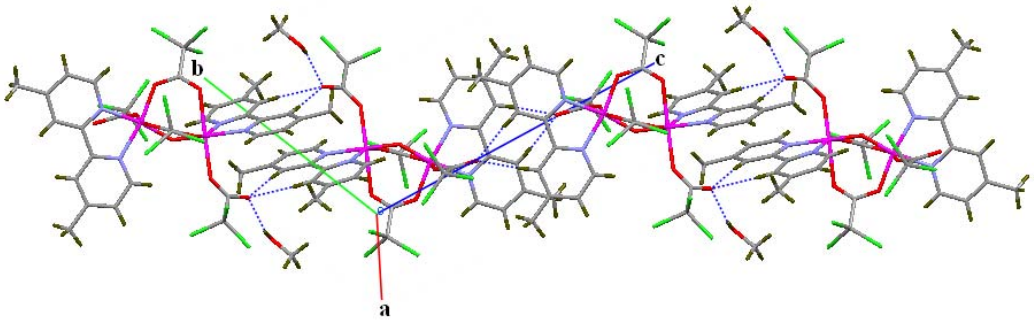

Figure 4.10. One dimensional hydrogen bonded chain of **5**

Table 4.8. Selected bond lengths [Å] and angles [°] for **5**

Mn(1)-O(1)	1.7828(18)	O(1)-Mn(1)-Mn(2)	24.82(6)
Mn(1)-O(3)	1.984(2)	O(3)-Mn(1)-Mn(2)	81.43(6)
Mn(1)-N(1)	2.048(2)	N(1)-Mn(1)-Mn(2)	108.17(7)
Mn(1)-N(2)	2.051(2)	N(2)-Mn(1)-Mn(2)	164.21(6)
Mn(1)-O(4)	2.133(2)	O(4)-Mn(1)-Mn(2)	102.88(6)
Mn(1)-O(6)	2.2417(19)	O(6)-Mn(1)-Mn(2)	73.21(5)
Mn(1)-Mn(2)	3.2200(8)	O(1)-Mn(2)-O(7)	97.63(8)
Mn(2)-O(1)	1.7680(18)	O(1)-Mn(2)-N(3)	170.24(9)
Mn(2)-O(7)	1.9789(19)	O(7)-Mn(2)-N(3)	92.02(8)
Mn(2)-N(3)	2.048(2)	O(1)-Mn(2)-N(4)	91.69(9)
Mn(2)-N(4)	2.055(2)	O(7)-Mn(2)-N(4)	161.52(8)
Mn(2)-O(8)	2.096(2)	N(3)-Mn(2)-N(4)	78.63(9)
Mn(2)-O(2)	2.326(2)	O(1)-Mn(2)-O(8)	91.50(8)
O(1)-Mn(1)-O(3)	99.43(8)	O(7)-Mn(2)-O(8)	89.76(8)
O(1)-Mn(1)-N(1)	91.50(9)	N(3)-Mn(2)-O(8)	89.97(8)
O(3)-Mn(1)-N(1)	168.76(8)	N(4)-Mn(2)-O(8)	105.97(9)
O(1)-Mn(1)-N(2)	169.44(9)	O(1)-Mn(2)-O(2)	92.50(8)
O(3)-Mn(1)-N(2)	90.54(8)	O(7)-Mn(2)-O(2)	83.50(7)
N(1)-Mn(1)-N(2)	78.72(9)	N(3)-Mn(2)-O(2)	87.15(8)
O(1)-Mn(1)-O(4)	87.50(8)	N(4)-Mn(2)-O(2)	80.18(8)
O(3)-Mn(1)-O(4)	85.21(9)	O(8)-Mn(2)-O(2)	172.56(8)
N(1)-Mn(1)-O(4)	97.93(9)	O(1)-Mn(2)-Mn(1)	25.04(6)
N(2)-Mn(1)-O(4)	89.88(8)	O(7)-Mn(2)-Mn(1)	80.55(5)
O(1)-Mn(1)-O(6)	91.20(8)	N(3)-Mn(2)-Mn(1)	158.94(6)
O(3)-Mn(1)-O(6)	86.66(8)	N(4)-Mn(2)-Mn(1)	102.53(6)
N(1)-Mn(1)-O(6)	90.55(8)	O(8)-Mn(2)-Mn(1)	109.54(6)
N(2)-Mn(1)-O(6)	92.87(8)	O(2)-Mn(2)-Mn(1)	72.51(5)

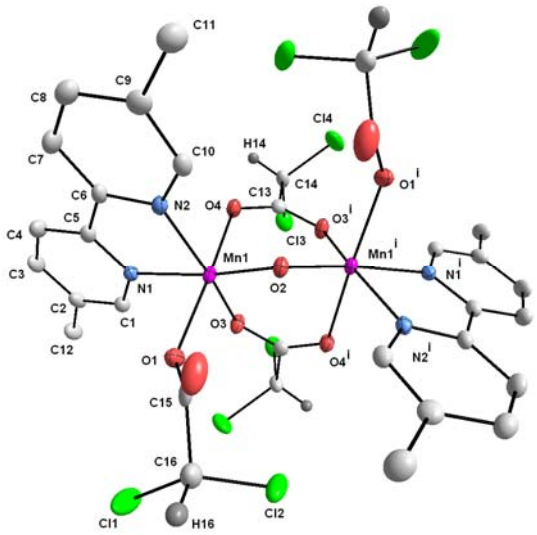

Figure 4.11. Thermal ellipsoid plot of the coordination environment of the complex molecules **6**. Atoms are represented as 50% probability ellipsoids. Dichloromethane, lattice water and ring hydrogens have been omitted for clarity. Symmetry code: (i) -x+1, y, -z+1/2.

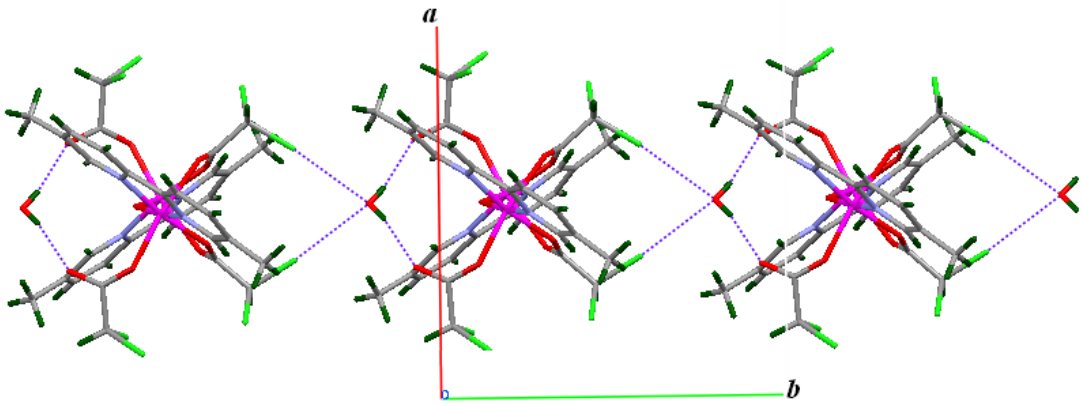

Figure 4.12. One-dimensional chain of **6** formed by O-H...O and Cl…O interactions

Table 4.9. Selected bond lengths [Å] and angles [°] for **6**

Mn(1)-O(2)	1.7876(10)	N(2)-Mn(1)-N(1)	78.25(7)
Mn(1)-O(3)	1.9742(15)	O(2)-Mn(1)-O(1)	94.95(5)
Mn(1)-N(2)	2.0596(18)	O(3)-Mn(1)-O(1)	88.10(7)
Mn(1)-N(1)	2.0751(18)	N(2)-Mn(1)-O(1)	97.75(7)
Mn(1)-O(1)	2.1142(16)	N(1)-Mn(1)-O(1)	86.77(6)
Mn(1)-O(4)	2.2508(15)	O(2)-Mn(1)-O(4)	92.93(5)
O(2)-Mn(1)-O(3)	98.94(7)	O(3)-Mn(1)-O(4)	85.39(6)
O(2)-Mn(1)-N(2)	93.08(7)	N(2)-Mn(1)-O(4)	87.14(6)
O(3)-Mn(1)-N(2)	166.14(7)	N(1)-Mn(1)-O(4)	86.24(6)
O(2)-Mn(1)-N(1)	171.32(7)	O(1)-Mn(1)-O(4)	170.48(6)
O(3)-Mn(1)-N(1)	89.61(7)		

Coming to crystal packing of compound **5**, molecules are assembled into one-dimensional chains by C-H…O interactions (Figure 4.10). These one-dimensional chains are further extended into three dimensions by C-H…Cl interactions (C21-H21…Cl3, 2.831Å; C11-H11c…Cl11, 2.845 Å) and π-stacking interactions (3.370-3.398 Å) between the bpy rings. In compound **6**, molecules are assembled into one dimensional chain by a O-H...O hydrogen bond (O7-H71…O5, 2.158 Å) as well as by a Cl…O interaction (Cl3…O7, 3.177 Å). These one dimensional chains are further builds into two-dimension by a C-H…C (C7-H7…C15, 2.521 Å) and π-stacking (C2…C2, 3.499 Å) interactions. As C–H…C interactions can exist at distances exceeding ν(H) + ν(C) + 0.3 Å (ν(H) and ν(C) are van der waals radii of hydrogen and carbon respectively), the C-H…C bond length is with in the "van der Waals cutoff" definition[15,16]. Nowadays it is well known that X-H…A

interactions with H…A distance up to 3.0 Å or even 3.2 Å should be considered as a potential hydrogen bonding interactions[17]. Two dimensional chains are further build into three-dimension by C-H…Cl (C16-H16…Cl6, 2.799 Å) interaction.

4.4.4 Crystal structure of $Mn_2(OMe)_2(dbm)_2(Cl_2HCOO)_2$ (7)

The molecular structure of the complex **7** is shown in Figure 4.12. Two manganese centers are related by crystallographic inversion centre. The coordination geometry around manganese is an elongated octahedron. Two dbm oxygen atoms and two methoxy oxygen atoms form the equatorial planes around the metal atoms. In plane bond distances are Mn1-O1, 1.876 Å, Mn1-O2, 1.876 Å Mn1-O3, 1.918 Å. Mn…Mn distance is 2.865Å which is comparable to the analogues reported complex[18]. Two Dichloro acetate oxygen atoms coordinate to the manganese atom via elongated axial direction. The axial bond distances are Mn1-O4, 2.278 Å and Mn1-O5, 2.217 Å. The Mn_2O_2 plane is exactly planar by symmetry. Coming to crystal packing molecules are assembled into one-dimensional chains with C-H…O interaction (Figure 4.13). These chains are further extends into two-dimension with π-stacking interactions (3.449-3.493Å).

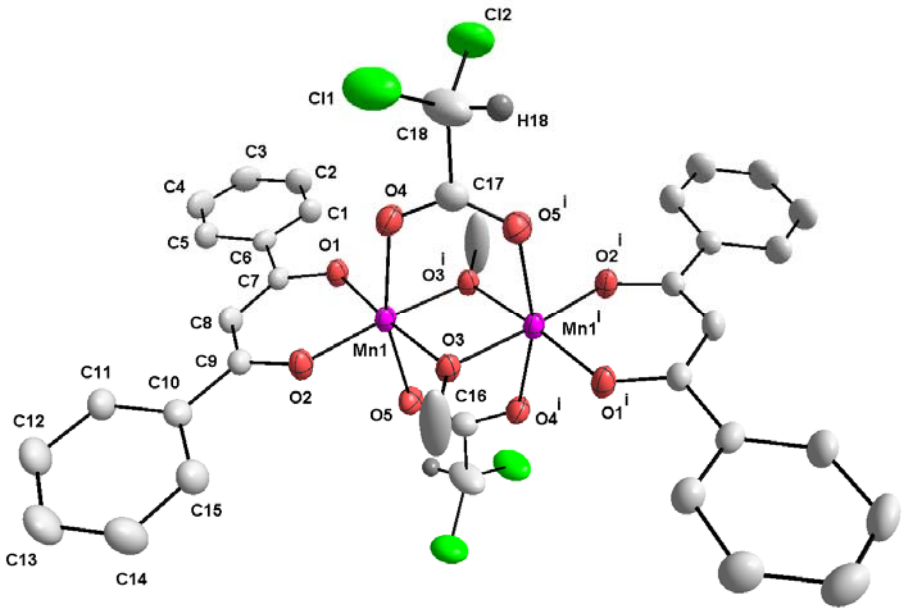

Figure 4.12. Thermal ellipsoid plot of the coordination environment of the complex molecules **7**. Atoms are represented as 50% probability ellipsoids and ring hydrogens have been omitted for clarity. Symmetry code : (i) -x+1, -y, -z.

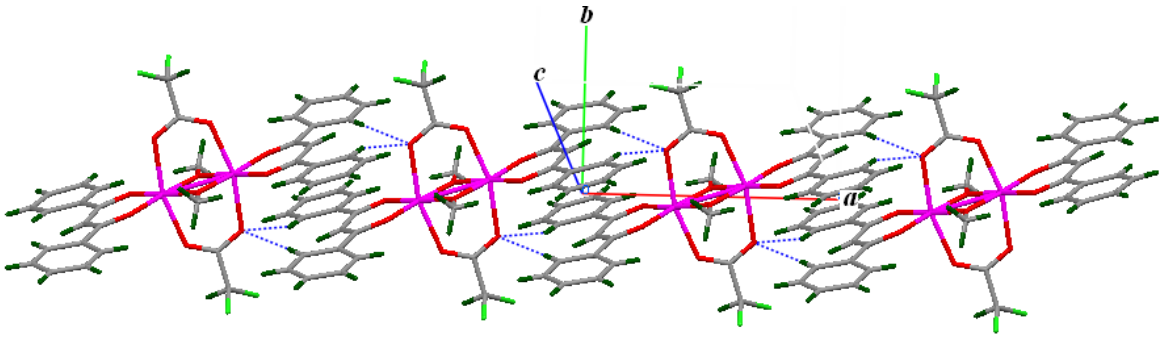

Figure 4.13. One-dimensional chain of **7** formed by C-H…O interactions.

Table 4.10. Crystallographic data for **7**, **8** and **9**

	7	**8**	**9**
Formula	$Mn_2C_{36}H_{30}Cl_4O_{10}$	$Mn_2C_{29}H_{32}N_5O_6S$	$Mn_2C_{30}H_{35}N_4O_8$
Formula weight	874.28	688.54	689.50
Crystal system	Monoclinic	Monoclinic	Monoclinic
Space group	$P2_1/c$	$P2_1/c$	$P2_1/c$
a (Å)	9.922(3)	14.6616(9)	15.0663(15)
b (Å)	20.265(6)	13.2530(8)	12.9039(13)
c (Å)	9.539(3)	16.2569(10)	16.0281(16)
β (º)	101.247(5)	103.3880(10)	03.592(2)
V (Å^3)	1881.2(10)	3073.0(3)	3028.8(5)
Z	2	4	4
T (ºC)	100(2)	100(2)	298(2)
D_{calc} (g cm^{-3})	1.543	1.488	1.512
μ (mm^{-1})	1.011	1.047	0.891
F(000)	888	1420	1428
Crystal size (mm)	0.22 x 0.10 x 0.08	0.4 x 0.18 x 0.18	0.40 x 0.20 x 0.18
θ Range (º)	2.01 to 25.00	2.00 to 25.00	1.39 to 28.29
h/k/l	-11<=h<=11, -24<=k<=24, -11<=l<=11	-17<=h<=17, -15<=k<=15, -19<=l<=19	-19<=h<=19, -16<=k<=16, -20<=l<=20
Reflection collected	17811	28932	34673
Unique reflect.,[R_{int}]	3303 [0.0602]	5400 [0.0426]	7275 [0.0347]
Goodness of fit on F^2	1.053	1.047	1.048
R_1 [I>2σ(I)]	0.0570	0.0594	0.0517
wR_2 (all data)	0.1280	0.1713	0.1387

Table 4.11. Selected bond lengths [Å] and angles [°] for **7**[a]

Mn(1)-O(2)	1.876(3)	O(3)#1-Mn(1)-O(4)	84.20(11)
Mn(1)-O(1)	1.876(2)	O(3)-Mn(1)-O(4)	82.96(11)
Mn(1)-O(3)	1.918(2)	O(5)#1-Mn(1)-O(4)	164.26(10)
Mn(1)-O(4)	2.278(3)	O(2)-Mn(1)- Mn(1)#1	134.36(8)
Mn(1)-Mn(1)#1	2.8647(13)	O(1)-Mn(1)-Mn(1)#1	134.46(9)
O(2)-Mn(1)-O(1)	91.18(11)	O(3)#1-Mn(1)-Mn(1)#1	41.68(7)
O(2)-Mn(1)-O(3)#1	92.70(11)	O(3)-Mn(1)-Mn(1)#1	41.61(7)
O(1)-Mn(1)-O(3)#1	175.76(11)	O(5)#1-Mn(1)-Mn(1)#1	82.88(7)
O(2)-Mn(1)-O(3)	175.61(11)	O(4)-Mn(1)-Mn(1)#1	81.39(7)
O(1)-Mn(1)-O(3)	92.88(11)	C(7)-O(1)-Mn(1)	129.2(3)
O(3)#1-Mn(1)-O(3)	83.29(11)	C(9)-O(2)-Mn(1)	128.6(2)
O(2)-Mn(1)-O(5)#1	92.95(12)	C(16)-O(3)-Mn(1)#1	131.5(3)
O(1)-Mn(1)-O(5)#1	97.04(11)	C(16)-O(3)-Mn(1)	131.8(3)
O(3)#1-Mn(1)-O(5)#1	84.48(11)	Mn(1)#1-O(3)-Mn(1)	96.71(11)
O(3)-Mn(1)-O(5)#1	84.89(11)	C(17)-O(4)-Mn(1)	122.6(3)
O(2)-Mn(1)-O(4)	98.47(11)	C(17)-O(5)-Mn(1)#1	123.8(3)
O(1)-Mn(1)-O(4)	93.54(11)		

a. symmetry code (#1) -x+1, -y, -z

4.4.5 Crystal structures of $Mn_2(dfppn)(OAc)_2(NCS)$ (8) and $Mn_2(dfppn)(OAc)_3$ (9)

The molecular structures of the complexes are described in Figure 4.14 and 4.15. Structurally characterized valence trapped Mn(II,III) complexes are few in number[19]. In both structures two manganese atoms are bridged by a phenolate oxygen and one carboxylate group of acetate ligand. In both structures second phenolate oxygen is bonded only to Mn1. In plane coordination of the both Mn1 and Mn2 atoms is completed by the two nitrogen atoms of propylene diamine macrocylic ligand. The coordination sphere of Mn1 is completed by one nitrogen atom of the NCS ligand in **8** and by one monodentate acetate ligand in **9**. Coordination sphere of Mn2 atom of the both complex is completed by chelating bidentate acetate ligand. N2O4 octahedron around Mn2 is typical of high spin Mn(II). Examination of the tables (Table 4.12 and 4.13) which summaries important bond lengths shows that all distances from Mn1 to donor atoms are significantly shorter than Mn2. Indeed these distances are average to 2.0375 Å vs 2.2471 Å for **8** and 2.0285 Å vs 2.2477 Å for **9** respectively. The most obvious differences are found in distances from two manganese ions to the bridging phenolate oxygen: Mn1-O1, 1.895 Å; Mn2-O1, 2.195 Å for **8** and Mn1-O1, 1.907 Å; Mn2-O1, 2.192 Å for **9**. This observations leads to conclude that valences of two ions are localized and that of Mn1 is Mn(III). The observed Mn…Mn distance is 3.261 Å in **8** and 3.308 in **9**. Interestingly Mn1 is laying approximately in macrocyclic N, N, O and O mean plane (deviation 0.034 Å for **8** and 0.095 Å for **9**) but Mn2 is laying considerably above the mean plane by 1.160 Å for **8** and

1.194 Å for **9**. These structural parameters are comparable to the previously reported complexes[19k].

Table 4.12. Selected bond lengths [Å] and angles [°] for **8**.

Mn(1)-O(1)	1.895(3)	O(1)-Mn(1)-O(3)	95.30(13)
Mn(1)-O(2)	1.910(3)	O(2)-Mn(1)-O(3)	85.82(12)
Mn(1)-N(2)	1.988(4)	N(2)-Mn(1)-O(3)	86.22(15)
Mn(1)-N(1)	2.021(4)	N(1)-Mn(1)-O(3)	89.12(13)
Mn(1)-N(5)	2.200(5)	N(5)-Mn(1)-O(3)	173.17(16)
Mn(1)-O(3)	2.211(3)	O(4)-Mn(2)-O(1)	105.50(12)
Mn(2)-O(4)	2.132(3)	O(4)-Mn(2)-N(4)	91.92(14)
Mn(2)-O(1)	2.195(3)	O(1)-Mn(2)-N(4)	128.52(13)
Mn(2)-N(4)	2.248(4)	O(4)-Mn(2)-N(3)	174.28(13)
Mn(2)-N(3)	2.269(4)	O(1)-Mn(2)-N(3)	80.03(13)
Mn(2)-O(6)	2.317(4)	N(4)-Mn(2)-N(3)	85.60(15)
Mn(2)-O(5)	2.322(4)	O(4)-Mn(2)-O(6)	92.02(13)
O(1)-Mn(1)-O(2)	83.76(12)	O(1)-Mn(2)-O(6)	131.81(12)
O(1)-Mn(1)-N(2)	176.42(14)	N(4)-Mn(2)-O(6)	94.34(13)
O(2)-Mn(1)-N(2)	93.12(14)	N(3)-Mn(2)-O(6)	83.04(14)
O(1)-Mn(1)-N(1)	89.75(14)	O(4)-Mn(2)-O(5)	90.74(15)
O(2)-Mn(1)-N(1)	171.36(13)	O(1)-Mn(2)-O(5)	79.31(12)
N(2)-Mn(1)-N(1)	93.53(15)	N(4)-Mn(2)-O(5)	149.79(14)
O(1)-Mn(1)-N(5)	91.18(16)	N(3)-Mn(2)-O(5)	88.84(16)
O(2)-Mn(1)-N(5)	97.07(15)	O(6)-Mn(2)-O(5)	55.48(13)
N(2)-Mn(1)-N(5)	87.44(18)	Mn(1)-O(1)-Mn(2)	105.54(13)
N(1)-Mn(1)-N(5)	88.74(16)		

Table 4.13. Selected bond lengths [Å] and angles [°] for **9**

Mn(1)-O(8)	1.8937(17)	O(8)-Mn(1)-O(5)	85.41(8)
Mn(1)-O(1)	1.9072(18)	O(1)-Mn(1)-O(5)	92.42(8)
Mn(1)-N(3)	1.989(2)	N(3)-Mn(1)-O(5)	83.85(9)
Mn(1)-N(2)	2.013(2)	N(2)-Mn(1)-O(5)	87.51(8)
Mn(1)-O(6)	2.095(2)	O(6)-Mn(1)-O(5)	176.60(9)
Mn(1)-O(5)	2.273(2)	O(4)-Mn(2)-O(1)	106.47(7)
Mn(2)-O(4)	2.114(2)	O(4)-Mn(2)-N(1)	173.73(8)
Mn(2)-O(1)	2.1924(17)	O(1)-Mn(2)-N(1)	79.70(8)
Mn(2)-N(1)	2.264(3)	O(4)-Mn(2)-N(4)	91.15(9)
Mn(2)-N(4)	2.272(2)	O(1)-Mn(2)-N(4)	125.61(8)
Mn(2)-O(3)	2.286(2)	N(1)-Mn(2)-N(4)	85.99(9)
Mn(2)-O(2)	2.358(2)	O(4)-Mn(2)-O(3)	90.96(8)
O(8)-Mn(1)-O(1)	84.87(8)	O(1)-Mn(2)-O(3)	133.78(8)
O(8)-Mn(1)-N(3)	92.85(9)	N(1)-Mn(2)-O(3)	83.78(8)
O(1)-Mn(1)-N(3)	175.78(9)	N(4)-Mn(2)-O(3)	95.56(8)
O(8)-Mn(1)-N(2)	170.84(9)	O(4)-Mn(2)-O(2)	91.40(9)
O(1)-Mn(1)-N(2)	89.62(8)	O(1)-Mn(2)-O(2)	80.85(8)
N(3)-Mn(1)-N(2)	92.17(9)	N(1)-Mn(2)-O(2)	88.45(9)
O(8)-Mn(1)-O(6)	95.59(9)	N(4)-Mn(2)-O(2)	151.20(9)
O(1)-Mn(1)-O(6)	90.91(9)	O(3)-Mn(2)-O(2)	55.72(8)
N(3)-Mn(1)-O(6)	92.85(10)	Mn(1)-O(1)-Mn(2)	107.36(8)
N(2)-Mn(1)-O(6)	91.80(9)		

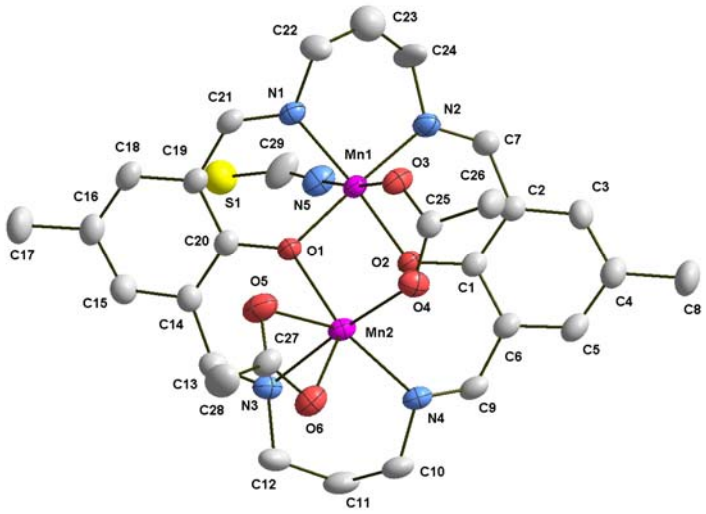

Figure 4.14. Thermal ellipsoid plot of the coordination environment of the complex molecules **8**. Atoms are represented as 50% probability ellipsoids and ring hydrogens have been omitted for clarity.

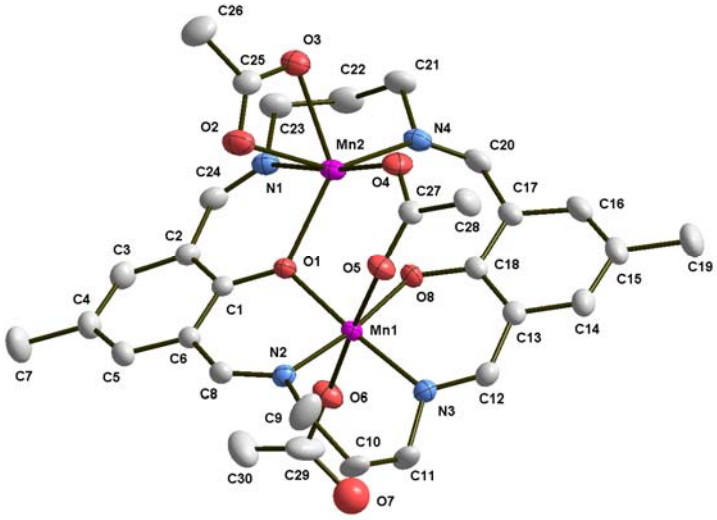

Figure 4.15. Thermal ellipsoid plot of the coordination environment of the complex molecule **9**. Atoms are represented as 50% probability ellipsoids and ring hydrogens have been omitted for clarity.

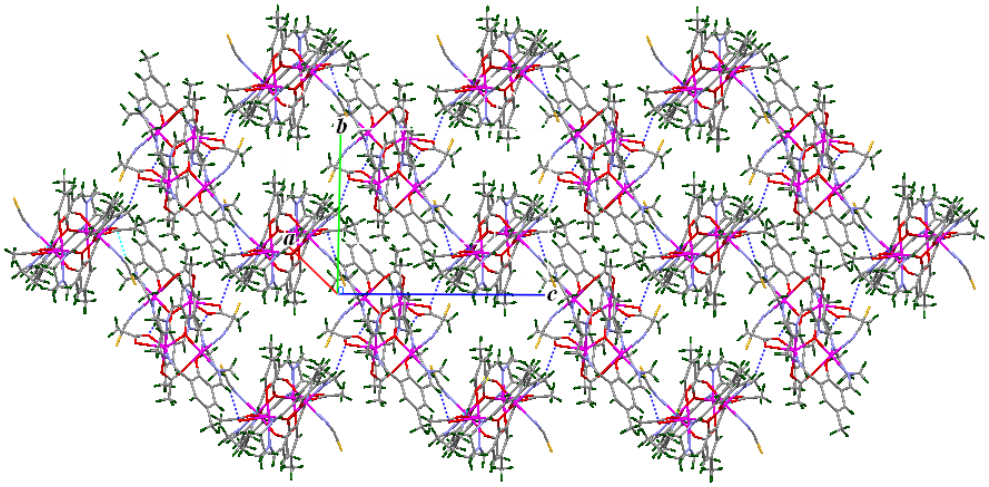

Figure 4.16. Two-dimensional networks of **8** formed by C-H…O interactions.

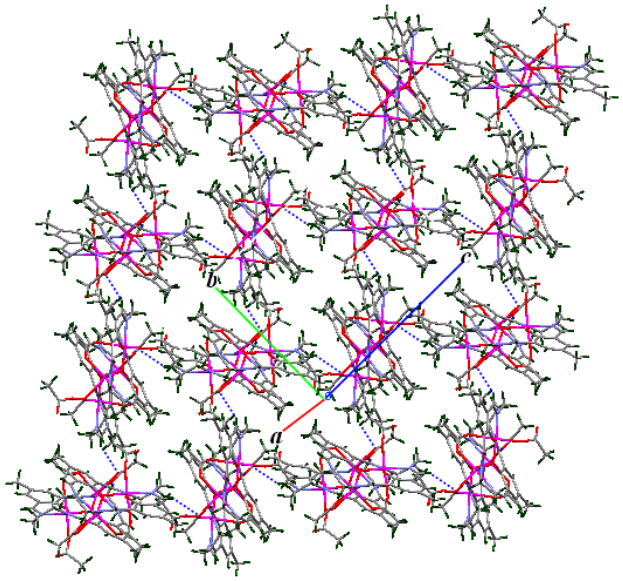

Figure 4.17. Two-dimensional networks of **9**

Coming to crystal packing of **8**, molecules are arranged into two-dimensional networks by C-H…O and π-stacking interaction (Figure 4.16). In **9** molecules are assembled into two-dimensional networks with the help C-H…O (C8-H8…O2, 2.359 Å and C12-H12…O3, 2.518 Å) interactions. These two dimensional chains are further develop into three-dimension by π-stacking interactions (3.380-3.494 Å) (Figure 4.17).

4.4.6 Mononuclear manganese complexes of 2,2',6,6'-terpyridine

An attempt was made to synthesize dinuclear manganese complexes of halogenated acetic acid and 2,2',6,6'-terpyridine by an analogous procedure described above for the dinuclear complexes of diimine ligands. Surprisingly all of the resulted complexes were mononuclear. In general isolation of mononuclear manganese carboxylate complexes is difficult. In order to isolate mononuclear complexes, the carboxylate has to be at least bidentate. However there have been no reports of mononuclear manganese complexes with simple carboxylate ligands. The mononuclear complexes reported are mostly with hydroxylcarboxylate and β-diketones and related ligands[20]. Contrary to this we have synthesized three mononuclear complexes which containing monodentate carboxylate group.

4.4.7 Crystal structure of $Mn(terp)(Cl_3CCOO)_3$ (10), $Mn(terp)(F_3CCOO)_3$ (11) and $Mn(terp)(Cl_2HCCOO)_3$ (12)

Molecular structures of the complexes are shown in Figures 4.18, 4.19 and 4.20. All of the complexes are analogues to the previously reported[21] $Mn(terp)(N_3)_3$ and

$Mn(terp)F_3$. Complex **12** contains two crystallographically independent manganese(III) centers. The Mn(III) ions exhibit a highly distorted octahedron coordination sphere, with three oxygen atoms of the three carboxylate ligand and one nitrogen atom of the terpyridine ligand defining the equatorial plane. The presence of one nitrogen atom of the terpyridine in the equatorial plane causes a distortion of the octahedron because Mn-terp bond is longer than Mn-carboxylate bonds. The average distances of the carboxylate ligands are 1.940 Å for **10**, 1.918 Å for **11** and 1.911 Å for **12**. The axial positions are occupied by two other nitrogen of terpy which display a tetragonal elongation as result of Jahn-Teller distortion expected for the high spin manganese(III) complex (d^4). The average axial distances (Å) are 2.231 for **10**, 2.247 for **11** and 2.241 for Mn1, 2.242 for Mn2 for **12.** In **10**, molecules are assembled into a one-dimensional chain with C-H…O interactions (C8-H8…O6, 2.480 Å, C9-H9…O4, 2.455 Å, C12-H12…O4, 2.496 Å) and these chains are further connected to three-dimension by π-stacking as well as by a Cl...O (Cl4…O2, 3.23 Å) interactions. C-H…F (C4-H4…F5, 2.524 Å; C8-H8…F9, 2.569 Å; C12-H12…F7, 2.585 Å) as well as π-stacking (3.370-3.460 Å) interactions pack molecules of 11 into three-dimension. Coming to the crystal packing of **12**, molecules are assembled into (4, 4) networks by Cl…O (3.403-3.450 Å) interactions as well as by C-H…Cl interactions (C7-H7…Cl3, 2.718 Å and C28-H28…Cl10, 2.709 Å) with pores down the *c* axis. However these pores are blocked by a two-fold parallel interpenetration of identical networks (Figure 4.21).

Table 4.14. Crystallographic data for **10**, **11** and **12**

	10	**11**	**12**
Formula	$MnC_{21}H_{11}Cl_9N_3O_6$	$MnC_{21}H_{11}F_9N_3O_6$	$MnC_{21}H_{14}Cl_6\ N_3O_6$
Formula weight	775.32	627.27	671.99
Crystal system	Triclinic	Monoclinic	Monoclinic
Space group	$P\bar{1}$	$P2_1/c$	$P2/c$
a (Å)	10.0151(7)	10.1223(8)	20.472(2)
b (Å)	10.2319(8)	17.3551(14)	12.0272(15)
c (Å)	15.7481(12)	15.6951(10)	27.994(3)
a (°)	93.7130(10)	90	90
β (°)	90.7380(10)	123.508(4)	132.059(6)
γ(°)	117.5960(10)	90	90
V (Å^3)	1425.49(18)	2299.0(3)	5117.5(10)
Z	2	4	8
T (ºC)	100(2)	100(2)	100(2)
D_{calc} (g cm^{-3})	1.806	1.812	1.744
μ (mm^{-1})	1.350	0.693	1.187
F(000)	768	1248	2688
Crystal size (mm)	0.24 x 0.18 x 0.12	0.26 x 0.18 x 0.18	0.40 x 0.24 x 0.20
θ Range (º)	1.30 to 26.03	1.95 to 26.06	1.34 to 26.03
h/k/l	-12<=h<=12, -12<=k<=12, -19<=l<=19	-12<=h<=12, -21<=k<=21, -19<=l<=19	-25<=h<=25, -14<=k<=14, -34<=l<=34
Reflection collected	14868	23649	52089
Unique reflect.,[R_{int}]	5581 [0.0201]	4547 [0.0360]	10095 [0.0555]
Goodness of fit on F^2	1.029	1.081	1.055
R_1 [I>2σ(I)]	0.0276	0.0466	0.0379
wR_2 (all data)	0.0715	0.1255	0.0918

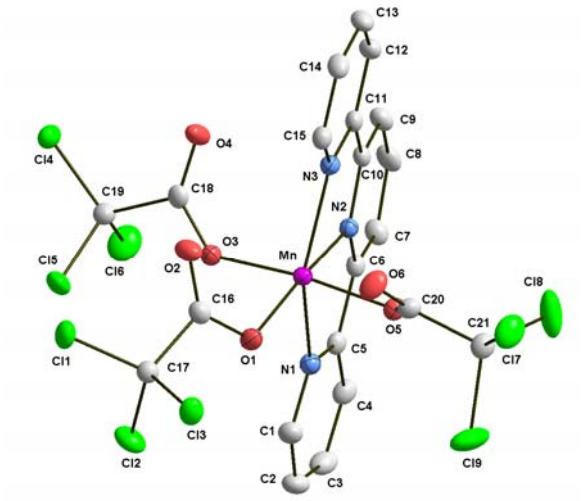

Figure 4.18. Thermal ellipsoid plot of the coordination environment of the complex molecules **10**. Atoms are represented as 50% probability ellipsoids and ring hydrogens have been omitted for clarity.

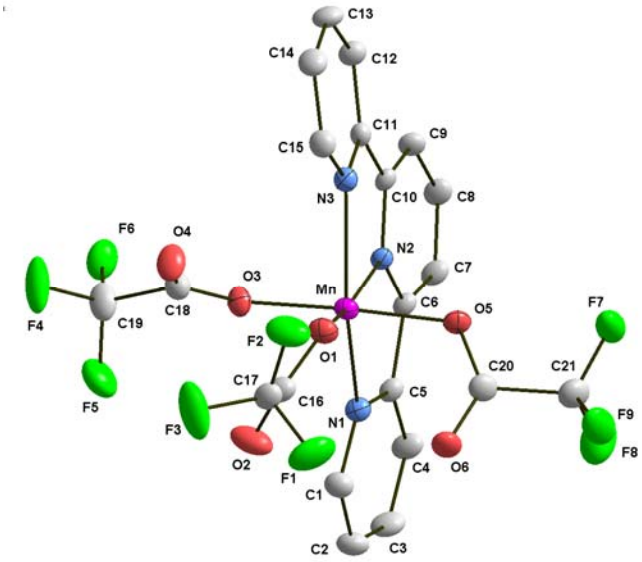

Figure 4.19. Thermal ellipsoid plot of the coordination environment of the complex molecules **11**. Atoms are represented as 50% probability ellipsoids and ring hydrogens have been omitted for clarity.

Table 4.15. Selected bond lengths [Å] and angles [°] for **10**

Mn-O(1)	1.9396(13)	O(1)-Mn-N(2)	165.03(6)
Mn-O(3)	1.8983(13)	O(3)-Mn-N(3)	97.27(5)
Mn-O(5)	1.9208(12)	O(5)-Mn-N(3)	89.71(5)
Mn-N(2)	2.0944(15)	O(1)-Mn-N(3)	119.40(6)
Mn-N(3)	2.2155(15)	N(2)-Mn-N(3)	74.91(6)
Mn-N(1)	2.2474(15)	O(3)-Mn-N(1)	86.23(6)
O(3)-Mn-O(5)	172.84(5)	O(5)-Mn-N(1)	86.97(5)
O(3)-Mn-O(1)	86.25(5)	O(1)-Mn-N(1)	91.59(6)
O(5)-Mn-O(1)	91.72(5)	N(2)-Mn-N(1)	74.40(6)
O(3)-Mn-N(2)	87.54(5)	N(3)-Mn-N(1)	148.92(6)
O(5)-Mn-N(2)	92.78(5)		

Table 4.16. Selected bond lengths [Å] and angles [°] for **11**

Mn-O(1)	1.9168(18)	O(3)-Mn-N(2)	86.15(7)
Mn-O(5)	1.9085(18)	O(5)-Mn-N(1)	88.86(8)
Mn-O(3)	1.9293(18)	O(1)-Mn-N(1)	91.90(8)
Mn-N(2)	2.088(2)	O(3)-Mn-N(1)	95.20(7)
Mn-N(1)	2.242(2)	N(2)-Mn-N(1)	74.76(7)
Mn-N(3)	2.252(2)	O(5)-Mn-N(3)	86.53(8)
O(5)-Mn-O(1)	96.04(8)	O(1)-Mn-N(3)	119.21(8)
O(5)-Mn-O(3)	172.93(7)	O(3)-Mn-N(3)	87.00(8)
O(1)-Mn-O(3)	89.62(7)	N(2)-Mn-N(3)	74.40(7)
O(5)-Mn-N(2)	89.34(7)	N(1)-Mn-N(3)	148.85(8)
O(1)-Mn-N(2)	165.54(8)		

Table 4.17. Selected bond lengths [A] and angles [°] for **12**

Mn(1)-O(1)	1.9042(18)	N(2)-Mn(1)-N(3)	74.60(8)
Mn(1)-O(3)	1.9052(18)	O(1)-Mn(1)-N(1)	88.44(8)
Mn(1)-O(5)	1.9179(18)	O(3)-Mn(1)-N(1)	88.23(8)
Mn(1)-N(2)	2.105(2)	O(5)-Mn(1)-N(1)	91.66(8)
Mn(1)-N(3)	2.235(2)	N(2)-Mn(1)-N(1)	74.13(8)
Mn(1)-N(1)	2.247(2)	N(3)-Mn(1)-N(1)	148.51(8)
Mn(2)-O(10)	1.8979(18)	O(10)-Mn(2)-O(7)	177.48(8)
Mn(2)-O(7)	1.9050(18)	O(10)-Mn(2)-O(12)	88.31(8)
Mn(2)-O(12)	1.9342(18)	O(7)-Mn(2)-O(12)	89.84(8)
Mn(2)-N(5)	2.092(2)	O(10)-Mn(2)-N(5)	96.84(8)
Mn(2)-N(6)	2.216(2)	O(7)-Mn(2)-N(5)	84.47(8)
Mn(2)-N(4)	2.268(2)	O(12)-Mn(2)-N(5)	163.23(8)
O(1)-Mn(1)-O(3)	175.58(8)	O(10)-Mn(2)-N(6)	92.17(8)
O(3)-Mn(1)-O(5)	87.86(8)	O(7)-Mn(2)-N(6)	90.24(8)
O(1)-Mn(1)-O(5)	89.33(8)	O(12)-Mn(2)-N(6)	120.65(8)
O(1)-Mn(1)-N(2)	83.43(8)	N(5)-Mn(2)-N(6)	75.24(8)
O(3)-Mn(1)-N(2)	98.44(8)	O(10)-Mn(2)-N(4)	88.10(8)
O(5)-Mn(1)-N(2)	164.17(8)	O(7)-Mn(2)-N(4)	90.19(8)
O(1)-Mn(1)-N(3)	91.67(8)	O(12)-Mn(2)-N(4)	90.10(8)
O(3)-Mn(1)-N(3)	92.69(8)	N(5)-Mn(2)-N(4)	74.20(8)
O(5)-Mn(1)-N(3)	119.83(8)	N(6)-Mn(2)-N(4)	149.25(8)

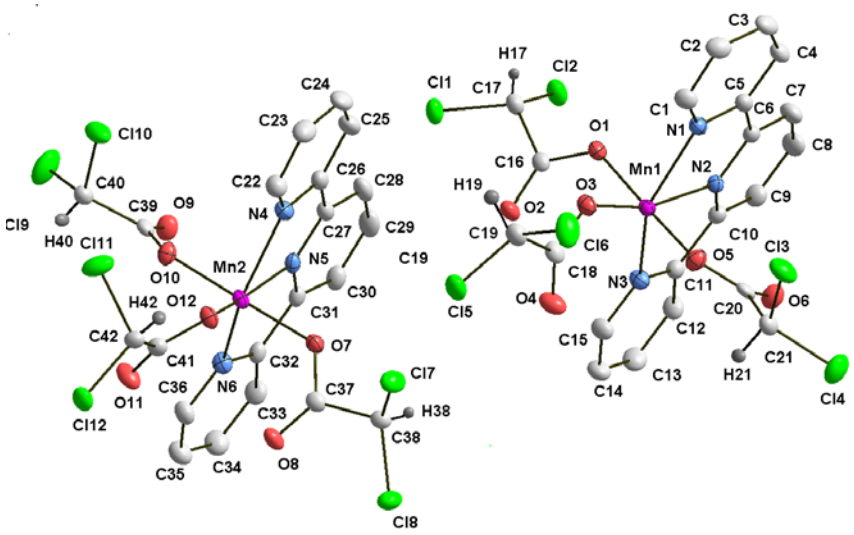

Figure 4.20. Thermal ellipsoid plot of the coordination environment of the complex molecules **12**. Atoms are represented as 50% probability ellipsoids and ring hydrogens have been omitted for clarity.

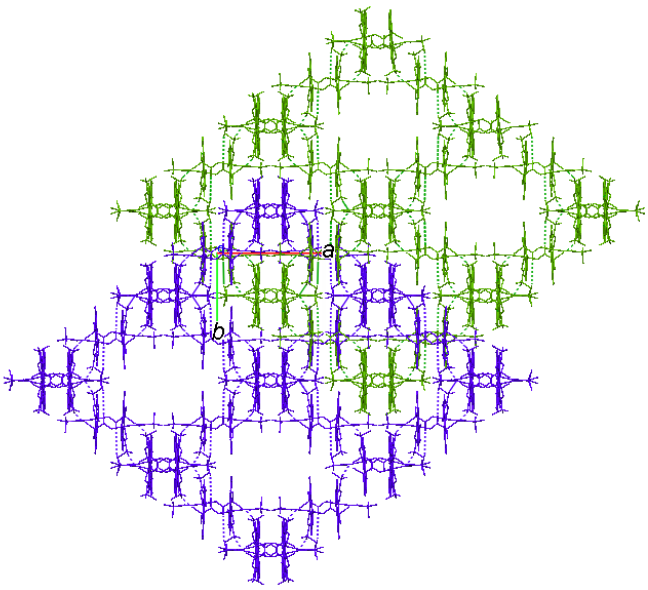

Figure 4.21. Two-fold parallel interpenetrating (4,4) networks of **12**

4.5 Magnetic properties

The magnetic moments are 3.34 BM for **1** and 3.3 BM for **3** are lower than expected for uncoupled S=2 ions at 300 K. This suggest anti-ferromagnetic coupling in the dimers as confirmed by the variable temperature susceptibility study. The cryogenic behaviors of the complexes were shown in Figure 4.22 and Figure 4.23. Magnetic susceptibility data were recorded for compounds **1** and **3** from 300 K to 1.98 K. The $\chi_M T$ product is 5.82 cm^3 mol^{-1} K for **1** and 5.58 cm^3 mol^{-1} K for **3** at room temperature. The $\chi_M T$ value for **1** and **3** seen to be much lower than the calculated value of 5.99 cm^3 mol^{-1} K for two uncoupled spins (S1 = 2, S2 = 2) with g= 2. These values indicate that the local spin states of both the manganese centers are quintects. With decrease of temperature, $\chi_M T$ decreases slowly reaching a value 0.106 cm^3 mol^{-1} K for **1** and 0.699 cm^3 mol^{-1} K for **3** at 1.98 K. The magnetic data for **1** was fitted by using dimer model including inter-dimer interactions with in the molecular field approximation. For complex **1** the data was fitted form 220 - 1.98 K because above 220 K it shows a sudden deviation for which we could not able to give a reasonable explanation. It was found that a good fit of the $\chi_M T$ *vs* temperature data could be obtained, except at the lowest temperatures where the theoretical values of $\chi_M T$ were found to be smaller than the observed. In the case of antiferromagnetically-coupled complexes, it is frequently the presence of a small amount of paramagnetic impurity that causes this deviation. Thus, in the fitting of the data for the complex **1**, we have included a susceptibility term (Curie law behavior) for a paramagnetic

S = 2 impurity (4 %). The parameters obtained by least square fitting[11] are: J = -15.50 cm^{-1}, zJ' = 9.703, g = 1.901. Error =0.00027. The magnetic data for **3** was simulated by using a modified dimer model.

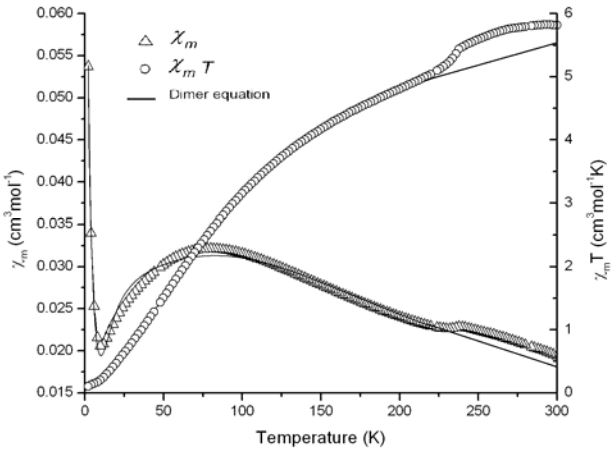

Figure 4.22. Molar paramagnetic susceptibility (χ_M) and product of molar paramagnetic susceptibility and temperature ($\chi_M T$) vs. Temperature curves for **1**.

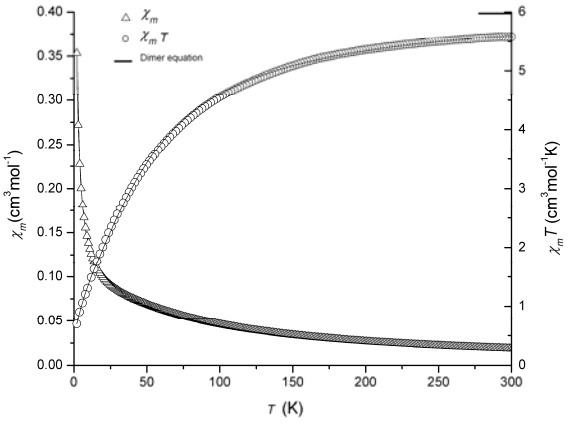

Figure 4.23. Molar paramagnetic susceptibility (χ_M) and product of molar paramagnetic susceptibility and temperature ($\chi_M T$) vs. Temperature curves for **3**.

Here too we have included a susceptibility term (Curie law behavior) for a paramagnetic S = 2 impurity (18 %). The parameters obtained by least square fitting[11] are: J = -5.34 (3) cm^{-1}, g = 2.02, Error = 0.00014.

4.6 ESR spectra

X-band ESR spectra were run for polycrystalline samples of **8** and **9** at 133 K (Figure 4.24). The spectral features are typical for the Mn(II,III) systems and are comparable with the previously reported structures[19k]. Relative population of the complexes in the S = ½ ground state and S = 3/2, 5/2, 7/2 and 9/2 excited states will vary according to the temperature. We could not assign the spectra since the J value for Mn(II, III) complexes are small (-1.1 to -2.0 cm^{-1}) and all of these states will be populated in various amounts even at very low temperatures[19k] (10 K). Averaged spectra of all these populations are obtained at 133 K. For both complexes, 6 line manganese(II) hyperfine pattern is observed when the spectra were run for 1:1 methanol/toluene glass at 133 K. It indicates that the complexes are dissociating in solution.

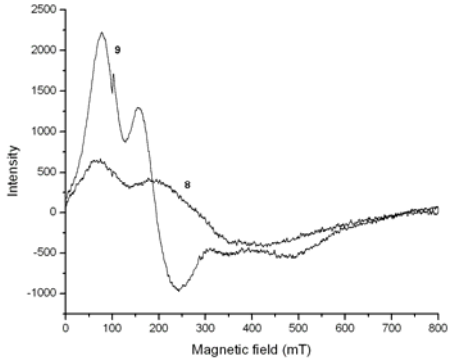

Figure 4.24. ESR spectra (X band,ν = 9.156 GHz) of polycrystalline samples of **8** and **9** at 133 K.

4.7 Conclusion

The $[Mn_2O(O_2CR)_2X_2(N\text{-}N)_2]$ (where N-N=bpy or phen) complexes with variety of monodentate ligands like H_2O, N_3^- and Cl^- have been reported earlier[7] and such complexes were invaluable in proving the influence of X on the structural parameters. It has been shown that a series of neutral binuclear manganese(III, III) complexes can be readily synthesized with X = halogenated acetate anion. Under the same reactions conditions, when a tridentate ligand, 2,2',6,6'-terpyridine was used instead of bpy/phen, corresponding mononuclear complexes were obtained. To the best of our knowledge, structural characterization of mononuclear complex with three monodentate carboxylate ligand was never reported. Here we have reported three of such complexes. Apart from a Schiffbase complex[18], $[Mn_2(\mu\text{-alkoxo})_2(\mu\text{-carboxylato})_2]^{2+}$ core have never been observed. Here we have reported one of such a rare complex (**7**) with dibenzoyl methane as a bidentate ligand. Valence trapped, macrocyclic $Mn^{II}Mn^{III}$ complexes are very rare. We have reported two such complexes (**8** and **9**). It has been said[19k] that ESR spectra of $Mn^{II}Mn^{III}$ complexes are broad and hard to detect above 60 K but complex **9** gave reasonably good ESR spectra at 133 K.

4.8 References

1. Debus, R. J. *Biochim. Biophys. Acta* **1992**, *1102*, 269.
2. Barber, J.; Andersson, B. *Nature* **1994**, *370*, 31.
3. Diner, B. A.; Babcock, G. T. Ort, D. R.; Yocum, C. F. *Oxygenic Photosynthesis: The Light Reactions*, Kluwer, Dordrecht, The Netherlands, **1996**, 213.
4. Nordlund, P. Sjőberg, B. M.; Eklund, H. *Nature* **1990**, *345*, 593.
5. (a) Barynin, V. V.; Hempstead, P. D.; Vagin, A. A.; Antonyuk, S. V.; Melik-Adamyan, W. R.; Lamzin, V. S.; Harrison, P. M.; Artymiuk, P. J. *J. Inorg. Biochem.* **1997**, *67*, 196. (b) Antonyuk, S. V.; Melik-Adamyan, W. R.; Popov, A. N.; Lamzin, V. S.; Hempstead, P. D.; Harrison, P. M.; Artymiuk, P. J.; Barynin, V. V. *Crystallogr. Rep.* **2000**, *45*, 105.
6. Barynin, V. V.; Whittaker, M. M.; Antonyuk, S. V.; Lamzin, V. S.; Harrison, P. M.; Artymiuk, P. J.; Whittaker, J. W. *Structure* **2001**, *9*, 725.
7. (a) Dave, B. C.; Czernuszewickz, R. S. *Inorg. Chim. Acta*. **1998**, *281*, 25. (b) Ruiz, R.; Sangregorio, C.; Caneschi, A.; Rossi, P.; Gaspar, A. B.; Real, J. A.; Muňoz, M. C. *Inorg. Chem. Commun*. **2000**, *3*, 361. (c) Reddy, K. R.; Rajasekharan, M. V.; Sukumar, S. *Polyhedron* **1996**, *15*, 4161. (d) Albela, B.; Corbella, M.; Ribas, J. *Polyhedron* **1996**, *15*, 91. (e) Corbella, M.; Costa, R.; Ribas, j. Fries, P. H.; Latour, J. M.; Ohstrom, L. Solans, X.; Rodríguez, V. *Inorg. Chem*. **1996**, *35*, 1857. (f) Romakh, V. B.; Therrien, B.; Karmazin-Brelot, L.; Labat, G.; Stoeckli-Evans, H.; Shuĺpin, G. B.; Süss-Fink, G. *Inorg. Chim. Acta* **2006**, *359*, 1619. (g) de

Boer, J. W.; Brinksma, Browne, W. R.; Meetsma, A.; Alsters, P. L.; R.; Hoge, R.; Feringa, B. L. *J. Am. Chem. Soc*. **2005**, *125*, 7990. (h) Bolm, C.; Meyer, N.; Raabe, G.; Weyhermüller, T.; Bothe, E. *Chem. Commun*. **2000**, 2435. (i) Caňada-Vilalta, C.; Streib, W. E.; Huffman, J. C.; O'Brien, T. A.; Davidson, E. R.; Christou, G. *Inorg. Chem.* **2004**, *43*, 101. (j) Caňada-Vilalta, C.; Huffman, J. C.; Streib, W. E.; Davidson, E. R., Christou, G. *Polyhedron* **2001**, *20*, 1375. (k) Ménage, S.; Girerd, J.-J.; Gleizes, A. *J. Chem. Soc., Chem. Commun.* **1988**, 431. (l) Corbella, M.; Costa, R.; Ribas, J.; Fries, P. H.; Latour, J. M.; Ohrstrom, L.; Solans, X.; Rodríguez, V. *Inorg. Chem.* **1996**, *35*, 1857. (m) Wieghardt, K.; Bossek, U.; Ventur, D.; Weiss, J. *J. Chem. Soc., Chem. Commun.* **1985**, 347. (n) Wieghardt, K.; Bossek, U.; Nuber,B.; Weiss, J.; Bonvoisin, J.; Corbella, M.; Vitols, S. E.; Girerd, J. J. *J. Am. Chem. Soc.* **1988**, *110*, 7398. (o) Bolm, C.; Meyer, N.; Raabe, G.; Weyhermüller, T.; Bothe, E. *Chem. Commun.* **2000**, 2435. (p) Vincent, J. B.; Folting, K.; Huffman, C. J.; Christou, G. *Biochem. Soc. Trans.* **1988**, *16*, 2. (q) Vincent, J. B.; Tsai, H. L.; Blackman, A. G.; Wang, S.; Boyd, P. D.; Folting, K.; Huffman, J. C.; Lobkovsky, E. B.; Hendrickson, D. N.; Christou, G. *J. Am. Chem. Soc.* **1993**, *115*, 12353. (r) Sheats, J. E.; Czernuszewicz, R. S.; Dismukes, G. C.; Rheingold, A. L.; Petrouleas, V.; Stubbe, J. A.; Armstrong, W. H.; Beer, R. H.; Lippard, S. J. *J. Am. Chem. Soc.* **1987**, *109*, 1435. (s) Wu, F. J.; Kurtz, D. M., Jr.Hagen, K. S.; Nyman, P. D.; Debrunner, P. G.; Vankai, V. A. *Inorg. Chem.* **1990**, *29*, 5174. (t) Mitra, K.; Mishra, D.; Biswas, S.; Lucas, C. R.; Adhikary, B. *Polyhedron* **2006**, *25*, 1681. (u) Fernández, G.; Corbella, M.;

Alfonso, M.; Stoeckli-Evans, H.; Castro, I. *Inorg. Chem.* **2004**, *43*, 6684.
(v) Fernández, G.; Corbella, C.; Aullón, G.; Maestro, M. A.; Mahía, J. *Eur. J. Inorg. Chem*. **2007**, 1285.

8 Brauer, G. Ed. *Handbook of Preparative Inorganic Chemistry*: Academic Press: New York. 2, **1965**, 1469.

9. Verani, C. N; Rentschler, E.; Weyhermüller, T.; Bill, E.; Chaudhuri, P.

11. M. Sheldrick, *SHELXS* and *SHELXL-97*, University of Gottingen, *J. Chem. Soc. Dalton. Trans*. **2000**, 251.

10 Pascal, P. *Ann. Chim. Phys*. **1910**, *19*, 5.

11. Chandramouli, G. V. R.; Balagopalakrishna, C.; Rajasekharan, M. V.; Manoharana, P. T. *Comput. Chem.* **1996**, *20*, 353.

12. O'Connor, C. J. Prog. *Inorg. Chem.* **1982**, *29*, 203.

13. *SAINTPLUS*, Bruker AXS Inc. Madison, Wisconsin, USA.

14. Sheldrick, G. M. *SADABS*, *Program for Empirical Absorption Correction*, University of Gottingen, Germany, **1996**.

Gottingen, Germany, **1997**.

15. Taylor, R.; Kennard, O. *J. Am. Chem. Soc.* **1982**,*104*, 5063.(b)

16. Steiner, T.; Desiraju G. R. *Chem. Commun.* **1998**, 891.

17. Steiner, T. *Angew Chem. Int. Ed. Engl*. **2002**, *41*, 48.

18. Zhang, C. G.; Janiak, C. *Acta Cryst.*. **2001**, *C57*, 719.

19. (a) Dubois, L.; Xiang, D.-F.; Tan, S.-S.; Pecaut, J.; Jones, P.; Baudron, S.; Le Pape, L.; Latour, J.-M.; Baffer, C.; Chardon-Noblat, S.; Collomb, M.-N.; Deronzier, A. *Inorg. Chem*. **2003**, *42*, 750. (b) Suzuki, M.; Mikuriya, M.; Murata, S.; Uehara, A.; Oshio, H.; Kida, S.; Saito, K. *Bull. Chem. Soc. Jpn.* **1987**, *60*, 4305. (c) Karsten, P.; Neves, A.; Bortoluzzi, A.; Strhle, J.; Maichle-Mossmer, C. *Inorg. Chem. Commun.* **2002**, *5*, 434. (d) Mikuriya, M.; Fujii, T.; Tokii, T.; Kawamori, A. *Bull. Chem. Soc. Jpn.* **1993**, *66*, 1675. (e) Huang, P.; Shaikh, N.; Anderlund, M. F.; Styring, S.; Hammarström, L. *J. Inorg. Biochem*. **2006**, *100*, 1139. (f) Jensen, K. B.; Johansen, E.; Larsen, F. B.; McKenzie, C. J. *Inorg. Chem*. **2004**, *43*, 3801. (g) Darovsky, A.; Kezerashvili, V.; Coppens, P.; Weyhermüller, T.;H. Hummel, H.; Wieghardt, H. *Inorg. Chem.* **1996**, *35,* 6916 (h) Chang, H.R.; Drill, H.; Nilges, M. J.; Zhang, X.; Potenza, J. A.; Schugar, H. J.; Hendrickson, D. N.; Isied, S. S. *J. Am. Chem. Soc.* **1988**, *110*, 625. (i) Boisen, A; Hazell, A.; McKenzie, C. J. *Chem. Commun.* **2001**, 2136. (j) Gou, S.; Zeng, Q.; Yu, Z.; Qian, M.; Zhu, J.; Duan, C.; You, X. *Inorg. Chim. Acta* **2000**, 303, 175. (k) Chang, H. R.; Larsen, S. K.; Boyd, P. D. W.; Pierpont, C .G.; Hendrickson, D. N. *J. Am. Chem. Soc*. **1988**, *110*, 4565. (l) Drill, H.; Chang, H. R.; Zhang, X.; Larsen, S. K.; Potenza, J. A.; Pierpont, C. G.; Schugar, H. J.; Isied, S. S.; Hendrickson, D. N. *J. Am. Chem. Soc.* **1987**, 109, 6207.

20. (a) Matzapetakis, M.; Karligiano, N.; Bino, A.; Dakanali, M.; Raptopoulou, C. P.; Tnagoulis, V.; Terzis, A.; Giapintzakis, J.; Salifoglou, A. *Inorg. Chem*. **2000**, *39*. 4044. (b) Bouwman, E.; Caulton, K. G.; Christou, G.; Folting, K.; Gasser, C.; Hendrickson, D. N.; Huffman, J. C.; Lobkovsky, E. B.; Martin, J. D. *Inorg. Chem*. **1993**, *32*, 3463. (c) Weighardt, K.; Pohl, K.; Bossek, U.; Nuber, B.; Weiss, J. *Z. Naturforsch. B*, **1998**, *43*, 1184. (d) Barra, A-L.; Gatteschi, D.; Sessoli, R.; Abbati, G. L.; Cornia, A.; Fabretti, a. C.; Uytterhoeven, M. G.; *Angew. Chem.; Int. Ed.* **1997**, *36*, 2329. (e) Yamaguchi, K. S.; Sawyer, D. T. *Inorg. Chem*. **1985**, *24*, 971. (f) Swarnabala, G; Reddy, K. R.; Tirunagar, J.; Rajasekharan, M. V. *Transition Met. Chem*. **1994**, *19*, 506.

21. (a) Limburg, J.; Vrettos, J. S.; Crabtree, R. H.; Brudvig, G. W.; de Paula, J. C.; Hassan, A.; Barra, A.-L.; Duboc-Toia, C.; Collomb, M.-N. *Inorg. Chem*. **2001**, *40*, 1698. (b) Mantel, C.; Hassan, A. K.; Pécaut, J.; Deronzier, A.; Collomb, M.-N.; Duboc-Toia, C. *J. Am. Chem. Soc.* **2003**, *125*, 12337.

CHAPTER V

High nuclearity manganese complexes

5.1. Introduction

The chemistry of polynuclear manganese complexes with carboxylate ligand was developed initially to prepare the synthetic models of water oxidizing active site in photo synthetic protein photosystem II and later on for the development of novel molecular magnetic materials[1-6]. $[Mn_4O_2]$ core was one of the earliest structures which were prepared among high nuclearity complexes[7]. Various tertranuclear complexes of diimine ligands (bpy and phen) with $[Mn_4O_2(OAC)_7]^+$ cores have been reported[8]. The WOC comprises a tetranuclear, oxide-bridged Mn cluster whose precise structure is still unclear, even with preliminary crystallographic results available[9]. The relevance of synthetic oxo-bridged multinuclear high-valent manganese complexes to the water oxidation center (WOC) in photosystem II (PS II) has in the recent past stimulated mechanistic studies of redox reactions of these oxidants. $[Mn_3O_4]^{4+}$ complexes of α-diimine ligands have important features common to oxygen evolving complex (OEC) of PSII[10]:. Oxo-bridged Mn ions in higher oxidation state, two sets of Mn…Mn contacts ca 2.7 Å and 3.3 Å and two fully protonated water molecule coordinated to two manganese centers. Very few structures have been reported earlier[11]. So in

order to study further about the trinuclear and tetranuclear complexes we have synthesized two Mn(IV) trimers and two Mn(III) tetrames.

5.2. Experimental

5.2.1. Reagents

All chemicals were purchased from Ranbaxy chemicals and used without further purification. $Mn(OAc)_3.2H_2O$ was prepared using a reported procedure[13].

5.2.2 Synthesis

$[Mn_3O_4(bpy)_4(Cl_3CCOO)_2](Cl_3COO)_2(Cl_3COOH)_4$ (1)

Manganese(II) acetate (0.245 g, 1.00 mmol) was dissolved in 1:1 acetic acid water mixture (30 mL). 2,2' bipyridine (0.160 g, 1.02 mmol) and trichloroacetic acid (0.50 g, 3.06 mmol) was added to the above solution and stirred continuously. Ceric ammonium nitrate (1.0 g, 1.824 mmol) which was dissolved in 10 mL of water was added slowly to the above solution. The dark brown solution was filtered and kept in desiccator for crystallization. Dark brown crystas deposited with in few days. Yield 0.426 g (0.20 mmol. 60 %). Anal. Calcd. for $Mn_3C_{56}H_{36}Cl_{24}N_8O_{20}$ (M.W. 2156.55): C, 31.18; H, 1.68; N, 5.20. Found: C, 31.42; H, 1.96; N, 5.65. Important IR absorptions (KBr disk, cm^{-1}): 3414, 3074, 2926, 2629, 1983, 1768, 1639, 1602, 1568, 1454, 1294, 1149, 1107, 817, 765, 694, 505, 609 and 432.

$[Mn_3O_4(bpy)_4(H_2O)_2][Ce(NO_3)_6\ (NO_3)_2(H_2O)_2$ (2)

2,2' bipyridine (0.200 g, 1.280 mmol) and manganese(II) acetate (0.245 g, 1.00 mmol) were dissolved in 0.1 M trifluoroacetic acid (20 mL). Ammoniumceric nitrate (1.00 g, 1.82 mmol) which was dissolved in 0.1 M trifluroacetic acid (10 mL) was added to the above solution slowly while stirring . The dark brown solution was filtered and kept for crystallization. Within a week dark brown crystals were separated out. Yield 0.357 g (0.235 mmol, 70 %). Anal. Calcd. for $Mn_3C_{40}H_{42}CeN_{15}O_{30}$ (M.W. 1517.83): C, 31.65; H, 2.79; N, 13.84. Found: C, 31.42; H, 2.98; N, 13.63. Important IR absorptions (KBr disk, cm^{-1}): 3366, 3074, 2000, 1768, 1639, 1602, 1568, 1454, 1385, 1290, 1165, 1107, 1072, 1032, 817, 765, 694 and 609.

$[Mn_4O_2(bpy)_2(CH_3COO)_7]Br_3$ (3)

HBr (0.08 mL) and KBr (0.24 g, 2.02 mmol) were added to acetonitrile (20 mL). 2,2'-bipyridine (0.160 g, 1.04 mmol) and manganese(III) acetate (0.268 g, 1.00 mmol) was added to the above mixture and stirred continuously until a clear dark brown solution was formed. It was filtered and kept at 5° C for crystallization. With in few days dark brown crystals were deposited. Yield 0.050 g (0.077 mmol, 30 %). Anal. Calcd. for $Mn_4C_{34}H_{37}Br_3N_4O_{16}$ (M.W. 1217.17): C, 33.55; H, 3.06; N, 4.60. Found: C, 33.81; H, 3.01; N, 4.72. Important IR absorptions (KBr disk, cm^{-1}): 3441, 1620, 1597, 1556, 1494, 1469, 1433, 1379, 1331, 1172, 1155, 1099, 1057, 1030, 1012, 939, 819, 771, 733, 661, 599 and 414.

$Mn_4O_2(ClH_2CCOO)_7]ClO_4$ (4)

2,2'-bipyridine (0.077 g, 0.49 mmol), manganese(III) acetate (0.268 g, 1.00 mmol) and monochloroacetic acid (0.330 g, 3.49 mmol) were added to 30 mL acetonitrile and stirred continuously until a clear brown solution was formed. Sodium perchlorate (0.50g, 3.56 mmol) was dissolved in the above solution, filtered and kept at room temperature for crystallization. Dark brown crystals were deposited with in three to four days. Yield 0.225 g (0.170 mmol, 68.4 %) Anal. Calcd. for $Mn_4C_{34}H_{28}Cl_8N_4O_{20}$ (M.W. 1315.96): C, 31.03; H, 2.14; N, 4.26. Found: C, 31.83; H, 2.27; N, 4.94. Important IR absorptions (KBr disk, cm^{-1}): 3119, 3084, 2955, 2019, 1641, 1606, 1572, 1502, 1471, 1383, 1238, 1161, 1091, 1033, 937, 794, 773, 727, 665 and 416.

5.3. Measurements

IR spectra were obtained with a Shimadzu FT-IR 8000 spectrometer. Elemental analysis was obtained using a FLASH EA 1112 SERIES CHNS analyzer.

5.3.1. Crystallographic data collection and structure determination

Data were collected on a Bruker SMART APEX CCD X-ray diffractometer using graphite monochromated Mo Kα radiation. The data were reduced using SAINTPLUS[14], and multiscan absorption corrections using SADABS[15] were applied. The structures were solved using SHELXS-97 and refined using SHELXL-97[16]. All ring hydrogen atoms were assigned on the basis of geometrical considerations and were allowed to ride upon the respective carbon atoms. All water hydrogen atoms were located from the difference Fourier maps and bond

length constraints were applied. Crystal data are in Table 5.1 and 5.4 and important interatomic distances and angles in Table 5.2, 5.3, 5.5 and 5.6.

5.4. Crystal structure

5.4.1 Structure of $[Mn_3O_4(bpy)_4(Cl_3CCOO)_2](Cl_3COO)_2(Cl_3COOH)_4$ (1)

Molecule lies on a crystallographically imposed 2 fold axis passing through Mn(2), which is situates at special position. The structure (Figure 5.1) consists of trinuclear cation $[Mn_3O_4(bpy)_4(Cl_3CCOO)_2]^{2+}$, two trichloro acetate anions and four trichloroacetic acid molecules. Manganese atoms occupy the vertices of an isosceles triangle. Coordination octahedron of Mn2 consists of two pairs of nitrogen atoms of two bpy moieties and two μ-oxo groups. Whereas that of each Mn1 and Mn1(#1) atoms consists of a pair of nitrogen atoms of a bpy moiety, three μ-oxo oxygen atoms, and an oxygen atom of the trichloro acetate anion. The structural parameters are comparable to the reported Mn(IV) trimers[11]. Mn-Mn distances involving Mn2 are equal at 3.249 Å, and the distance between the doubly bridged manganese atoms Mn1 and Mn1(#1) is considerably shorter 2.687 Å. Four lattice free trichloroacetic acids play a major role in the crystal packing. Various interactions like O-H…O (1.624-1.797 Å), C20-H20…Cl19 (2.798 Å), Cl2…O5, (3.053 Å) and π stacking interaction of Cl3 (Cl3….C9, 3.145 Å) pack the molecules into a 2-dimensional networks (Figure 5.2). Various C-H…O interactions (2.276-2.477 Å) interconnect these 2-dimensional networks into a 3-dimensional networks.

Table 5.1. Crystallographic data for **1** and **2**

	1	**2**
Formula	$Mn_3C_{56}H_36Cl_{24}N_8O_{20}$	$Mn_3CeC_{40}H_{42}N_{15}O_{30}$
Formula weight	2156.55	1517.83
Crystal system	Monoclinic	Monoclinic
Space group	*C*2/*c*	*Cc*
a (Å)	22.1016(11)	24.642(2)
b (Å)	19.9503(10)	15.1775(15)
c (Å)	19.4355(10)	17.4441(17)
β (º)	114.0910(10)	123.071(6)
V (Å^3)	7823.3(7)	5467.2(9)
Z	4	4
T (K)	100(2)	100(2)
D_{calc} (g cm^{-3})	1.831	1.844
μ (mm^{-1})	1.371	1.603
F(000)	4284	3040
Crystal size	0.24 x 0.20 x 0.10	0.38 x 0.24 x 0.22
θ Range (º)	1.44 to 26.03	1.67 to 26.04
h/k/l	-27<=h<=27, -24<=k<=24, -23<=l<=23	-30<=h<=30, -18<=k<=18, -21<=l<=21
Reflection collected	40156	28014
Unique reflect., [R_{int}]	7711 [0.0393]	10510 [0.0300]
Goodness of fit on F^2	1.022	1.042
R_1 [$I>2\sigma(I)$]	0.0426	0.0289
wR_2 (all data)	0.1051	0.0691

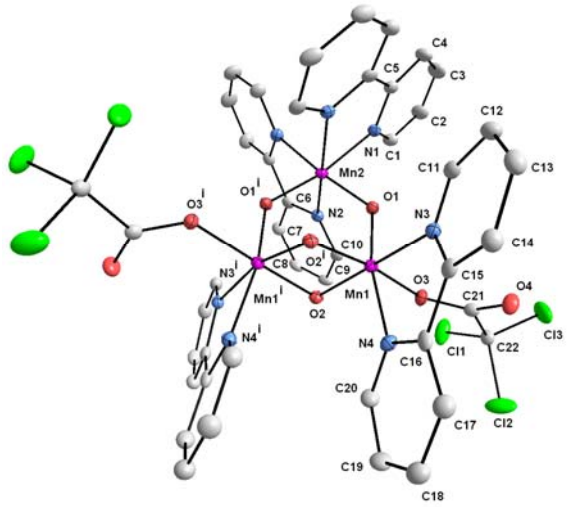

Figure. 5.1.Thermal ellipsoid plot of the coordination environment of the complex cation in **1**. Atoms are represented as 50% probability ellipsoids. Trichloroacetate anions, trichloro acetic acids, and ring hydrogens have been omitted for clarity. (i) Symmetry code: -x, y, -z+3/2.

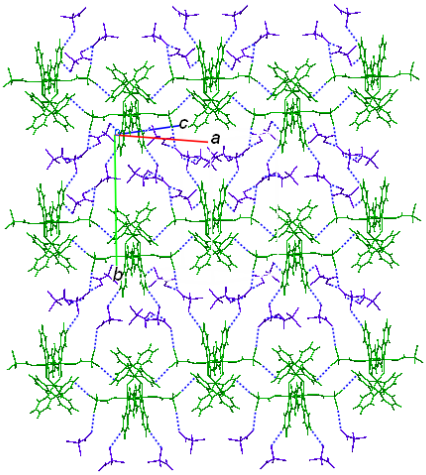

Figure. 5.2. 2-dimensional networks of **1** (blue = trichloroacetic acids and trichloroacetate anions. Green = $[Mn_3O_4(bpy)_4(Cl_3CCOO)_2]^{2+}$.)

Table 5.2 Selected bond lengths [Å] and angles [º] for **1**[a]

Mn(1)-O(2)	1.806(2)	O(1)-Mn(1)-N(3)	95.12(9)
Mn(1)-O(2)#1	1.814(2)	O(3)-Mn(1)-N(3)	101.60(9)
Mn(1)-O(1)	1.833(2)	N(4)-Mn(1)-N(3)	77.74(10)
Mn(1)-O(3)	1.977(2)	O(2)-Mn(1)-Mn(1)#1	42.18(6)
Mn(1)-N(4)	2.045(3)	O(2)#1-Mn(1)-Mn(1)#1	41.97(6)
Mn(1)-N(3)	2.075(2)	O(1)-Mn(1)-Mn(1)#1	90.49(6)
Mn(1)-Mn(1)#1	2.6865(9)	O(3)-Mn(1)-Mn(1)#1	131.27(6)
Mn(2)-O(1)#1	1.765(2)	N(4)-Mn(1)-Mn(1)#1	100.95(7)
Mn(2)-O(1)	1.765(2)	N(3)-Mn(1)-Mn(1)#1	127.09(7)
Mn(2)-N(2)	2.012(2)	O(1)#1-Mn(2)-O(1)	100.74(13)
Mn(2)-N(2)#1	2.012(2)	O(1)#1-Mn(2)-N(2)	89.28(9)
Mn(2)-N(1)	2.085(3)	O(1)-Mn(2)-N(2)	96.38(10)
Mn(2)-N(1)#1	2.085(3)	O(1)#1-Mn(2)-N(2)#1	96.38(10)
O(2)-Mn(1)-O(2)#1	82.98(9)	O(1)-Mn(2)-N(2)#1	89.27(9)
O(2)-Mn(1)-O(1)	95.31(9)	N(2)-Mn(2)-N(2)#1	171.14(14)
O(2)#1-Mn(1)-O(1)	96.97(9)	O(1)#1-Mn(2)-N(1)	170.29(10)
O(2)-Mn(1)-O(3)	89.67(9)	O(1)-Mn(2)-N(1)	88.05(9)
O(2)#1-Mn(1)-O(3)	172.13(9)	N(2)-Mn(2)-N(1)	93.86(10)
O(1)-Mn(1)-O(3)	86.51(9)	N(2)#1-Mn(2)-N(1)	79.48(10)
O(2)-Mn(1)-N(4)	93.47(10)	O(1)#1-Mn(2)-N(1)#1	88.06(9)
O(2)#1-Mn(1)-N(4)	91.38(10)	O(1)-Mn(2)-N(1)#1	170.29(10)
O(1)-Mn(1)-N(4)	168.55(10)	N(2)-Mn(2)-N(1)#1	79.49(10)
O(3)-Mn(1)-N(4)	86.20(9)	N(2)#1-Mn(2)-N(1)#1	93.86(10)
O(2)-Mn(1)-N(3)	165.07(10)	N(1)-Mn(2)-N(1)#1	83.50(14)
O(2)#1-Mn(1)-N(3)	85.17(9)		

5.4.2 Structure of $[Mn_3O_4(bpy)_4(H_2O)_2]$ $[Ce(NO_3)_5(H_2O)](NO_3)_2(H_2O)_2$ (2)

Molecular structure of the complex **2** is shown in figure 5.3. The structural parameters are comparable to that of the reported complexes[11]. Three manganese atoms occupies the vertices of an isosceles triangle. One of the manganese atoms Mn3 is linked to the other two manganese atoms Mn1 and Mn2 by means of individual μ-oxobridges, *viz* O6 and O5 respectively. Mn1 and Mn2 are themselves linked to each other by two mutual μ-oxobridges (O1 and O2). The Mn…Mn distances between Mn1 and Mn3 is 3.259 Å and Mn2 and Mn3 is 3.249 Å. The distance between the doubly bridged Mn1 and Mn2 is considerably shorter at 2.667 Å. The geometry of each manganese atom is octahedral. The coordination around Mn1 and Mn2 atoms consist of a pair of nitrogen atoms from bpy moiety, three μ-oxygen atoms and the oxygen atom of water molecules where as Mn3 consists of two pairs of nitrogen atoms of two bpy moieties and two μ-oxygen atoms. The average Mn-N distance is 2.085 Å and average Mn-O_{oxo} distance is 1.817 Å. However the average Mn-O_{water} distance is 2.006 Å. Three manganese atoms and two μ-oxo bridges O5 and O6 are coplanar. The $[Ce(NO_3)_5(H_2O)]^{2-}$ is 11 coordinate, being bonded to five nitrate anions and one water molecule. The average Ce-$O_{nitrate}$ distance is 2.616 Å and Ce-O_{water} distance is 2.474 Å. The structural parameters of $[Ce(NO_3)_5(H_2O)]^{2-}$ anion are comparable with the previous reports[17]. **2** forms three-dimensional hydrogen bonded structures with the help of two nitrate anions and $[Ce(NO_3)_5(H_2O)]^{2-}$ anion.

Various O-H…O (1.782 - 2.491 Å) and C-H…O (2.322 - 2.470 Å) interactions build the molecules into three-dimensional networks.

a

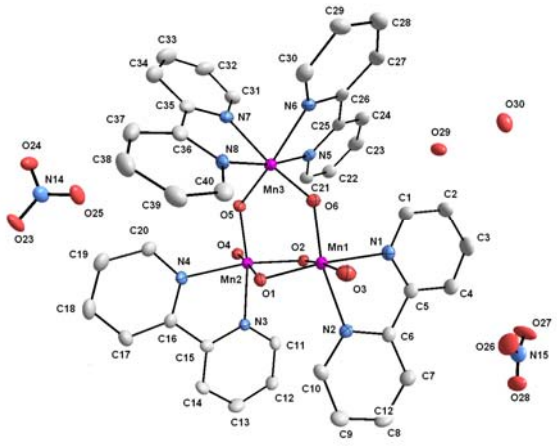

b

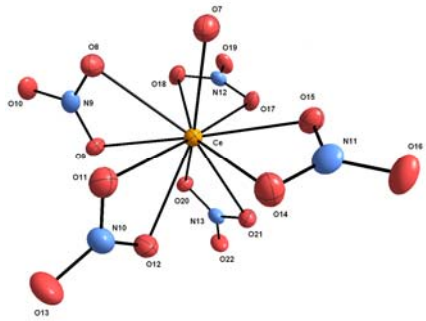

Figure.5.3. Thermal ellipsoid plot of the coordination environment of the complex in **2**: (a) cation, nitrate anions and water molecules, (b) $[Ce(NO_3)_5(H_2O)]^{2-}$ anion. Atoms are represented as 50% probability ellipsoids. Ring and water hydrogens hydrogens have been omitted for clarity.

Table 5.3 Selected bond lengths [Å] and angles [°] for **2**

Mn(1)-O(1)	1.811(2)	O(1)-Mn(2)-O(5)	98.64(11)
Mn(1)-O(2)	1.815(2)	O(2)-Mn(2)-O(4)	94.61(11)
Mn(1)-O(6)	1.823(2)	O(1)-Mn(2)-O(4)	174.15(11)
Mn(1)-O(3)	1.984(3)	O(5)-Mn(2)-O(4)	87.13(11)
Mn(1)-N(2)	2.050(3)	O(2)-Mn(2)-N(3)	93.24(11)
Mn(1)-N(1)	2.068(3)	O(1)-Mn(2)-N(3)	91.21(11)
Mn(1)-Mn(2)	2.6676(7)	O(5)-Mn(2)-N(3)	167.09(11)
Mn(2)-O(2)	1.802(2)	O(4)-Mn(2)-N(3)	83.23(11)
Mn(2)-O(1)	1.805(2)	O(2)-Mn(2)-N(4)	169.20(11)
Mn(2)-O(5)	1.836(2)	O(1)-Mn(2)-N(4)	89.55(11)
Mn(2)-O(4)	2.028(3)	O(5)-Mn(2)-N(4)	93.35(11)
Mn(2)-N(3)	2.053(3)	O(4)-Mn(2)-N(4)	91.10(11)
Mn(2)-N(4)	2.070(3)	N(3)-Mn(2)-N(4)	78.32(11)
Mn(3)-O(6)	1.768(2)	O(2)-Mn(2)-Mn(1)	42.66(8)
Mn(3)-O(5)	1.778(2)	O(1)-Mn(2)-Mn(1)	42.55(7)
Mn(3)-N(8)	1.993(3)	O(5)-Mn(2)-Mn(1)	91.53(8)
Mn(3)-N(5)	2.004(3)	O(4)-Mn(2)-Mn(1)	136.87(8)
Mn(3)-N(6)	2.066(3)	N(3)-Mn(2)-Mn(1)	101.37(8)
Mn(3)-N(7)	2.084(3)	N(4)-Mn(2)-Mn(1)	131.98(8)
O(1)-Mn(1)-O(2)	83.31(11)	O(6)-Mn(3)-O(5)	100.03(11)
O(1)-Mn(1)-O(6)	95.66(11)	O(6)-Mn(3)-N(8)	95.12(12)
O(2)-Mn(1)-O(6)	96.70(11)	O(5)-Mn(3)-N(8)	90.32(12)
O(1)-Mn(1)-O(3)	94.78(11)	O(6)-Mn(3)-N(5)	91.25(12)
O(2)-Mn(1)-O(3)	175.32(11)	O(5)-Mn(3)-N(5)	96.81(12)
O(6)-Mn(1)-O(3)	87.73(11)	N(8)-Mn(3)-N(5)	169.48(12)
O(1)-Mn(1)-N(2)	95.43(11)	O(6)-Mn(3)-N(6)	86.62(11)
O(2)-Mn(1)-N(2)	93.40(11)	O(5)-Mn(3)-N(6)	172.49(12)

O(6)-Mn(1)-N(2)	165.78(11)	N(8)-Mn(3)-N(6)	92.57(12)
O(3)-Mn(1)-N(2)	82.51(12)	N(5)-Mn(3)-N(6)	79.44(12)
O(1)-Mn(1)-N(1)	171.36(11)	O(6)-Mn(3)-N(7)	169.15(11)
O(2)-Mn(1)-N(1)	91.31(11)	N(8)-Mn(3)-N(7)	79.81(12)
O(6)-Mn(1)-N(1)	91.67(11)	N(5)-Mn(3)-N(7)	92.48(12)
O(3)-Mn(1)-N(1)	90.07(11)	N(6)-Mn(3)-N(7)	84.05(12)
N(2)-Mn(1)-N(1)	78.09(12)	Mn(2)-O(1)-Mn(1)	95.08(11)
O(1)-Mn(1)-Mn(2)	42.37(8)	Mn(2)-O(2)-Mn(1)	95.06(11)
O(2)-Mn(1)-Mn(2)	42.29(8)	Mn(3)-O(5)-Mn(2)	128.02(14)
O(6)-Mn(1)-Mn(2)	89.98(8)	Mn(3)-O(6)-Mn(1)	130.30(14)
O(3)-Mn(1)-Mn(2)	136.59(8)	O(2)-Mn(2)-O(5)	96.08(11)
N(2)-Mn(1)-Mn(2)	104.21(8)	O(5)-Mn(3)-N(7)	89.64(11)
N(1)-Mn(1)-Mn(2)	133.34(8)	O(2)-Mn(2)-O(1)	83.85(11)

5.4.3 Crystal structure of $[Mn_4O_2(bpy)_2(CH_3COO)_7]Br_3$ (3)

Molecular structure of **3** is shown in figure 5.4. The molecule lies on a symmetric imposed *C*2 axis through the centre of two bridging oxo units. The molecule posses a Mn_4O_2 core which can be considered as two-edge sharing Mn_3O units. The resulting arrangement has a butterfly like structure with Mn1 atoms occupy on the hinge sites and Mn2 atoms occupy on the edges sites. The C2 axis is bisecting the carboxylate group which bridges the hinge Mn1 atoms. Two terminal bpy groups complete the peripheral ligation with each of the four Mn(III) ion possessing distorted octahedral geometry. The μ_3-oxide atom O1 lies 0.598 below the Mn_3 plane. The average Mn-$O_{\mu 3}$ distance is 1.878 Å. Mn1 atom, which occupy on hinge side of the structure has Jahn-Teller elongation along the Mn1-

O2 and Mn1-O6 carboxylate bonds with distances 2.229 Å and 2.169Å respectively. Mn2 atom, which occupy on wing site has an elongation along Mn2-O5 and Mn2-O8 carboxylate bonds with distances 2.150 Å and 2.172 Å. The average Mn-N_{bpy} distance is 2.071 Å. All of the carboxylate groups are having considerable amount of asymmetry in their coordination as one oxygen atom of the each carboxylate ligand is coordinated through Jahn-Teller axis. The structural parameters are comparable with the previous reports[18]. The Br1-Br2 distance is 2.495 Å.

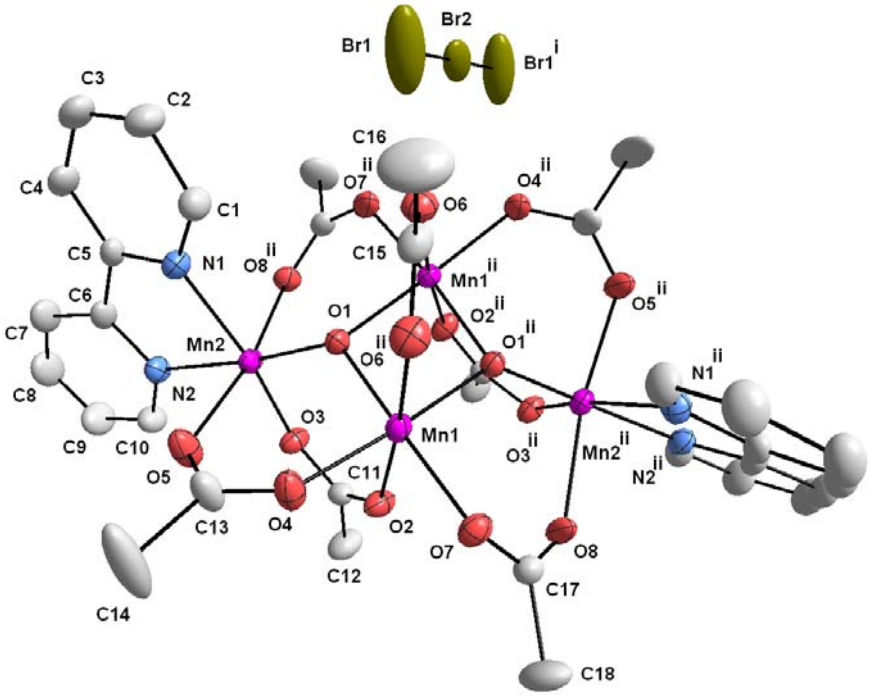

Figure 5.4. Thermal ellipsoid plot of the coordination environment of the complex molecule in **3**. Atoms are represented as 50% probability ellipsoids and ring hydrogens have been omitted for clarity. Symmetry code: (i) -x+1/2, -y+1/2, -z, (ii) -x, y, -z+1/2.

Table 5.4. Crystallographic data for **3** and **4**

	3	**4**
Formula	$Mn_4C_{34}H_{37}Br_3N_4O_{16}$	$Mn_4C_{34}H_{28}Cl_8N_4O_{20}$
Formula weight	1217.17	1315.96
Crystal system	Monoclinic	Triclinic
Space group	C2/c	$P\bar{1}$
a (Å)	28.011(2)	12.2343(6)
b (Å)	11.8988(8)	12.6575(7)
c (Å)	16.1194(11)	17.0899(9)
α (º)	90	89.5970(10)
β (º)	121.2570(10)	89.3860(10)
γ (º)	90	62.4020(10)
V (Å^3)	4592.7(6)	2345.2(2)
Z	4	2
T (K)	298(2)	100(2)
D_{calc} (g cm^{-3})	1.760	1.864
μ (mm^{-1})	3.753	1.590
F(000)	2408	1312
Crystal size	0.36 x 0.20 x 0.13	0.40 x 0.20 x 0.16
θ Range (º)	1.70 to 28.28	1.82 to 25.00
h/k/l	-37<=h<=36, -15<=k<=15, -21<=l<=21	-14<=h<=14, -15<=k<=15, -20<=l<=20
Reflection collected	25757	22545
Unique reflect., [R_{int}]	5479 [0.0497]	8198 [0.0245]
Goodness of fit on F^2	1.016	1.022
R_1 [$I>2\sigma(I)$]	0.0593	0.0780
wR_2 (all data)	0.1932	0.2294

Table 5.5 Selected bond lengths [Å] and angles [º] for **3**

Mn(1)-O(1)	1.900(3)	O(4)-Mn(1)-O(2)	88.57(18)
Mn(1)-O(1)#1	1.908(3)	O(6)-Mn(1)-O(2)	175.20(17)
Mn(1)-O(7)	1.935(4)	O(1)-Mn(1)-Mn(1)#1	41.93(10)
Mn(1)-O(4)	1.944(4)	O(1)#1-Mn(1)-Mn(1)#1	1.72(10)
Mn(1)-O(6)	2.169(4)	O(7)-Mn(1)-Mn(1)#1	135.60(12)
Mn(1)-O(2)	2.229(4)	O(4)-Mn(1)-Mn(1)#1	136.20(13)
Mn(1)-Mn(1)#1	2.8369(15)	O(6)-Mn(1)-Mn(1)#1	81.83(11)
Mn(2)-O(1)	1.829(3)	O(2)-Mn(1)-Mn(1)#1	100.88(11)
Mn(2)-O(3)	1.913(4)	O(1)-Mn(2)-O(3)	97.77(16)
Mn(2)-N(2)	2.064(4)	O(1)-Mn(2)-N(2)	173.40(17)
Mn(2)-N(1)	2.077(5)	O(3)-Mn(2)-N(2)	88.78(17)
Mn(2)-O(5)	2.149(4)	O(1)-Mn(2)-N(1)	95.05(17)
Mn(2)-O(8)#1	2.172(4)	O(3)-Mn(2)-N(1)	167.00(18)
O(1)-Mn(1)-O(1)#1	82.90(15)	N(2)-Mn(2)-N(1)	78.37(19)
O(1)-Mn(1)-O(7)	173.59(16)	O(1)-Mn(2)-O(5)	92.66(15)
O(1)#1-Mn(1)-O(7)	94.00(15)	O(3)-Mn(2)-O(5)	91.94(19)
O(1)-Mn(1)-O(4)	96.51(15)	N(2)-Mn(2)-O(5)	87.90(17)
O(1)#1-Mn(1)-O(4)	173.06(18)	N(1)-Mn(2)-O(5)	89.61(19)
O(7)-Mn(1)-O(4)	87.24(16)	O(1)-Mn(2)-O(8)#1	92.69(15)
O(1)-Mn(1)-O(6)	90.70(15)	O(3)-Mn(2)-O(8)#1	95.43(16)
O(1)#1-Mn(1)-O(6)	86.34(16)	N(2)-Mn(2)-O(8)#1	85.85(16)
O(7)-Mn(1)-O(6)	94.71(16)	N(1)-Mn(2)-O(8)#1	81.77(17)
O(4)-Mn(1)-O(6)	86.75(18)	O(5)-Mn(2)-O(8)#1	170.22(16)
O(1)-Mn(1)-O(2)	88.77(14)	Mn(2)-O(1)-Mn(1)	125.11(18)
O(1)#1-Mn(1)-O(2)	98.32(16)	Mn(2)-O(1)-Mn(1)#1	129.99(19)
O(7)-Mn(1)-O(2)	86.12(15)	Mn(1)-O(1)-Mn(1)#1	96.34(15)

5.4.4 Crystal structure of $[Mn_4O_2(bpy)_2(CH_2ClCOO)_7]ClO_4$ (4)

The molecular structure of the complex **4** is shown in Figure.5.5. Unlike structure **3** the asymmetric unit contains complete cation with no imposed symmetry. The molecule again does posses Mn_4O_2 core which can be considered as two edge sharing Mn_3O units with butterfly structure with Mn1 and Mn2 occupy hinge sites and Mn3 and Mn4 occupy wing sites. The terminal bpy groups complete the peripheral ligation with each of the four Mn atoms possessing distorted octahedral geometry. The average Mn-N_{bpy} distance is 2.046Å. The two μ-oxide atoms O1 and O2 lie 0.523 and 0.522 Å below their respective Mn3 planes. The average Mn-$O_{\mu 3}$ distance is 1.894 Å. The structural parameters are comparable with the previous reports[18].

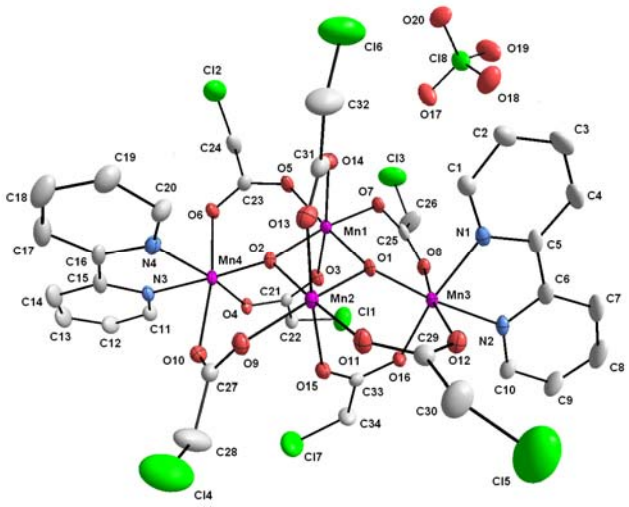

Figure 5.5..Thermal ellipsoid plot of the coordination environment of the complex molecule in **4**. Atoms are represented as 50% probability ellipsoids and ring hydrogens have been omitted for clarity.

Table 5.6 Selected bond lengths [Å] and angles [º] for **4**

Mn(1)-O(2)	1.894(3)	O(2)-Mn(2)-O(13)	86.50(13)
Mn(1)-O(1)	1.896(3)	O(1)-Mn(2)-O(13)	90.04(13)
Mn(1)-O(5)	1.939(3)	O(11)-Mn(2)-O(13)	87.19(14)
Mn(1)-O(7)	1.949(3)	O(9)-Mn(2)-O(13)	97.78(14)
Mn(1)-O(3)	2.193(3)	O(2)-Mn(2)-O(16)	96.85(13)
Mn(1)-O(14	2.199(3)	O(1)-Mn(2)-O(16)	86.84(12)
Mn(1)-Mn(2)	2.8227(9)	O(11)-Mn(2)-O(16)	89.49(14)
Mn(2)-O(2)	1.887(3)	O(9)-Mn(2)-O(16)	85.58(13)
Mn(2)-O(1)	1.897(3)	O(13)-Mn(2)-O(16)	175.11(13)
Mn(2)-O(11)	1.940(3)	O(2)-Mn(2)-Mn(1)	41.81(9)
Mn(2)-O(9)	1.950(3)	O(1)-Mn(2)-Mn(1)	41.89(9)
Mn(2)-O(13)	2.166(3)	O(11)-Mn(2)-Mn(1)	137.74(10)
Mn(2)-O(16)	2.233(3)	O(9)-Mn(2)-Mn(1)	135.49(10)
Mn(3)-O(1)	1.844(3)	O(13)-Mn(2)-Mn(1)	82.59(9)
Mn(3)-O(15)	1.924(3)	O(16)-Mn(2)-Mn(1)	97.52(9)
Mn(3)-N(2)	2.035(4)	O(1)-Mn(3)-O(15)	97.00(13)
Mn(3)-N(1)	2.049(4)	O(1)-Mn(3)-N(2)	172.75(15)
Mn(3)-O(8)	2.168(3)	O(15)-Mn(3)-N(2)	90.24(15)
Mn(3)-O(12)	2.192(3)	O(1)-Mn(3)-N(1)	93.80(15)
Mn(4)-O(2)	1.849(3)	O(15)-Mn(3)-N(1)	168.89(15)
Mn(4)-O(4)	1.919(3)	N(2)-Mn(3)-N(1)	78.94(16)
Mn(4)-N(3)	2.041(4)	O(1)-Mn(3)-O(8)	93.67(13)
Mn(4)-N(4)	2.057(4)	O(15)-Mn(3)-O(8)	90.60(13)
Mn(4)-O(6)	2.164(3)	N(2)-Mn(3)-O(8)	85.90(13)
Mn(4)-O(10)	2.172(3)	N(1)-Mn(3)-O(8)	86.14(14)
O(2)-Mn(1)-O(1)	83.04(13)	O(1)-Mn(3)-O(12)	92.55(13)
O(1)-Mn(1)-O(5)	173.58(14)	O(15)-Mn(3)-O(12)	93.71(13)

O(2)-Mn(1)-O(7)	171.23(14)	N(2)-Mn(3)-O(12)	87.28(13)
O(1)-Mn(1)-O(7)	94.32(13)	N(1)-Mn(3)-O(12)	88.36(14)
O(5)-Mn(1)-O(7)	86.34(13)	O(8)-Mn(3)-O(12)	171.95(12)
O(2)-Mn(1)-O(3)	87.00(13)	O(2)-Mn(4)-O(4)	97.34(13)
O(1)-Mn(1)-O(3)	96.85(13)	O(2)-Mn(4)-N(3)	172.29(15)
O(5)-Mn(1)-O(3)	89.57(14)	O(4)-Mn(4)-N(3)	90.06(15)
O(7)-Mn(1)-O(3)	85.01(13)	O(2)-Mn(4)-N(4)	93.87(15)
O(2)-Mn(1)-O(14)	89.57(13)	O(4)-Mn(4)-N(4)	168.78(15)
O(1)-Mn(1)-O(14)	86.19(13)	N(3)-Mn(4)-N(4)	78.72(16)
O(5)-Mn(1)-O(14)	87.40(14	O(2)-Mn(4)-O(6)	92.80(13)
O(7)-Mn(1)-O(14)	98.61(13)	O(4)-Mn(4)-O(6)	92.96(14)
O(3)-Mn(1)-O(14)	175.11(12)	N(3)-Mn(4)-O(6)	88.95(14)
O(2)-Mn(1)-Mn(2)	41.63(9)	N(4)-Mn(4)-O(6)	86.88(14)
O(1)-Mn(1)-Mn(2)	41.92(9)	O(2)-Mn(4)-O(10)	93.31(13)
O(5)-Mn(1)-Mn(2)	137.14(10)	O(4)-Mn(4)-O(10)	92.09(13)
O(7)-Mn(1)-Mn(2)	136.24(10)	N(4)-Mn(4)-O(10)	86.85(14)
O(3)-Mn(1)-Mn(2)	97.59(9)	N(3)-Mn(4)-O(10)	84.23(14)
O(14)-Mn(1)-Mn(2)	82.10(9)	O(6)-Mn(4)-O(10)	171.52(12)
O(2)-Mn(2)-O(1)	83.19(13)	Mn(3)-O(1)-Mn(1)	130.48(17)
O(2)-Mn(2)-O(11)	173.64(14)	Mn(3)-O(1)-Mn(2)	126.04(17)
O(1)-Mn(2)-O(11)	97.56(13)	Mn(1)-O(1)-Mn(2)	96.19(13)
O(2)-Mn(2)-O(9)	93.69(13)	Mn(4)-O(2)-Mn(2)	130.79(17)
O(1)-Mn(2)-O(9)	171.40(14)	Mn(4)-O(2)-Mn(1)	125.59(17)
O(11)-Mn(2)-O(9)	86.44(14)	Mn(2)-O(2)-Mn(1)	96.56(13)

5.5 Conclusion

The oxidation of manganese(II) acetate with ceric ammonium nitrate was done in the presence of trichloroacetic acid and trifluroacetic acid. In both cases two new trinuclear manganese(IV) complexes were obtained. The $[Mn_3O_4X_2(N\text{-}N)_4]$ (where N-N=bpy or phen) core with monodentate ligand like Cl- and H_2O have been reported[11]. It is for first the time $[Mn_3O_4X_2(N\text{-}N)_4]$ core has been reported with Cl_3CCOO^- ion. Two new manganese(III) tetranuclear complexes have been synthesized. The treatment of trinuclear complexes containing the Mn_3O core with chelating bpy gives the Mn_4O_2 tetranuclear complexes. Both complexes **3** and **4** are having $[Mn_4O_2(OOCR)_7]^+$ core and a butterfly structure which is in accordance with the previous reports[18].

5.6 References

1. Christou, G.; Gatteschi, D.; Hendrickson, D. N.; Sessoli, R. *MRS Bull.* **2000**, *25*, 66.
2. Christou, G. *Acc. Chem. Res*. **1989**, *22*, 328.
3. Wieghardt, K. *Angew. Chem. Int. Ed.* **1989**, *28*, 1153.
4. Pecoraro, V. L.; Baldwin, M. J.; Gelasco, A. *Chem. Rev.* **1994**, *94,* 807.

5. Manchandra, R.; Brudvig, G. W.; Crabtree, R. H. *Coord. Chem. Rev.* **1995**, *144,* 1.

6. Rütinger, W.; Dismukes, G. *Chem. Rev*. **1997**, *97*, 1.

7. Vincent, J. B.; Christmas, C.; Chang, H. R.; Li, Q.; Boyd, P. D. W.; Huffman, J. C.; Hendrickson, D. N.; Christou. G. *J. Am. Chem. Soc*. **1989**, *111*, 2086.

8. (a) Vincent, J. B.; Christmas, C.; Chang, H. R.; Li, Q.; Boyd, P. D. W.; Huffman, J. C.; Hendrickson, D. N.; Christou. G. *J. Am. Chem. Soc*. **1989**, *111*, 2086. (b) Vincent, J. B.; Christmas, C.; Huffman, J. C.; Christou. G.; Chang, H. R.; Hendrickson, D. N. *J. Chem. Soc. Chem*. *Commun*. **1987**, 236. (c) Bouwman, E.; Bolcar, M. A.; Libby, E.; Huffman, J. C.; Folting, K.; Christou, G. *Inorg. Chem*. **1992**, *31*. 5185. (d) Libby, E.; McCusker, J. K.; Schmitt, E. A.; Folting, K; Hendrickson, D. N.; Christou, G. *Inorg. Chem*. **1991**, *30*, 3486. (e) Boskovic, C.; Folting, K; Christou, G. *Polyhedron* **2000**, *19*, 2111. (f) Wang, S.; Huffman, J. C.; Folting, K.; Streib, W. E.; Lobokovsky, E. B.; Christou, G. *Angew. Chem*. **1991**, *103*, 1681.

9. (a) Ferreira, K. N.; Iverson, T. M.; Maghlaoui, K.; Barber, J.; Iwata, S. *Science* **2004**, *303*, 1831. (b) Loll, B.; Kern, J.; Saenger, W.; Zouni, A.; Biesadka, J. *Nature* **2005**, 438.

10. (a) Guils, R. D.; Zimmerman, J. L.; McDerrnott, A. E. ; Yachandra, V. K.; Cole, J. L.; Dexheimer, S. L.; Britt, R. D. ; Weighardt, K.; Bossek, U.

Sauer, K.; Klein, M. P. *Biochemistry* **1990**, *29*, 486. (b) George, G. N.; Prince, R. C.; Cramer, S. P. *Science* **1989**, *243*, 789. (c) Rüettinger, W. Dismukes, G. C. *Chem. Rev.*, **1997**, *97*, 1. (d) Robblee, J. H.; Cince, R. M.; Yachandra, V. K. *Biochim. Biophys. Acta* **2001**, *1503*, 7. (e) Sproviero, E. M.; Gascón, J. A.; McEvoy, J. P.; Brudvig, G. W.; Batista, V. S. *J. Inorg. Biochem.* **2005**, *100*, 780. (f) Sproviero, E. M.; Gascón, J. A. ; McEvoy, J. P.; Brudvig, G. W.; Batista, V. S. *J. Chem. Theory Comput.* **2006**, *2*, 1119.

11. (a) Sarneski, J. E.; Thorp, H. H.; Brudvig, G. W.; Crabtree, R. H.; Schulte, G. K. *J.Am.Chem.Soc.* **1990**, *112*, 7255. (b) Auger, N. Girerd, J.-J. Corbella, M.; Gleizes, A.; Zimmermann, J.-L. *J. Am. Chem. Soc.* **1990**, *112***,** 448. (c) Reddy, K. R.; Rajasekharan, M. V.; Arulsamy, N.; Hodgson, D. J. *Inorg. Chem.* **1996**, *35***,** 2283.

13. Brauer, G. Ed. *Handbook of Preparative Inorganic Chemistry*: Academic Press: New York. 2, **1965**, 1469.

14. SAINTPLUS, Bruker AXS Inc. Madison, Wisconsin, USA.

15. Sheldrick, G.M. SADABS Programm for Empirical Absorption Correction, University of Gottingen, Germany, **1996**.

16. Sheldrick, M. SHELXS and SHELXL-97, University of Gottingen, Gottingen, Germany, **1997**.

17. (a) Chen, D.-G.; Cheng, W.-D.; Zhang, H.; Zhang, Y.-C. *Chin. J. Struct. Chem.* **2004***, 23*, 870. (b) Chan, G. Y. S.; Drew, M. G. B.; Hudson, M. J.;

Isaacs, M. J. N. S.; Byers, P.; Madic, C. *Polyhedron* **1996**, *15*, 3385. (c) Xue, G.-L; Yang, Y.- X.; Li, H.-X.; Shui-Yang.; Li, J. *Chin. Chin. J. Inorg. Chem.* **2001**, ***17,*** 423.

18. (a) Vincent, J. B.; Christmas, C.; Chang, H. R.; Li, Q.; Boyd, P. D. W.; Huffman, J. C.; Hendrickson, D. N.; Christou. G. *J. Am. Chem. Soc*. **1989**, *111*, 2086. (b) Vincent, J. B.; Christmas, C.; Huffman, J. C.; Christou. G.; Chang, H. R.; Hendrickson, D. N. *J. Chem. Soc. Chem*. *Commun*. **1987**, 236. (c) Bouwman, E.; Bolcar, M. A.; Libby, E.; Huffman, J. C.; Folting, K.; Christou, G. *Inorg. Chem*. **1992**, *31*. 5185. (d) Libby, E.; McCusker, J. K.; Schmitt, E. A.; Folting, K; Hendrickson, D. N.; Christou, G. *Inorg. Chem*. **1991**, *30*, 3486. (e) Boskovic, C.; Folting, K; Christou, G. *Polyhedron*, **2000**, *19*, 2111. (f) Wang, S.; Huffman, J. C.; Folting, K.; Streib, W. E.; Lobokovsky, E. B.; Christou, G. *Angew. Chem*. **1991**, 103, 1681.

APPENDIX 1

Silver and platinum complexes of 4,5-diazafluoren-9-one

A.1 Introduction

4,5-Diazafluoren-9-one (dafone) is a bidentate ligand. It is a derivative of 1,10-phenanthroline (phen), having an exocyclic keto function[1]. Dafone attracted attention of researchers due perhaps to its DNA intercalation properties[2]. The reactive exocyclic keto function in dafone offers distinct advantages for further derivatization to yield multinuclear metal complexes having interesting catalytic and biological properties.

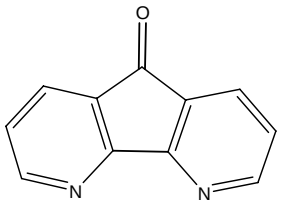

(dafone)

Unlike phen / bpy (1,10-phenanthroline/2,2'-bipyridine), coordination chemistry of bidentate, neutral ligand dafone is still restricted to a few metals[3-9]. Even though silver(I) and platinum(II) complexes of other diimine ligands like 2,2'-biyridine (bpy) and 1,10-phenanthroline (phen) are known in the literature[10-14], little is known about the dafone complexes. Unlike phen and bpy, dafone has a large N-N bite distance (2.99Å) enforced by the rigid five-membered centre ring, which makes it unique among the diimine ligands[15]. In order to explore the effect of the geometry of dafone on silver and platinum we have synthesized some of its complexes with these metals.

A.2. Experimental

A.2.1 Reagents

All chemicals were purchased from Ranbaxy chemicals and used without further purification. Dafone was prepared using a reported procedure[1]

A.2.2 Synthesis

Preparation of $[Ag(dafone)_2]NO_3.H_2O$ (1): Dafone (0.181 g , 1.00 mmol) dissolved in acetonitrile (15 mL) was added to an aqueous solution (15 mL) of $AgNO_3$ (0.085 g, 0.50 mmol), with constant stirring. It was filtered and kept for crystallization at room temperature to yield yellow needle type crystals suitable for X-ray data collection. Yield 0.25 g, (0.45 mmol, 90 %). Anal. cald. for $AgC_{22}H_{14}N_5O_6$ (M.W. 552.25 g): C, 47.85; H, 2.56; N, 12.68. Found: C, 47.72; H, 2.52; N, 12.93. Important IR absorptions (KBr disk, cm^{-1}): 3576, 3425, 3034, 1834, 1718, 1593, 1462, 1259, 916 and 758.

Preparation of $[Ag_2(4,4'\text{-bipyridine})(dafone)_4](BF_4)_2$ (2): Acetonitrile solution (20 mL) of 4,4'-bipyridine (0.039 g, 0.250 mmol) and dafone (0.181 g, 1.00 mmol) was slowly added to an acetonitrle solution (10 mL) of $AgBF_4$ (0.098 g, 0.50 mmol) while stirring. It was filtered and kept for crystallization at room temperature to yield yellow block crystals suitable for X-ray data collection. Yield 0.295 g (0.232 mmol, 93 %). Anal. cald. for $Ag_2C_{54}H_{32}B_2F_8N_{10}O_4$ (M.W. 1274.25 g): C, 50.90; H, 2.53; N, 10.99 . Found: C, 50.84; H, 2.58; N, 10.73. Important IR absorptions (KBr disk, cm^{-1}): 3097, 1728, 1593, 1566, 1464, 1406, 1259, 1055, and 758.

Preparation of Pt(dafone)Cl_2 (3): K_2PtCl_4 (0.104 g, 0.25 mmol) was dissolved in 5 mL water. Acetonitrile (40 mL) was added to the above solution and it was heated while stirring. Dafone (0.045 g, 0.25 mmol) in acetonitrile (10 mL) was added to the above solution. After 10 minutes, the yellow solution was filtered and volume of the solution was reduced considerably by heating under constant stirring. When the volume of the solution was reduced considerably, it was kept aside at room temperature. Within 2 days crystalline precipitate was formed. Yield 0.067g (0.145 mmol, 60 %). X-ray quality crystals were obtained by layering the original solution (concentration) with methanol in a long tube. Anal. cald. for $PtC_{11}H_6Cl_2N_2O$ (M.W. 448.17): C, 29.48; H, 1.35; N, 6.25. Found: C, 29.87; H, 1.41; N, 6.09. Import IR absorptions (KBr disk, cm^{-1}): 1790, 1736, 1593, 1570, 1423, 1283, 1219, 1099, 891, 823, 750, 707 and 412.

A.3 Measurements

IR spectra were obtained with a Shimadzu FT-IR 8000 spectrometer. Elemental analysis was obtained using a FLASH EA 1112 SERIES CHNS analyzer.

A.3.1 X-ray crystallography

Data were collected on a Bruker SMART APEX CCD X-ray diffractometer using graphite monochromated Mo Kα radiation. The data were reduced using SAINTPLUS[16], and multiscan absorption corrections using SADABS[17] were applied. The structures were solved using SHELXS-97 and refined using

SHELXL-97[18]. All ring hydrogen atoms were assigned on the basis of geometrical considerations and were allowed to ride upon the respective carbon atoms. All water hydrogen atoms were located from the difference Fourier maps and bond length constraints were applied.

A.4 Crystal structure

A.4.1 Crystal structure of $[Ag(dafone)_2]NO_3.H_2O$ (1) and $[Ag_2(4,4'\text{-bipyridine})(dafone)_4](BF_4)_2$ (2) : There are two crystallographically independent, but chemically similar $Ag(dafone)_2^+$ cations in the unit cell of **1** (Figure A.1). Each four-coordinate silver atom is situated on a crystallographic inversion centre. The coordination is, therefore, strictly planar. However, there is a large asymmetry in the chelating bond distances of dafone (Ag(1)-N(1), 2.222(3); Ag(1)-N(2), 2.695(3); Ag(2)-N(3), 2.254(3); Ag(2)-N(4), 2.650(3) Å).

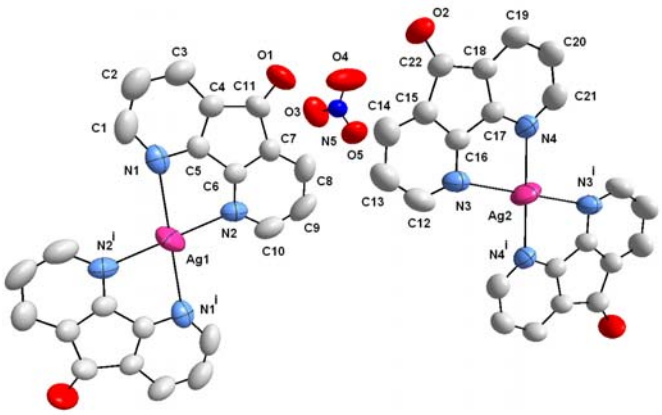

Figure A.1. Thermal ellipsoid plot of the coordination environment of the complex molecules **1.** Atoms are represented as 50% probability ellipsoids. Lattice water and ring hydrogen atoms have been omitted for clarity. [Symmetry code: (i) –x + 1, –y + 2, –z + 1. (ii) –x, –y, –z + 1]

Table .A.1 Crystallographic data for **1** and **2**

	1	**2**	**3**
Formula	Ag C_{22} H_{14} N_5O_6	Ag_2C_{54} H_{32} B_2 F_8 $N_{10}O_4$	Pt $C_{11}H_6Cl_2N_2O$
Formula weight	552.25	1274.26	448.17
Crystal system	Triclinic	Triclinic	Monoclinic
Space group	$P\bar{1}$	$P\bar{1}$	$P2_1/c$
a (Å)	7.5988(9)	8.8909(14)	5.1296(12)
b (Å)	11.4730(13)	10.2543(17)	16.638(4)
c (Å)	13.2265(15)	14.229(2)	2.785(3)
α (º)	114.849(2)	91.856(2)	90
β (º)	90.815(2)	101.272(2)	98.419(18)
γ(º)	93.866(2)	107.774(2)	90
V (Å^3)	1042.8(2)	1205.6(3)	1079.4(4)
Z	2	1	4
μ (mm^{-1})	1.019	0.905	2.758
D_{calc} (g cm^{-3})	1.759	1.755	13.474
T (K)	298(2)	298(2)	100(2)
Crystal size (mm)	0.40 x 0.20 x 0.06	0.32 x 0.24 x 0.14	0.26 x 0.16 x 0.14
θ Range (º)	1.70 to 26.05	1.47 to 26.07	2.02 to 25.99
Reflection collected	10950 /	12608	10986
Unique reflect., [R_{int}]	4100 [0.0213]	4747 [0.0175]	2122 [0.0337]
Goodness of fit	1.030	1.042	1.097
R_1 [$I>2\sigma(I)$]	0.0427	0.0319	0.0227
wR_2	0.1027	0.0839	0.0516

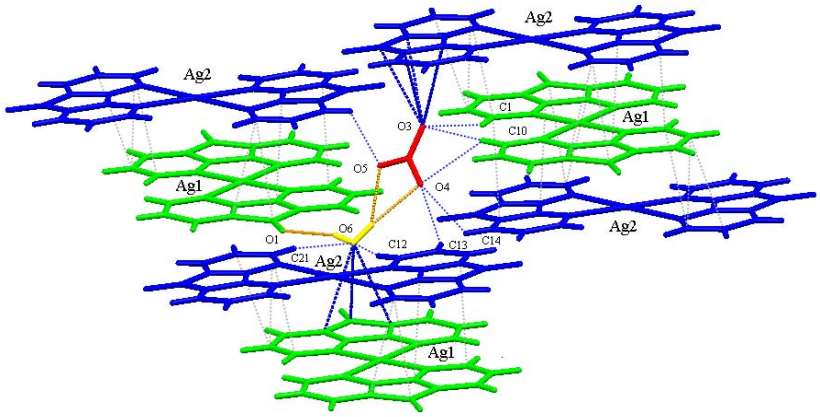

Figure A.2 Weak interactions involving the complex cations, anion and lattice water in **1**.

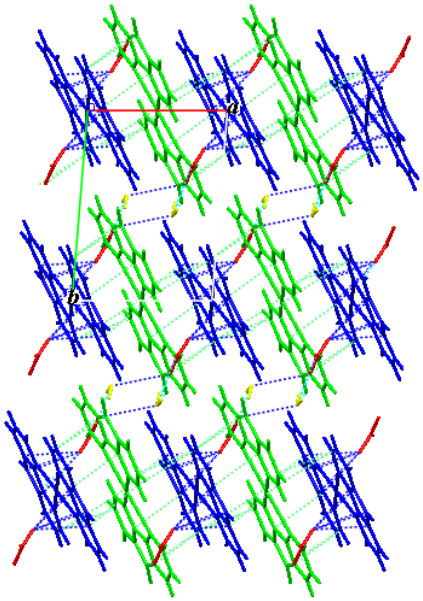

Figure A.3 Crystal packing of **1** viewed down the *c* axis

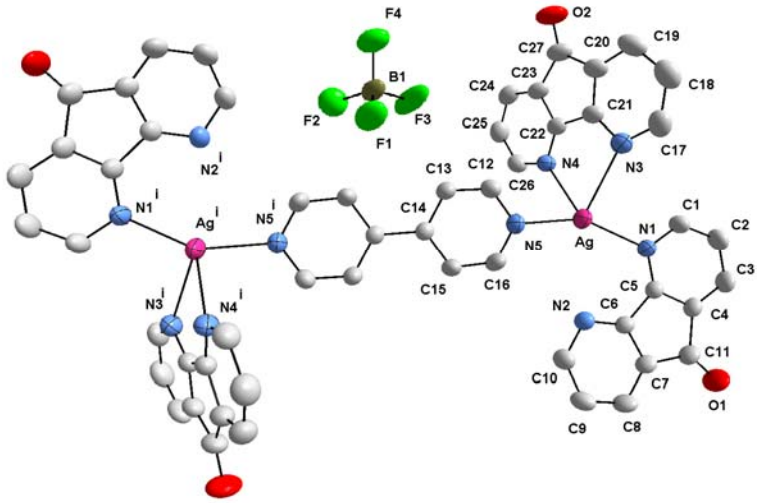

Figure A.4 Thermal ellipsoid plot of the coordination environment of the complex molecule **2.** Atoms are represented as 50% probability ellipsoids and ring hydrogen atoms have been omitted for clarity. [Symmetry code: (i) –x + 1, –y + 1, –z + 1.]

Table A.2 Selected bond lengths [Å] and angles [°] for **1**

Ag(1)-N(1)	2.222(3)	Ag(2)-N(4)	2.650(3)
Ag(1)-N(2)	2.695(3)	N(1)-Ag(1)-(N2)	74.59 (9)
Ag(2)-N(3)	2.254(3)	N(3)-Ag(2)-N(4)	75.01(9)

[Symmetry code : (i) -x+1, -y+2, -z+1. (ii) -x, -y, -z+1]

Table A.3 Selected bond lengths [Å] and angles [°] for **2**

Ag-N(1)	2.2464(19)	N(5)-Ag-N(3)	109.97(7)
Ag –N(5)	2.2433(19)	N(5)-Ag-N(4)	85.80(7)
Ag-N(3)	2.593(2)	N(1)-Ag-N(3)	92.97(7)
Ag-N(4)	2.644(2)	N(1)-Ag-N(4)	122.61(6)
N(5)-Ag-N(1)	148.87(7)	N(3)-Ag-N(4)	70.45(6)

Most previously reported $[Ag(N\text{-}N)_2]^+$ complexes are near-symmetric chelates exhibiting flattened tetrahedral coordination with dihedral angles in the range 27.9-80.4° [10-14,19]. The two complex cations interact through π-stacking (3.365(5) - 3.495(5) Å) leading to an interdigitized packing. The nitrate ion and the lattice water molecule participate in H-bonding (O-H…O, C-H…O) and O…π interactions (Figures A.2 and A.3). The cation in **2** is dinuclear with a crystallographic inversion centre (Figure A.4). The coordination polyhedron at each silver atom is a highly distorted tetrahedron with two short and two long bonds (Ag-N(1), 2.246(2); Ag-N(5), 2.243(2); Ag-N(3), 2.593(2); Ag-N(4), 2.644(2) Å). Of the two coordinated dafone molecules, one forms a single short bond, while the other forms two weak chelating bonds. The cations are assembled into porous two-dimensional sheets by C-H…F and C-H…O interactions. However these pores are blocked by the 2-dimensional interpenetration of identical networks with the adjacent networks connected by π…π stacking (3.295(7) - 3.48(1) Å) interactions (Figures A.5 and A.6).

As early as 1986, Goodwin et al.,[19h] after considering electronic as well as steric factors concluded that the flattening distortion in bis-chelate complexes of Ag(I) with hetero-aromatic ligands is imposed by π-stacking interactions in the lattice. The wide range of the observed torsion angles reveal that there is considerable

plasticity in the coordination polyhedron of this class of four-coordinate Ag(I) complexes. Compound **1**, represents the extreme situation of perfect planarity.

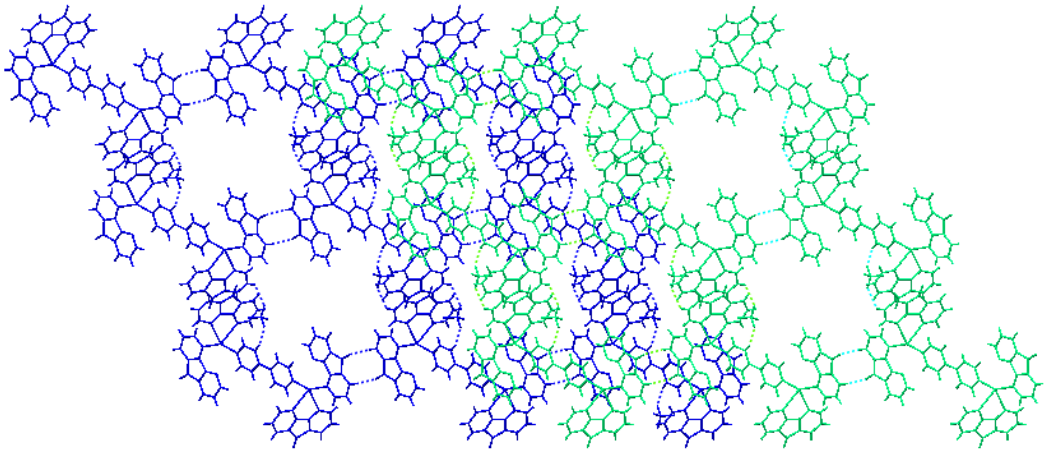

Figure A.5. Two-fold interpenetrating layers of **2** viewed down the *a* axis.

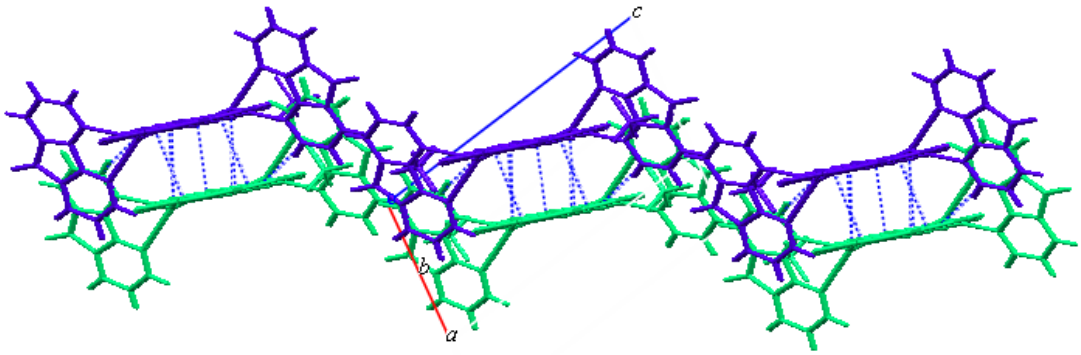

Figure A.6. Side view showing stacking interactions between the interpenetrating layers in **2**.

However, it should be noted that the flattening is accompanied by a highly unsymmetrical (to the extent of 15 - 20 %) chelate bonds. Further, Ag(I) in this

compound has an abnormally low bond valence sum (bvs)[20] of 0.78 - 0.81 (expected value 1.0). Other complexes, for example $Ag(bpy)_2^+$, typically have a bond valence sum of 0.98. It appears that the relatively weak metal-ligand interaction is compensated by intermolecular interactions, especially π-stacking. The dominant role of lattice interactions in controlling the coordination geometry of Ag(I) complexes has been previously noted[21]. Compound **2** further illustrates the weakness of Ag-dafone interaction. The chelating dafone presents the unusual picture of two long Ag-N bonds, while the singly bonded dafone forms a normal Ag-N bond. Even in this compound, the bvs is only 0.82.

A.4.2 Crystal structure of $Pt(dafone)Cl_2$

In complexes **3**, platinum shows square planar coordination, with two nitrogen atoms and two chlorine atoms are in *cis* position. Molecular diagram of the complex is shown in Figure A.7. The N1-Pt-N2 angle 83.6° is determined by the geometrical constrains inside the chelating ring. Other angles Cl1-Pt-Cl2, 91.7°; Cl2-Pt-N1, 93.4° and Cl1-Pt-N2, 91.3 are very close to 90°.

Table A.4. Selected bond lengths [Å] and angles [°] for **3**

Pt-N(2)	2.053(4)	N(2)-Pt-Cl(2)	176.76(11)
Pt-N(1)	2.070(4)	N(1)-Pt-Cl(2)	93.36(11)
Pt-Cl(2)	2.2776(13)	N(2)-Pt-Cl(1)	91.33(11)
Pt-Cl(1)	2.2782(13)	N(1)-Pt-Cl(1)	174.86(11)
N(2)-Pt-N(1)	83.56(15)	Cl(2)-Pt-Cl(1)	91.73(5)

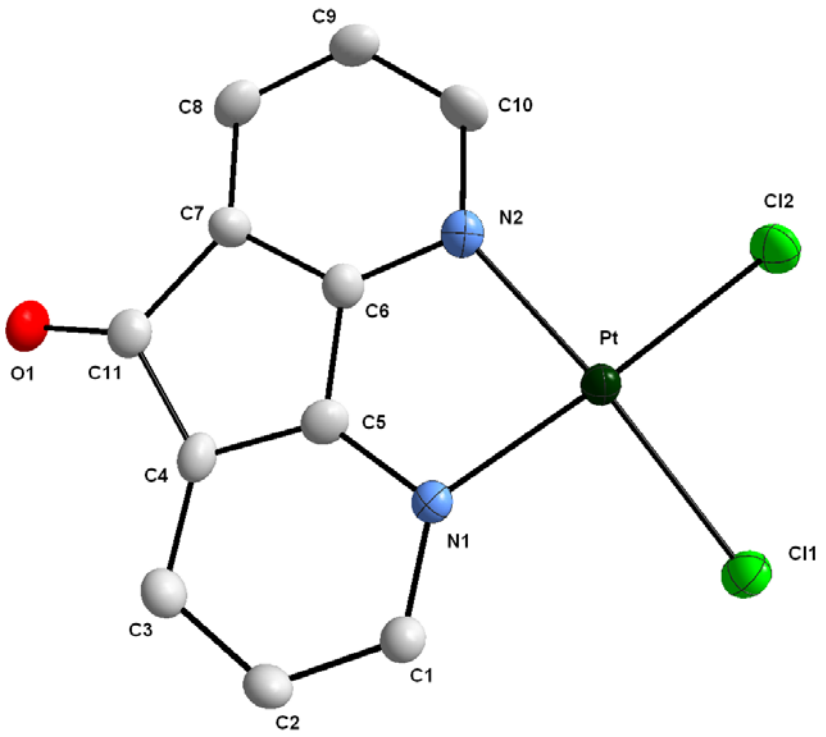

Figure A.7. Thermal ellipsoid plot of the coordination environment of the complex molecules **3**. Atoms are represented as 50% probability ellipsoids and ring hydrogen atoms have been omitted for clarity.

Coming to crystal packing, molecules are arranged into a zig-zag two-dimensional layers by C10-H10…Cl1 (2.758 Å), C8-H8…Cl2 (2.719 Å) and C3-H3…O1 (2.452 Å) interactions (Figure. A.8). These zig-zag layers are further connected by π-stacking interactions (3.357-3.459 Å) as well as by a C1-H1…Cl1 (2.733 Å) interaction into 3-dimesion (Figure. A.9)

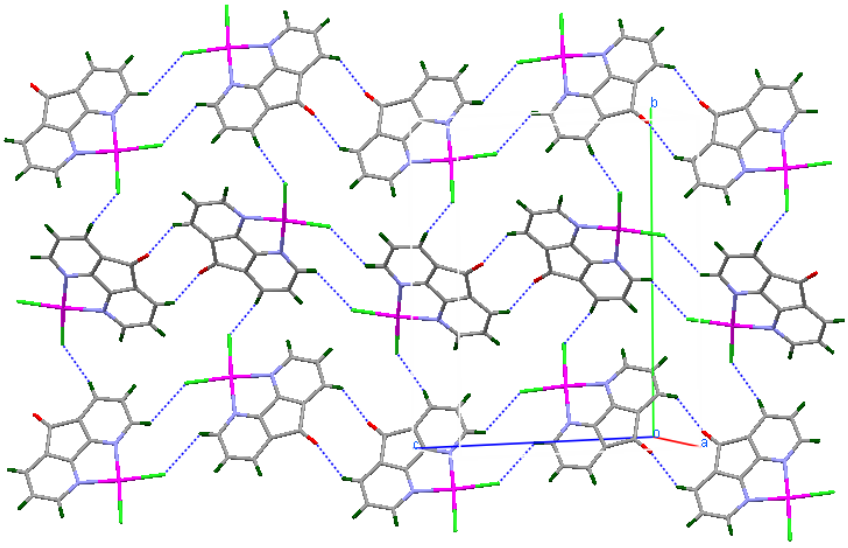

Figure A.8. C-H…Cl and C-H…O interactions in a zig-zag two-dimensional layer of **3**.

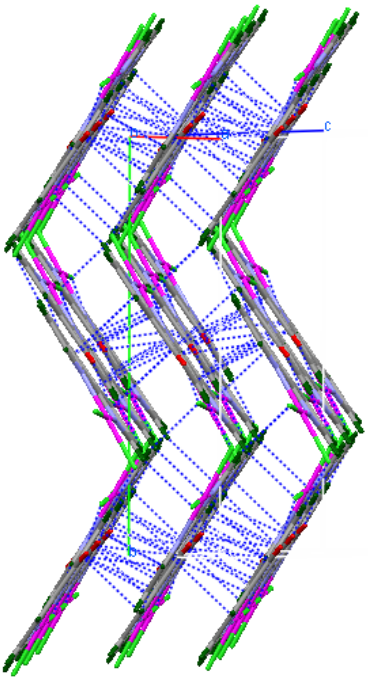

Figure A.9 2-dimensional zig-zag layers interconnected by π-stacking and C-H…Cl interactions in **3**.

A.5 Conclusion

Dafone form a variety of coordination modes with silver. In compound **1**, it forms a tetracoordinated complex with an extreme case of planarity. However planarity of the tetracordinate silver complex is associated with highly unsymmetrical chelate bonds as observed for other diminine complexes. Bond valance sum of complex **1** is low indicates a weak Ag-dafone bonds, which was further confirmed by the weakness of Ag-dafone interaction in compound **2**. In compound **3** dafone has a planar rectangular structure with a symmetric chelation. Its structure is analogous to cisplatin[22] [*cis*-$(NH3)_2PtCl_2$], which is one of the most effective drugs to treat testicular, ovarian, bladder and neck cancers.

A.6 References

1. Henderson Jr. L. J.; Fronczek, F. R.; Cherry, W. R. *J. Am. Chem. Soc.* **1984**, *106*, 5876.

2. Pyle, M.; Rahman, R.; Meshoyrer, J. P.; Kumar, C. V.; Turro, N. J.; Barton, J. K. *J. Am. Chem. Soc.* **1989**, *111*, 3051.

3. Menon, S.; Balagopalakrishna, C.; Rajasekharan, M. V.; Ramakrishna, B. L. *Inorg. Chem.* **1994**, *33*, 950.

4. Balagolalakrishna, C.; Rajasekharan, M. V.; Bott, S.; Atwood, J. L.; Ramakrishna, B. L. *Inorg. Chem.* **1992**, *31*, 2843.

5. Menon, S.; Rajasekharan. M. V. *Inorg. Chem.* **1997***, 36*, 4983.

6. Menon, S.; Rajasekharan. M. V. *Polyhedron* **1998**, *17*, 2463.

7. Miao, S.; Kang, H.; Du, C.; Ji. B. *X-Ray Struct. Anal. Online,* **2006**, *22***,** 45.

8. Lu, Z.; Duan, C.; Tian, Y.; You, X. *Inorg*. *Chem*. **1996**, *35*, 2253.

9. Wang, Y.; Jackman, D. C.; Woods, C.; Rillema, D. P. *J*. *Chem*. *Crystal*. **1995**, *25*, 549.

10. Bowmaker, G. A.; Effendy.; Marfuah, S.; Skelton, B. W.; White, A. H. *Inorg. Chim. Acta* **2005**, *358*, 4371.

11. Li, P.-G.; Wang, Q.-L.; Li, D.-S.; Fu, F.; Qi, G.-C. *Z. Kristallogr. New Cryst. Struct.* **2006**, *221*, 391.

12. Atwood, J. L.; Simms, M. L.; Zatko, D. A.; *Cryst. Struct. Commun.* **1973**, *2*, 279.

13. Leschke, M.; Rheinwald, G.; Lang, H.; *Z. Anorg. Allg. Chem.* **2002**, *628*, 2470. (b) Paramonov, S. E.; Kuzmina, N. P.; Troyanov, S. I.; *Polyhedron* **2003**, *22*, 837.

14. (a) Osborn, R. S.; Rogers, D. *J. Chem. Soc., Dalton Trans.* **1974**, 1002. (b) Canty, A. J.; Skelton, B. W.; Traill, P.R.; White, A.H. *Aust. J. Chem.* **1992**, *45***,** 417. (c) Textor, M.; Oswald, H. R. *Z. Anorg. Allg. Chem.* **1974**, *407***,** 244. (d) Connick, W. B.; Henling, L. M.; Marsh, R. E.; Gray, H. B. *Inorg. Chem.* **1996**, *35*, 6261. (e) Falvello, L. R.; Garde, R.; Miqueleiz, E. M.; Tomas, M.; Urriolabeitia, E. P. *Inorg. Chim. Acta* **1997**, *264***,** 297. (f)

Falvello, L. R.; Garde, R.; Miqueleiz, E. M.; Soler, T.; Tomas, M. *Private Communication ,* **2003**, (g).Hambley, T. W. *Acta Cryst.* **1986**, *C42***,** 49. (h) Nakabayashi, Y.; Erxleben, A.; Letinois, U.; Pratviel, G.; Meunier, B.; Holland, L.; Lippert, B. *Chem.-Eur. J.* **2007**, *13*, 3980. (i) Vicente, J.; Arcas, A.; Fernandez-Hernandez, J. M.; Bautista, D. *Organometallics* **2006**, *25*, 4404. (j) Grzesiak, A. L.; Matzger, A. J. *Inorg. Chem.* **2007**, *46***,** 453.

15. Menon, S.; Rajasekharan. M. V. Polyhedron **1998**, 17, 2463.

16. *SAINTPLUS*, Bruker AXS Inc. Madison, Wisconsin, USA.

17. Sheldrick, G. M. *SADABS*, *Program for Empirical Absorption Correction*, University of Gottingen, Germany, **1996.**

18. M. Sheldrick, *SHELXS* and *SHELXL-97*, University of Gottingen, Gottingen, Germany, **1997**.

19. (a) Stephenson, M. D.; Hardie, M. J. *Cryst. Growth Des.* **2006**, *6*, 423. (b) Ashton, P. R.; Balzani, V.; Credi, A.; Kocian, O.; Pasini, D.; Prodi, L.; Spencer, N.; Stoddart, J. F.; Tolley, M. S.; Venturi, M.; White, A. J. P.; Williams, D. J. *Chem. Eur. J.* **1998**, *4*, 590. (c) Wen, M.; Kejia, E.; Munakata, M.; Suenaga, Y.; Sowa, T. K.; Maekawa, M.; Yan, S. G. *Mol. Cryst. Liq. Cryst. Sci. Technol., Sect. A* **2006**, *457*, 203. (d) Constable, E.C.; Housecroft, C. E.; Neuburger, M.; Poleschak, I.; Zehnder, M. *Polyhedron* **2003**, *22*, 93. (e) Pallenberg, A. J.; Marschner, T. M.; Barnhart, D. M. *Polyhedron* **1997**, *16*, 2711. (f) Titze, C.; Kaim,

W.; Zalis, S.; *Inorg. Chem.* **1997**, *36*, 2505. (g) Wu, H.-P.; Janiak, C.; Rheinwald, G.; Lang, H. *J. Chem. Soc., Dalton Trans.* **1999**, 183. (h) Goodwin, K. V.; McMillin, D. R.; Robinson, W. R. *Inorg. Chem.* **1986**, *25*, 2033. (i) Ward, M. D.; Couchman, S. M.; Jeffery, J. C. *Acta Cryst.* **1998**, *C54*, 1820.

20. Keeffe, M. O'.; Brese, N. E. *J. Am. Chem. Soc.* **1991**, *113*, 3226.

21. Swarnabala, G.; Rajasekharan, M. V. *Polyhedron* **1996**, *15*, 3197.

22. Rosenberg, B.; Van Camp, L.; Trosko, J. E.; Mansour, V. H. *Nature*, **1969**, *222*, 385.

LIST OF PUBLICATIONS

(1) Fluoromanganese(III) complex of phenanthroline. Distortion isomers of $Mn(phen)F_3(H_2O)$ stabilised by intermolecular interactions – Crystal structures, electronic spectra and DFT calculations. **Biju, A. R.**; Rajasekharan, M. V. *J. Mol. Struct.* **2007**, *875*, 456.

(2) Unusual coordination geometries of silver(I) 4,5-diazafluoren-9-one complexes. **Biju, A. R.**; Rajasekharan, M. V. *Polyhedron* **2008**, *27*, 2065.

POSTERS AND WORKSHOPS

(1) Chattopadhyay, M. K.; Sharma, Y. V. R. K.; Raghu, G.; Shivaji, S.; Biju, A. R.; Rajasekharan, M. V. Abstract presented at Proceedings of biological chemist (India) 73rd annual meeting, (2004).

(2) Presented a poster entitled Higher valent manganese complexes; structure and properties. **Biju, A. R**.; Rajasekharan, M. V. at 11th National Symposium on Modern Trends in Inorganic Chemistry (MTIC-XI), IIT Delhi, December 8-10, (2005).

(3) SCD user training for APEXII or SMART APEXII at Bruker AXS CCD Single Crystal X-ray Diffractometer Workshop 2006. May 31- June 1. NCL Pune.

(4) Presented a poster entitled High Field-High Frequency EPR & Optical Studies of New Manganese(III) Complexes **Biju, A. R**.; Rajasekharan, M. V. at International Conference on Materials for the Millennium, CUSAT, Cochin, March 1-3, (2007).

(5) Presented a poster entitled Concomitant polymorphs of $[Mn(acac)_2(H_2O)_2]NO_3.H_2O$ **Biju, A. R.**; Rajasekharan, M. V. at 12th National Symposium on Modern Trends in Inorganic Chemistry (MTIC-XII), IIT Madrass. December 6-8, (2007).